EXTRACELLULAR VESICLES AND THEIR ROLE IN CANCER PROGRESSION AND THERAPY RESISTANCE

A Dissertation

Presented to the Faculty of the Graduate School

of Cornell University

In Partial Fulfillment of the Requirements for the Degree of

Doctor of Philosophy

by

Bridget Taylor Kreger

August 2016

EXTRACELLULAR VESICLES AND THEIR ROLE IN CANCER PROGRESSION AND THERAPY RESISTANCE

Bridget Taylor Kreger, Ph. D.

Cornell University 2016

Extracellular vesicles (EVs), including exosomes and microvesicles (MVs), have emerged as a major form of intercellular communication, playing important roles in several physiological processes and diseases including cancer. EVs generated by cancer cells contain a variety of proteins and RNA species that can be transferred between cancer cells, as well as between cancer and non-transformed (normal) cells, thereby impacting a number of aspects of cancer progression. We show how oncogenic transformation influences the biogenesis and function of EVs using a mouse embryonic fibroblast (MEF) cell line that can be induced to express an oncogenic form of Dbl (for diffuse B cell lymphoma). MVs isolated from onco-Dbl-transformed cells contain a unique signaling protein, the ubiquitously expressed non-receptor tyrosine kinase, focal adhesion kinase (FAK). The addition of MVs isolated from MEFs expressing onco-Dbl to cultures of normal fibroblasts strongly promoted their survival and induced their ability to grow under anchorage-independent conditions, outcomes that could be reversed by knocking-down FAK and depleting it from the MVs, or by inhibiting its kinase activity using a specific inhibitor. I then showed the same to be true for MVs isolated from aggressive MDAMB231 breast cancer cells. Together, these findings demonstrate that the induction of oncogenic transformation gives rise to MVs, which uniquely contain a signaling

protein kinase that helps propagate the transformed phenotype, and thus may offer a specific diagnostic marker of malignant disease.

Additionally, I have discovered that treating MDAMB231 breast cancer cells with the chemotherapy paclitaxel, which functions by stabilizing microtubules, significantly increases the amount of survivin in the EVs shed by these cells. I then go on to show that survivin is specifically enriched in the class of EVs known as exosomes. Exosomes collected from MDAMB-231 cancer cells treated with paclitaxel promoted the growth and survival of recipient fibroblasts and other breast cancer cells exposed to serum-starvation and paclitaxel treatment, an effect that was lost when survivin was depleted from these exosomes by siRNA. Overall, these results highlight how a specific protein is selectively packaged into exosomes, as well as shed light on a potential mechanism underlying paclitaxel resistance.

BIOGRAPHICAL SKETCH

Bridget Kreger was born in New Jersey and was raised in a small town with her four younger siblings until she was fourteen years old. Her family then moved to Rhode Island where she completed her high school years. Bridget's parents, Mary Beth and Christopher, encouraged her to view the world with curiosity and kindled her fascination of the natural world with frequent "backyard biology" classes. After a high school curriculum split between art and biology courses, Bridget followed her passion for science to the University of Vermont to pursue a degree in Medical Laboratory Sciences. While in Vermont, Bridget was accepted into the McNair Scholars program, which enabled her to join the laboratory of Dr. Chaudhry where she studied the effects of ionizing radiation on the microRNA profiles of human cell lines, and how these microRNAs played a role in the bystander effect (a phenomenon now attributed to extracellular vesicles). After graduating, Bridget drove across the country with her then-boyfriend Evan Sorel, to work as a research technician at the Fred Hutchinson Cancer Research Center in Seattle, Washington. Her time at the 'Hutch' focused on determining the mechanisms that lead to the onset of squamous cell carcinoma by studying cell adhesion in mouse hair follicle stem cells. Bridget was then accepted into the Biochemistry, Molecular and Cell Biology program at Cornell University where she joined the laboratory of Dr. Richard Cerione. There, she studied the role of extracellular vesicles in the context of cancer progression and resistance to chemotherapeutics. After graduation, Bridget, and her now-husband Evan, will be moving to Boston where she has secured a position as a Post-doctoral Scientist at the biopharmaceutical company AstraZeneca. Although she will miss the friends she has made in Ithaca, she is excited about this next phase of her life.

ACKNOWLEDGEMENTS

I would like to thank my parents for their constant love and encouragement over the years, as well as my siblings for keeping me in touch with what matters in life.

I would like to thank Rick for always doing everything he can to help all of his lab members, including myself. He has been a constant advocate; I couldn't have asked for a better mentor.

I would like to thank Marc for his time and patience, and for his infinite knowledge of science, laboratory techniques, and 80's rock.

I greatly appreciate all of the support and feedback from my committee members, John Lis and Bill Brown.

The Department of Molecular Medicine has been an endless source of help throughout my time at Cornell. I would especially like to thank Maurine, Debbie, Cindy, and Robin for their support.

I will never forget all of the friends I have made in the Cerione laboratory, and in the BMCB program, they have made these years fun and interesting beyond measure.

Finally, my husband Evan deserves my endless gratitude for being so supportive in all of our adventures together, and for making me laugh every day.

TABLE OF CONTENTS

LIST OF ABBREVIATIONS

ABCA3: ATP-binding cassette transporter A3
ABs: apoptotic bodies
Ago2: Argonaute 2
Arf6: ADP-ribosylation factor 6
CAV1: caveolin 1
Cdc42: Cell division control protein 42 homolog
CFDA: 5(6)-carboxyfluorescein diacetate
CFSE: carboxyfluorescein succinimidyl ester
CM: conditioned medium
DAPI: 4',6-diamidino-2-phenylindole
Dbl: Diffuse B-cell lymphoma
DMEM: Dulbecco's modified eagle medium
DMSO: dimethyl sulfoxide
EGF: epidermal growth factor
EGFR: epidermal growth factor receptor
EGFRvIII: epidermal growth factor receptor variant III
ERK: extracellular signal-related kinase
ES cells: embryonic stem cells
ESCRT: endosomal sorting complex required for transport
EVs: extracellular vesicles
Exos: exosomes
F-actin: filamentous actin
FAK: focal adhesion kinase
FBS: fetal bovine serum
FGFR: fibroblast growth factor receptor
GBM: glioblastoma
GEF: guanine nucleotide exchange factor
GFP: green fluorescent protein
GPI: glycosylphosphatidylinositol
HA: hemagglutinin
HDL: high-density lipoproteins
Hrs: hepatocyte growth factor-regulated tyrosine kinase substrate
ILV: intraluminal vesicle
Ind: Onco-Dbl Induced
JNK: c-Jun N-terminal kinase
KD: kinase dead
KRAS: Kirsten rat sarcoma viral oncogene homolog
LAMP: lysosome associated proteins
LimK: Lim Kinase

MAPK: mitogen activated protein kinase
mDia: mammalian homolog of Drosophila diaphanous
MEFs: mouse embryonic fibroblasts
MEK: MAPK/Erk kinase
miRNA: micro RNA
MLC: myosin light chain
MLCK: myosin light chain kinase
MMP: matrix metalloproteinases
mRNA: messenger RNA
MVB: multivesicular body
MVE: multivesicular endosome
MVs: microvesicles
NS: not significant
NTA: nanoparticle tracking analysis
PAK: p21-activated protein kinase
PBS: phosphate buffered saline
PI3K: phosphatidylinositol-3-kinase
PLD: phospholipase D
PS: phosphatidylserine
PTX: paclitaxel
PVDF: Polyvinylidene fluoride
Rab: Ras-related protein Rab
Rac1: Ras-related C3 botulinum toxin substrate 1
RhoA: Ras homology gene family member A
RISC: RNA-induced silencing complex
ROCK: Rho-associated protein kinase
SD: standard deviation
shRNA: short hairpin
siRNA: small interfering RNA
Syt-7: synaptotagmin-7
TEM: transmission electron microscopy
TNF-α: tumor necrosis factor alpha
TSG101: tumor suscetibility gene 101
tTG: tissue transglutaminase
UTR: untranslated region
VAMP3: v-SNARE-vesicle associated membrane protein
VEGF: vascular endothelial growth factor
WB: Western blot
WCL: whole cell lysate
WT: wild type
XIAP: X-linked inhibitor of apoptosis protein

CHAPTER 1

Introduction

Intercellular communication is critical for the development and functionality of multicellular organisms, while deregulation of these events often cause the onset of disease. A classical example of intercellular communication involves the secretion of a soluble factor, such as a growth factor or cytokine, by one cell into its local environment (1). The soluble factor then binds its corresponding receptor expressed in a neighboring cell, leading to the activation of signaling pathways that determines whether the target cell grows, differentiates, migrates, or even dies (2, 3). In addition to soluble factor-mediated interactions between two cells, there are several other forms of intercellular communication, including direct cell-to-cell contact (4).

The study of intercellular communication has expanded greatly with the discovery that membrane enclosed packets of information, collectively referred to as extracellular vesicles (EVs), are actively released by cells (5-8). Once thought to be nothing more than cellular debris, it is now appreciated that EVs are an evolutionarily conserved mechanism utilized by prokaryotes, eukaryotes, and plants for the transmission of signals by cells (8-12). While there is increasing evidence suggesting that EVs play important roles in several different biological contexts, to date, most of the studies on EVs have been in the field of cancer biology. Indeed, EVs have been shown to be potent mediators of tumor growth, metastasis, vascularization, and even chemoresistance (13-15).

EVs are able to carry out a diverse range of biological functions as a result of the unique cargo they contain, including microRNA (miRNA), messenger RNA (mRNA), DNA, cytokines, receptor and non-receptor tyrosine kinases, cytoskeletal components, and transcription factors

(16-20). Due to the findings that the contents of EVs often reflect their cell of origin, and that EVs can be found in the bloodstream, there are also significant implications for the use of EVs as diagnostic markers of disease (21, 22).

Biogenesis of distinct classes of EVs

EVs have been referred to by a variety of names, including ectosome, exosomes, oncosomes, microparticles, microvesicles (MVs), shedding vesicles, or simply small vesicles (23-26). This has created a good deal of confusion in the field, especially because there are distinct classes of EVs. The EVs generated by viable cells can be broken down into two major classes: 1) MVs, or those EVs that are shed from the plasma membrane, and 2) exosomes, or those EVs that are formed by a re-routing of the multivesicular bodies (MVBs)-containing endosomes to the cell surface (Figure 1.1) (27). It is worth mentioning that there is a third class of EVs, called apoptotic bodies (ABs), which are formed as a cell fragments during apoptosis (28). One of the main factors used to distinguish between the different classes of EVs, other than the mechanism underlying their biogenesis, is their size. Exosomes are the smallest type of EVs and are approximately 30-100nm in diameter, while MVs have the propensity to be much larger, ranging from 200nm-2μm. Lastly, apoptotic bodies are the largest class of EVs, with a diameter of 2-10μm (29).

Formation and shedding of Microvesicles

MVs are formed by the outward budding and fission of the plasma membrane and the subsequent release, or shedding, of the membrane-enclosed structure into the extracellular environment. MVs have been identified in the context of many different biological events, for

Figure 1.1. Exosomes and Microvesicles are generated by distinct mechanisms.
Exosomes are formed by the inward budding of the endosomal membrane to form intraluminal vesicles (ILV) within the multivesicular body (MVB). The MVB is re-routed from the lysosome, to the cell surface where it fuses with the plasma membrane and releases its contents (now called exosomes) in the extracellular space. Microvesicles bud directly from the cell's plasma membrane.

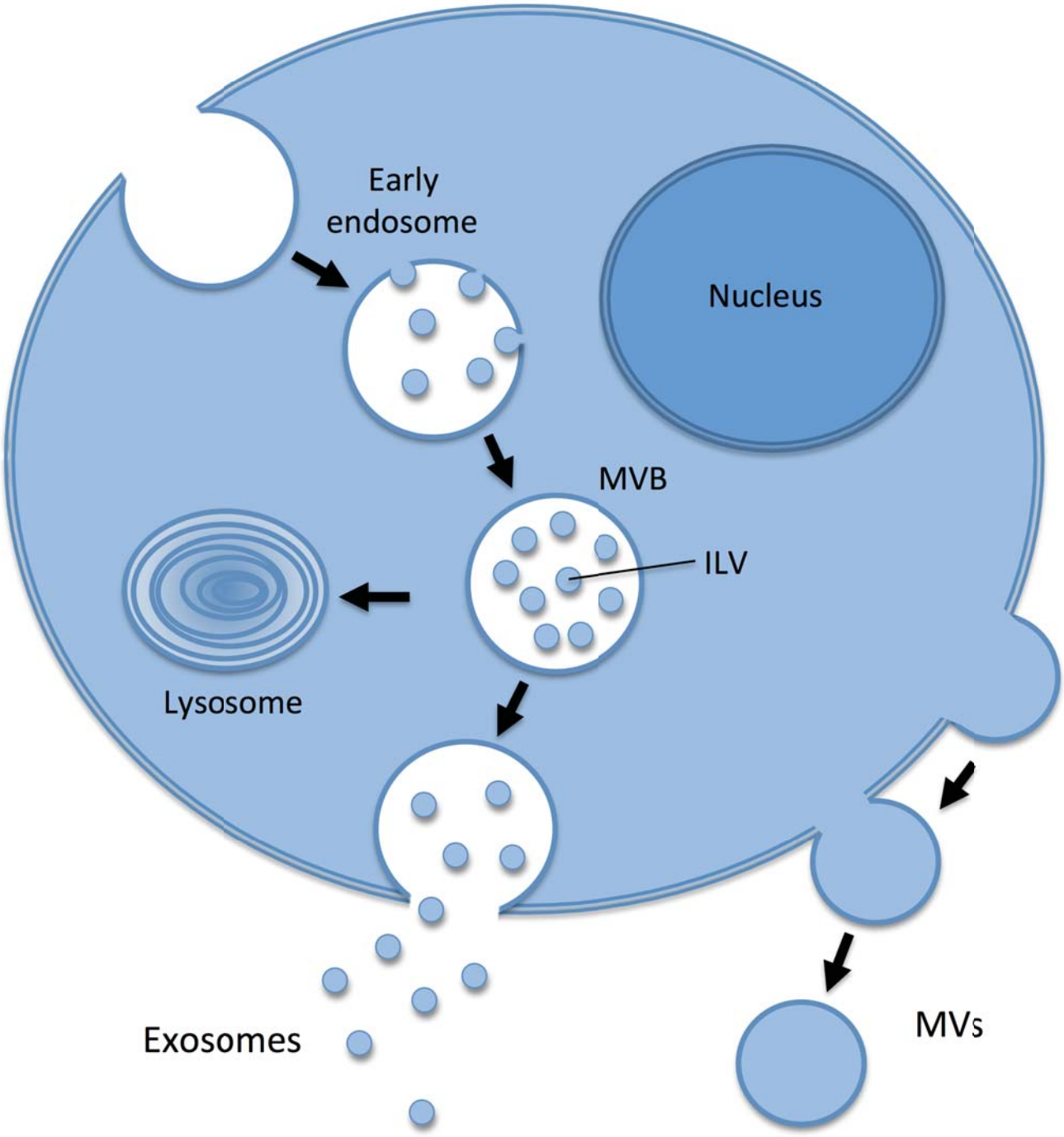
Early
endosome
Nucleus
MVB
ILV
Lysosome
Exosomes
MVs

example, early studies drew comparisons between viral budding and MV formation, noting the similarity in requirements for rearrangement of structural proteins, packaging of select cargo, and deforming the plasma membrane for release of the virus from the cell (30). For example, some retroviruses will assemble Gag proteins and hijack the endosomal sorting complex required for transport (ESCRT), recruiting it to the plasma membrane along with the tumor susceptibility gene 101 (TSG101) (31). The assembly of the ESCRT complexes leads to the formation of a semispherical complex that distorts the curvature of the plasma membrane until the assembled particle pinches off from the surface of the cell (30).

The mechanisms responsible for MV formation and shedding are still an active area of research, however, several studies have highlighted the importance of certain small GTPases and their ability to rearrange the actin cytoskeleton as key factors in the biogenesis of MVs. Both Ras homolog gene family member A (Rho A) and ADP-ribosylation factor 6 (Arf 6) have been shown to act as molecular switches in order to initiate changes in the actin cytoskeleton leading to MV formation (32, 33).

Early studies in our laboratory directed at understanding how MVs are formed and mediate biological outcomes involved the detection of large (between 200nm-2.0μm) vesicular structures decorating the surfaces of cancer cells as detected by immunofluorescence using an antibody against tissue transglutaminase (tTG) (32). tTG is a crosslinking enzyme that has an elevated expression in several cancers and has been associated with chemoresistance and cell growth. The vesicles could also be visualized as ring-like structures on the surfaces of cells stained with rhodamine-conjugated phalloidin to detect filamentous actin (F-actin). Interestingly, MVs could be consistently detected on the highly aggressive MDAMB-231 breast cancer cell

line and the U87 glioblastoma cell line. However, MV formation in the HeLa cervical carcinoma cell line required the addition of epidermal growth factor (EGF).

Discovering that MV biogenesis in HeLa cells was increased by EGF stimulation provided us with an opportunity to determine what might be functioning downstream of the EGF receptor (EGFR) to mediate this effect. Because MVs budding from the cell surface are likely to cause cytoskeletal rearrangements, proteins known to be activated by growth factor stimulation and regulate the actin cytoskeleton were investigated. The Rho family is a part of the larger Ras superfamily of small GTPases and includes a number of members, such as, RhoA, Rac, and Cdc42. Each of these small GTPases are activated by the EGFR and are known to mediate cytoskeletal rearrangements (34, 35). For example, RhoA has been shown to the activate Rho-associated coiled-coiled forming kinase (ROCK), which then can phosphorylate the myosin-binding subunit of myosin phosphatase to inactivate it, leading to actin assembly. The RhoA-ROCK signaling axis can also influence the cytoskeleton by activating the mammalian homolog of Drosophila diaphanous (mDia), a formin molecule that promotes actin nucleation (36-38). Other members of the Rho family include Rac and Cdc42 to regulate cytoskeletal changes (39, 40). Rac interacts with Arp2/3 to create a network of branched actin filaments for the formation of lamellipodia on the leading edge of a cell for migration (41). Cdc42 interacts with p21-activated protein kinase (PAK) to induce the formation of filopodia, actin-dependent membrane protrusions involved in migration (40, 42).

HA-tagged activated forms of Rac (Rac F28L), Cdc42 (Cdc42 F28L), or RhoA (RhoA F30L) were ectopically expressed in HeLa cells, and then cells were immunostained with tTG and HA antibodies to detect any MVs that were potentially forming on the surface of the transfected cells. Interestingly, only the HeLa cells expressing the activated form of RhoA were

found to have MVs on their surfaces. Consistent with this finding, knocking down RhoA expression in HeLa cells using a siRNA that specifically targeted this small GTPase were no longer able to form MVs in response to treatment with EGF. The study then went on to delineate the RhoA-mediated signaling pathway that was important for generating MVs in these cells. The pathway included the sequential activation of the kinases ROCK-1 and ROCK-2 and then Lim Kinase (LIMK) (37). LIMK, in turn phosphorylates cofilin on serine 3, which inhibits its actin filament severing activity (Figure 1.2) (43). Inhibiting cofilin activity at the sites of MV budding allows for the necessary changes to the actin cytoskeleton to occur (i.e. the formation of the characteristic actin rings seen in MVs from cancer cells) such that MVs are formed and release from a cell. Notably, if any component of this signaling pathway is inhibited, for example by using the ROCK inhibitor Y-27632, or by knocking down LIMK, the cell is no longer able to generate actin-based MVs (32).

Another study demonstrating the importance of a small GTPase in MV biogenesis came from the D'Souza-Schorey laboratory. In this case, they discovered that the Arf6 GTPase played an essential role in MV biogenesis (33) (Figure 1.3). Arf6 had been previously implicated in regulating the changes that need to occur to the actin cytoskeleton in order to turnover invadopodia (44). Invadopodia are actin-dependent protrusions of the plasma membrane involved in degradation of the extracellular matrix in cancer cell migration (45). However in this study, they showed that Arf6 could also influence MV formation. Whether Arf6 activity promoted invadopodia turnover or MV release was dependent on the stiffness of the surrounding extracellular matrix. In order to investigate this further, the group took advantage of an activated form of Arf6 (Arf6-Q67L), and a dominant-negative form of Arf6 (Arf6-T27N), to investigate the role that this small GTPase may play in MV biogenesis. Interestingly, they found that the

Figure 1.2. RhoA signaling regulates MV budding.
Growth factors (e.g. EGF) can lead to the activation of RhoA by exchanging GDP for GTP. RhoA signals through ROCK and LimK, which phosphorylates coflillin, inhibiting its actin-severing capabilities. This allows for the assembly of actin filaments at sites of MV budding. This pathway can be interrupted by treating the cells with a ROCK inhibitor (Y-27632), or with the depletion of LIMK expression by siRNA.

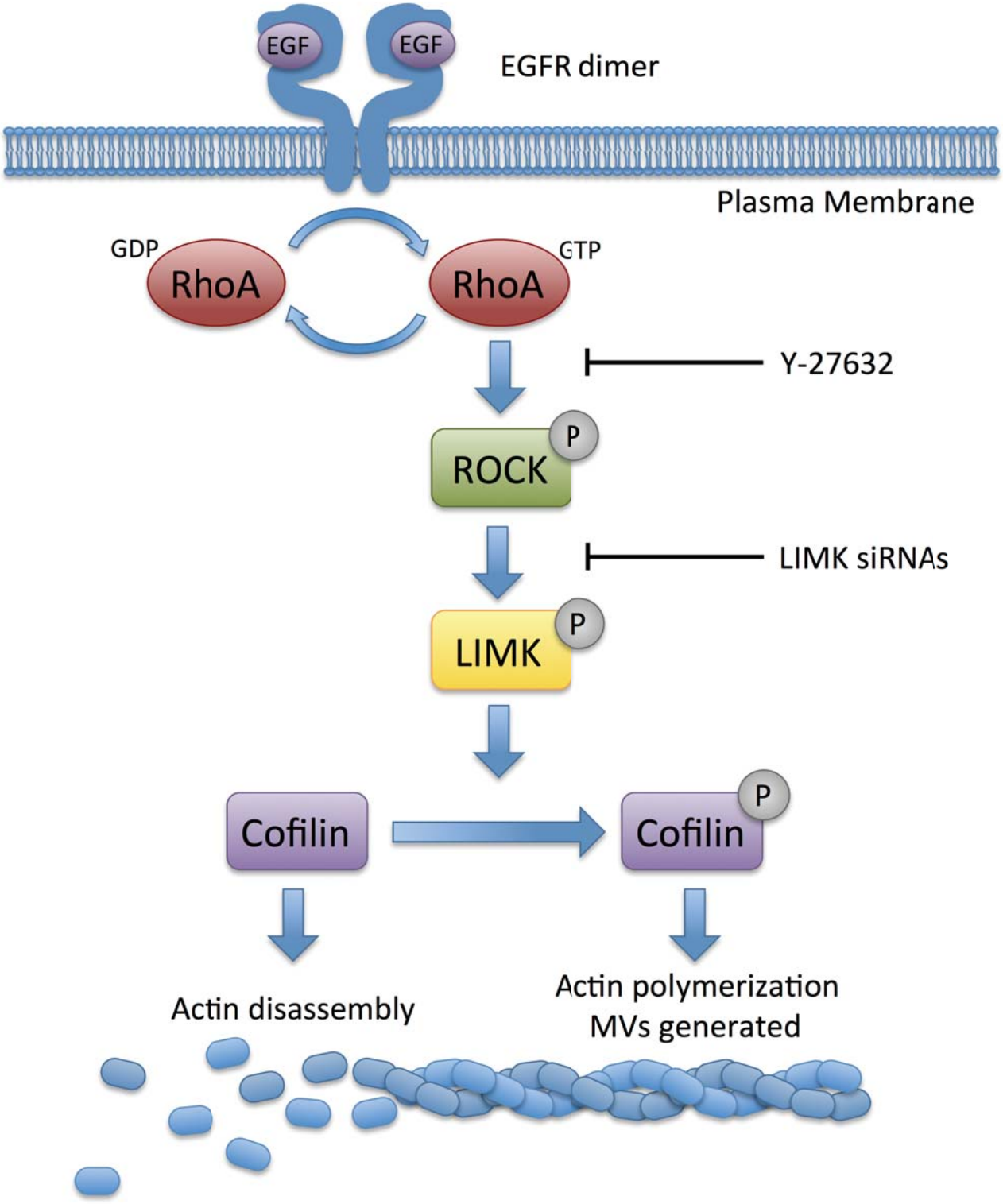
EGF
EGF
EGFR dimer
Plasma Membrane
GDP
RhoA
RhoA
GTP
Y-27632
ROCK
P
LIMK siRNAs
LIMK
P
Cofilin
Cofilin
P
Actin disassembly
Actin polymerization
MVs generated

Figure 1.3. Arf6 regulates MV shedding.
Active Arf6 (GTP-bound) signals through PLD to activate the mitogen activated protein kinase ERK. ERK in turn activates MLCK to phosphorylate myosin light chain (MLC) on Serine 18/19. The phosphorylated myosin is responsible for the actomysin-based fission of the plasma membrane for MV release. PD98059, the MEK/ERK inhibitor, blocks this signaling pathway.

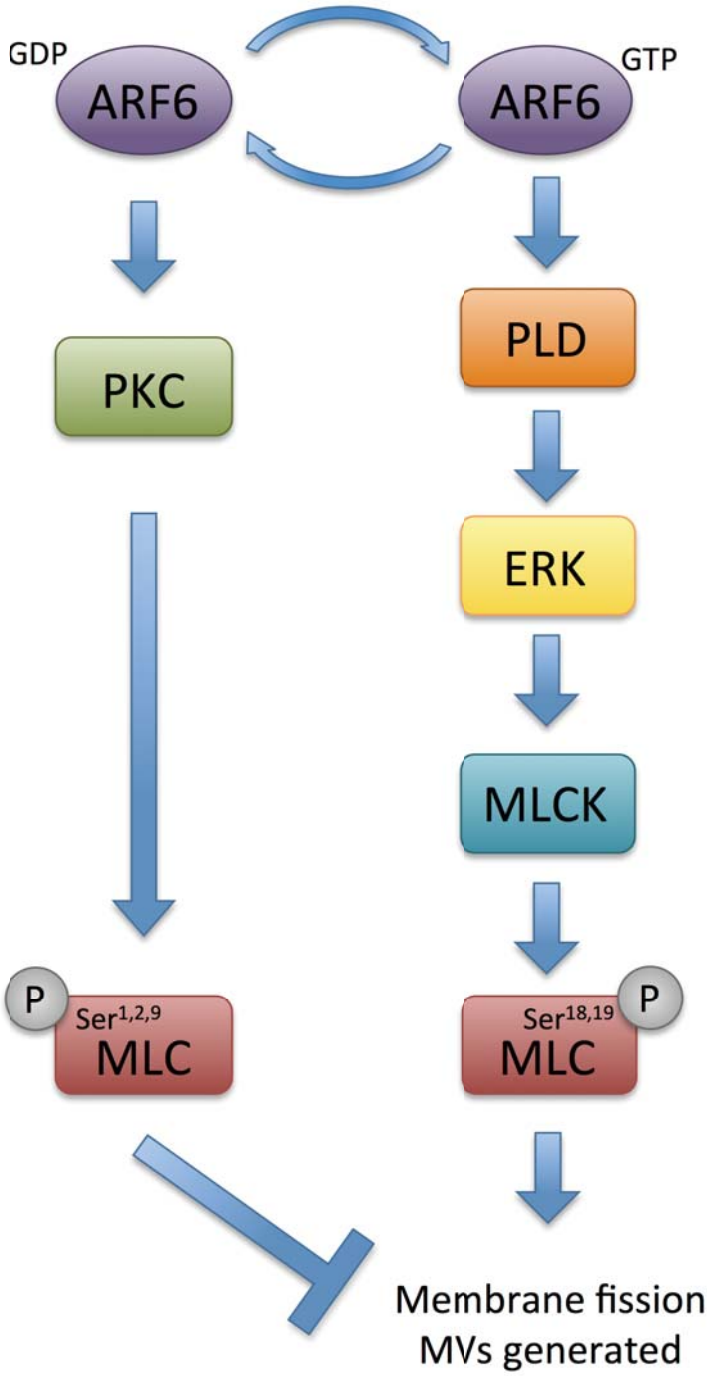
GDP
ARF6
ARF6
GTP
PKC
PLD
ERK
MLCK
P
Ser1,2,9
MLC
Ser18,19
MLC
P
Membrane fission
MVs generated

expression of the dominant-negative form of Arf6 lead to an increase in the amount of MVs that could be detected on the surfaces of the transfected cells, but an overall reduction in the amount of MVs released or shed by these cells into their media. Conversely, the expression of the activated mutant form of Arf6 led to fewer MVs on the surfaces of the cells, and an increase in the amount found in the media. This suggested that Arf6 activation is specifically required for the release of MVs from cells, rather than for their initial formation. The authors then went on to determine the signaling pathway through which ARF6 mediates its effects. Specifically, they found that Arf6 acts by signaling through phospholipase D (PLD) to activate extracellular signal-regulated kinase (ERK) (44, 46, 47). Phosphorylated ERK then activates myosin light-chain kinase (MLCK) to promote contraction of actin-based structures that form at the neck between the surface of the cell and the emerging MV. Ultimately, the neck continues to get smaller to the point that membrane fission occurs and the MV is released into the extracellular environment. Consistent with this finding, inhibiting ERK activation lead to the buildup of MVs along the surfaces of cells expressing an inactive form of Arf6 (48, 49).

In addition to the roles that proteins play in the formation and shedding of MVs, several studies have also focused on how changes in the lipid composition of the plasma membrane also influence this process. One of the best examples of this can be seen when considering the asymmetrical distribution of phosphadidylserine (PS) that occurs in MVs (50). PS is normally maintained in the inner leaflet of the plasma membrane by ATP-dependent flippases. However, as MVs are budding from the surface of cells, it is characteristic for PS to become enriched on the outer surface of the membrane due to the activity of the lipid transporter scramblase (51, 52). The localization of PS to the outer leaflet of MVs has several potential functional consequences including, promoting the outward curvature of the plasma membrane and detachment of the

underlying cytoskeleton to promote MV shedding (53, 54). As will be discussed later, PS on the outer surface of MVs also plays a role in the ability of MVs to dock onto recipient cells.

MV biogenesis has been associated with lipid rafts, a specialized microdomain of the plasma membrane that acts to compartmentalize cellular processes and serves as a center for assembly of signaling complexes (55). Lipid rafts are enriched with a specific set of proteins, glycosphingolipids, and cholesterol and are thought to be the site of MV biogenesis (56). MVs are enriched in cholesterol, and when cholesterol levels were depleted in cells due to treatment with MβCD (a reagent that removes cholesterol from membranes), MV generation by the monocytic cell line THP-1 was reduced (56, 57). It has also been shown that flotillin, a lipid raft marker, is also expressed in MVs, further suggesting that MVs form at sites of lipid rafts (58, 59).

Formation and shedding of exosomes

Exosomes are the class of EVs that are typically in the size range of 30-100nm in diameter (60). They are distinct from MVs in how they are formed (27). There has also been a good amount of discussion in the field recently regarding exactly what constitutes an exosome versus a MV; however, here I am referring to EVs shed by cells as a result of the re-routing of multivesicular bodies (MVBs) (also known as the multivesicular endosome (MVE)) from the lysosome to the plasma membrane (31). The MVB then fuses with the plasma membrane and releases its contents (endosomes) into the extracellular environment, at which point they are referred to as exosomes (Figure 1.1). The mechanisms involved in the formation of exosomes, are more established, compared to MVs.

The formation of MVBs begins as the early endosome is generated by the inward budding of the plasma membrane (Figure 1.4) (61). ESCRT-0 recognizes phosphatidylinositol 3-phosphate on the membrane of the endosome and initiates the assembly of the ESCRT complexes for the formation of intraluminal vesicles (ILVs) within the endosome (62). ESCRT-0 subunits contain binding motifs for ubiquitin, enabling the enrichment of cargo within the ILV (63). ESCRT-0 is also required for the recruitment of ESCRT-1 (64, 65). The ESCRT-I complex includes the protein TSG101, which acts as a link between ESCRT-0 and ESCRT-II, as well as engages cargo at the endosome mediating its sorting into MVBs through the formation of intraluminal vesicles (66). ESCRT-II promotes the interaction between the ESCRT complex and the endosomal membrane and plays a critical role in initiating ESCRT-III complex formation (67, 68).

While ESCRT-0, I, and II are responsible for initiating complex formation and cargo recruitment, it is ESCRT-III that is responsible for deforming the endosomal membrane for cargo sequestration into ILVs (69). ESCRT-III is composed of 4 subunits known as charged multivesicular body proteins (CHMPs) in mammalian systems (70). ESCRT-III exists in an auto-inhibited state in the cytoplasm, but upon interacting with the ESCRT-II subunit Vps25, the ESCRT-III subunit Snf-7 undergoes a conformational change and assembles into a filament that interacts with the endosomal membrane (71). Upon interacting with Vps4, Snf-7 induces the curvature and scission responsible for formation of the ILV (72). Another protein required for this process is Bro1/Alix (BCK1-like resistance to osmotic shock protein/ apoptosis-linked gene-2 interacting protein X), which aids in the stabilization of Snf-7 and recruits the de-ubiquitinating enzyme Doa4 for processing ILV cargo (73).

Figure 1.4. ESCRT complexes form intraluminal vesicles.
(A) The ESCRT complexes 0, I, II assemble sequentially on the surfaces of endosomes (MVB). ESCRT-III subunits polymerize into spiral filaments. (B) The ESCRT-III filaments remodel to deform the membrane and constrict it at the bud neck to generate an intraluminal vesicle.

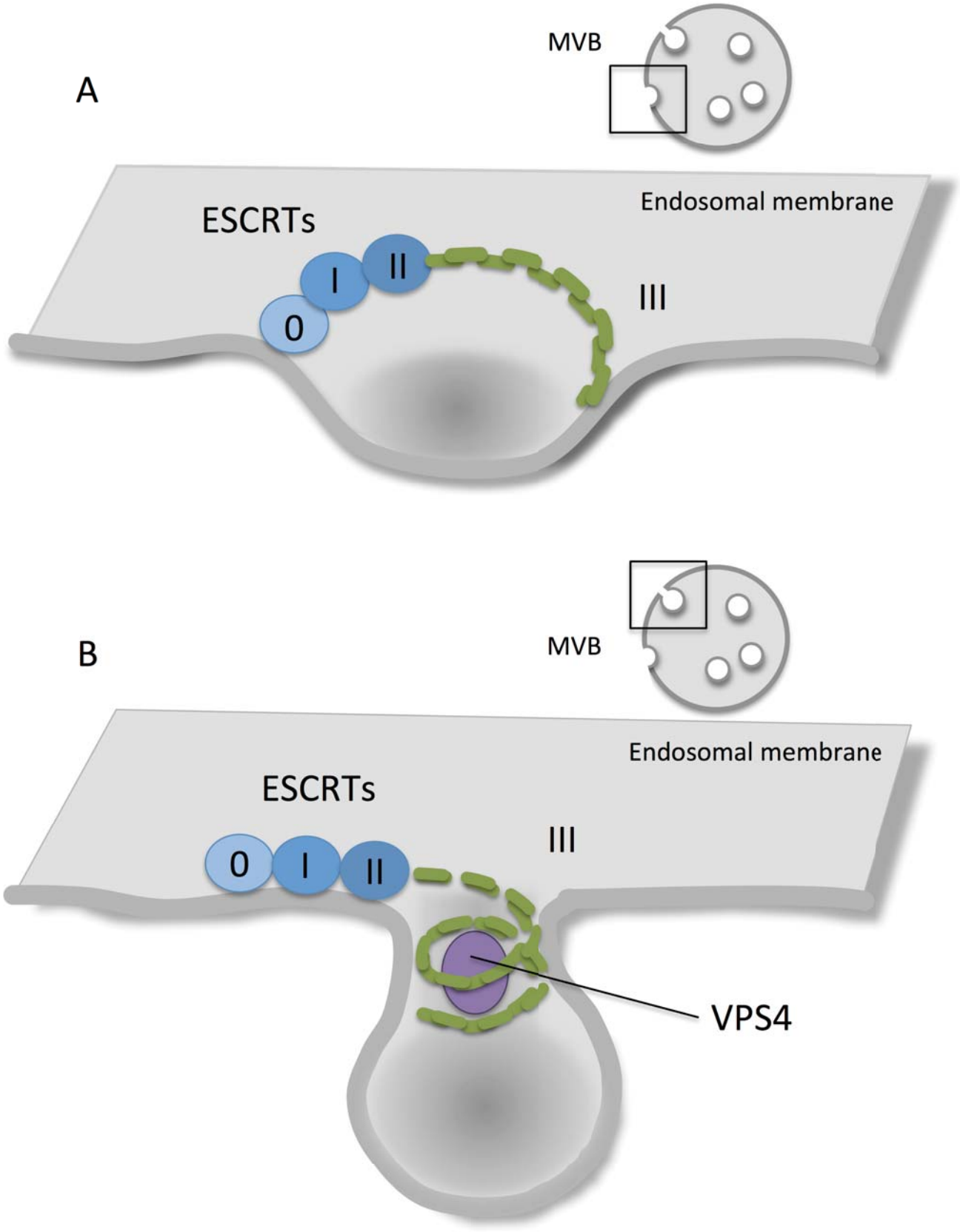
A
MVB
Endosomal membrane
ESCRTs
0
I
II
III
B
MVB
Endosomal membrane
ESCRTs
0
I
II
III
VPS4

Classically, MVBs go on to fuse with a lysosome to degrade the ILVs and their cargo. However studies are starting to reveal that some MVBs can instead be re-directed to the plasma membrane for release of ILVs as exosomes in the extracellular space (31). The mechanisms regulating this process have been discovered. For example, Rabs, monomeric GTPases and members of the Ras superfamily, have been shown to be important for promoting the association of MVBs with the plasma membrane. Rab GTPases are best known for their roles in directing the localization of membrane-bound organelles and for intracellular vesicle transport (74). Recently, Rab27a and Rab27b were shown to be necessary for the proper targeting of the MVB to the plasma membrane, both being required for the secretion of exosomes by HeLa cervical carcinoma cells (75). Moreover, the ectopic expression of a dominant-negative form of Rab35 in HeLa cells led to the accumulation of intracellular endosomal vesicles and impaired exosome secretion. The GTP-bound form of Rab35 was found to localize to the plasma membrane, suggesting that it can play a role in MVB docking or tethering to the plasma membrane (76). Yet, another study found that Rab11 regulates MVB targeting to the plasma membrane, culminating in a calcium-dependent fusion event (77). Overall, the release of exosomes is a highly regulated process that can occur in most cell types.

Apoptotic bodies

Apoptotic bodies are the largest class of vesicles, ranging from 2-10μm in diameter and are formed by cells undergoing programmed cell death (28, 78). The defining differences between apoptotic bodies and other types of EVs (exosomes and MVs) are that their cargo is non-specifically sorted into them and apoptotic bodies can contain entire organelles (78, 79). The formation of apoptotic bodies is thought to help break down dying cells into fragments that can

be more efficiently phagocytosed by macrophages, while avoiding rupturing the cell and releasing immunostimulatory molecules, as occurs in necrotic cells (80). This prevents the exposure of "self" proteins and DNA to immune cells, protecting against the initiation of an auto-immune response (81, 82).

Isolation of MVs and exosomes

The challenging questions in the field of EVs regarding the differences between MVs and exosomes in different biological processes are made even more difficult due to the lack of standardized nomenclature and isolation procedures for EVs. It is becoming increasingly clear that some laboratories are isolating MVs but calling them exosomes and vise versa. Other groups are simply isolating both MVs and exosomes together (referred to as "batch preparations"). This has lead to confusion and without standardizing the nomenclature and isolation procedures, advances in the field are impeded. Our laboratory has adopted the most widely accepted approach for distinguishing the different classes of vesicles, specifically, that microvesicles are larger and bud directly from the plasma membrane, while exosomes are smaller and are formed from a re-routing of the endosomal pathway. One of the areas being developed that will certainly help eliminate these concerns is the identification of markers for the different classes of EVs.

Several approaches for collecting EVs from cell culture media have been developed including those involving precipitation, membrane filtration, gel filtration, differential ultracentrifugation, and affinity purification (28, 83-86). There are benefits and drawbacks for each approach. For example, the precipitation-based method results in the non-specific aggregation of all vesicles and macromolecular structures, and although it is a relatively easy procedure to carry out, the vesicles they isolate have been shown to be less bioactive, and have

different particle sizes, compared to other EV isolation procedures (87). Gel filtration, also known as size exclusion chromatography has been effectively used for the purification of nucleic acids, proteins, peptides, and lipids by passing samples through a column of porous beads. However, EVs and high-density lipoproteins (HDL) have a similar density and were found to co-isolate, and further studies are required to determine the effects of bead type and buffer composition for the fractionation of EVs using gel filtration (88). Differential centrifugation is the most prevalent method of isolating EVs. Generally it involves a low-speed centrifugation step (300xg for 5-30 minutes) to remove cells and cellular debris, a high-speed centrifugation (10,000-20,000xg for 30 minutes), and finally an ultracentrifugation step (100,000xg for 1-18 hours) (89). It was determined that longer spin times in the ultracentrifugation step led to greater yields of EVs, however, it also caused the aggregation of vesicles, decreasing their functionality in biological assays. Additionally, the vesicle populations in the 10,000xg and 100,000xg fractions were found to be heterogeneous in size and vary significantly depending on the type of rotor, centrifuge tube, and centrifuge model (83, 89).

A method for separating vesicles by size involves the use of membrane filters with successively smaller pore sizes, resulting in a population of vesicles with improved size homogeneity while avoiding high g-forces and precipitants that may be present with the use of other methods (83). Limitations of the membrane filter method include clogging of the filter, potentially disrupting the vesicles due to sheer force, and the possibility for different forms of vesicles to be of a similar size, however, this limitations can be overcome by proper sample handling techniques.

For the purposes of separating out different fractions of EVs from a homogeneous cell population, our laboratory developed an approach that combines differential centrifugation and

membrane filtration (Figure 1.5) (90). Cell culture supernatant, also known as conditioned media, was collected from serum starved cells and subjected to two consecutive centrifugations at 300×g to clarify the media of cells and large cellular debris. Due to the presence of EVs in the media supplemented with fetal bovine serum (FBS), it is vital to use serum depleted of EVs, or preferably to use serum-free media for EV collection, when possible (91).

The partially clarified media was filtered using a Steriflip PVDF filter with a 0.22 μm pore size and extensively rinsed to remove soluble factors with special care taken to avoid clogging the filter, or subjecting the vesicles to physical stress. The EVs retained by the filter are considered MVs, as they represent EVs that are 200 nM and larger. The larger EVs retained by the filter could be resuspended in medium for use in cell-based (biological) assays, or lysed directly off the filter membrane to generate MV lysates. Exosomes were isolated from the conditioned medium that flowed-through the 0.22 μm Steriflip filter (i.e. vesicles smaller than 220 nm) by centrifugation at 100,000xg for 2 hours, or alternatively, they were collected from the flow-though using a filter with a 100,000 kDa size cut-off. EV fractions were then confirmed using nanoparticle tracking analysis (NTA) to determine the sizes and amount of EVs in a given preparation, as well as Western blot analysis with EV-specific markers. This method has been used to reliably separate exosomes and MVs by size, while removing cells, debris, and apoptotic bodies.

To follow the fate of the isolated EVs and demonstrate the transfer of EV cargo to the cytoplasm of a donor cell, several biochemical assays have been developed. A chemical compound such as a carboxyfluorescein succinimidyl ester (CFSE) or 5(6)-carboxyfluorescein diacetate (CFDA) can be incorporated into EVs. EVs containing these chemical compounds are then added to the culture medium of recipient cells. If the CFSE or CFDA is transferred to the

Figure 1.5. Isolation procedure for exosomes and MVs
Serum-free culturing medium is collected from cells and then centrifuged at low speeds to remove cells and large cellular debris. The partially clarified medium is then passed through a 220 μm filter. The larger class of EVs, known as MVs, are retained on top of the filter. The smaller exosomes that passed through the filter can be collected from the flow through by a high-speed centrifugation step, or by collecting the exosomes retained by a 100,000 kDa cut-off filter.

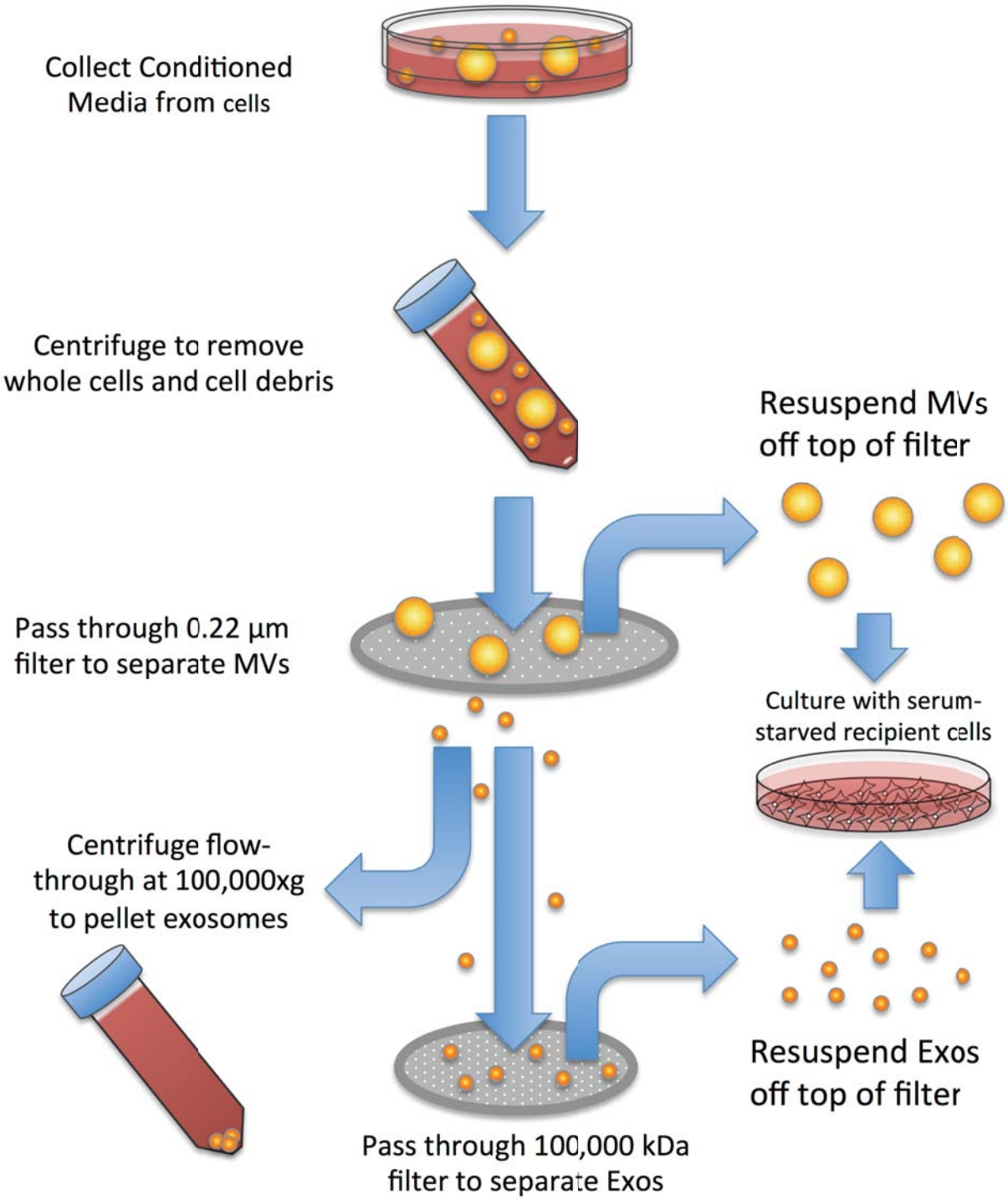
Collect Conditioned Media from cells
Centrifuge to remove whole cells and cell debris
Pass through 0.22 µm filter to separate MVs
Resuspend MVs off top of filter
Culture with serum-starved recipient cells
Centrifuge flow-through at 100,000xg to pellet exosomes
Pass through 100,000 kDa filter to separate Exos
Resuspend Exos off top of filter

recipient cell, the cell will fluoresce due to the esterification of the chemical compounds. This makes it possible to distinguish between EVs that fuse with the recipient cell to transfer cargo, and EVs that dock on the surface of the recipient cell without fusing (92, 93).

EV cargo

The importance of EVs for diagnostic purposes, and for their ability to perform diverse biological functions, is dependent on the cargo they contain. The contents of EVs are often representative of their cell of origin and includes cell surface receptor tyrosine kinases, cytosolic signaling proteins, metabolic proteins, metalloproteases (MMPs), nuclear proteins, messenger RNA transcripts, micro-RNAs, and cytoskeletal components (16, 19, 33, 94-99). A great effort is being made to catalog the various protein, lipid, and nucleic acid content of EVs in order to identify markers that can be used to identify each class of EV (i.e. MV versus exosome), as well as EVs shed by diseased cells (Figure 1.6). Although there have been challenges in demonstrating cargo specificity between different classes of EVs, there is evidence of cargo found preferentially expressed in one class of EV over the other (8).

RNA as EV cargo

Perhaps the most investigated types of EV cargo are RNA transcripts and miRNAs, which are sometimes referred to as exRNAs or evRNAs. RNA can be isolated from EVs from nearly all tested biofluids, and have garnered great interest due to their ability to alter protein expression in recipient cells, and for their potential use in the clinics as biomarkers for disease, and even as potential therapeutic agents (100, 101).

Figure 1.6. Cargo in Extracellular Vesicles
A list of cargoes in common to all EVs, as well as those that are specific to either exosomes or MVs.

Exo-enriched cargo:	Shared cargo:	MV-enriched cargo:
CD-63	flotillin	FAK
CD-81	tissue transglutaminase	Ran GTPase
Survivin	cytoskeletal proteins	EGFR
	actin	
	microRNA	
	mRNA	
	DNA	

Mechanisms that target certain RNA species to EVs have been uncovered by comparing the mRNAs expressed by cancer cells and the EVs that these cells generate. It was found that many mRNAs are highly enriched in EVs compared to their levels in the cells, indicating that the trafficking of mRNAs into EVs is a highly regulated process (16, 20). For example, a landmark study in the EV field focused on identifying the most abundant mRNA transcripts in MVs shed by glioblastoma cells (16). The most abundant mRNAs detected belonged in ontologies related to tumor growth, including angiogenesis, cell proliferation, and cell migration. The authors went on to show that mRNAs delivered to recipient cells via MVs could be translated and generate a functional protein using a luciferase reporter sequence. The researchers demonstrated that tumor-specific RNA sequences, such as epidermal growth factor receptor variant type III (EGFRvIII), were found in MVs collected from the serum of glioblastoma patients, highlighting the potential for mRNA sequences such as EGFRvIII to be used as biomarkers.

A large effort is being made to identify specific sequences contained within the RNA transcripts that are important for targeting them to EVs. In fact, studies have identified specific cis-acting RNA elements common to at least some of the mRNAs detected in EVs (102). These ~25 nucleotide length sequences are sometimes referred to as “zip code”-like sequences, and are found in the 3’-untranslated region (3’UTR). When these “zip codes” were incorporated into the 3’UTR of a reporter mRNA, the levels of the receptor RNA detected in the EVs derived from the cells were increased (103). More importantly, mRNA cargo delivered by EVs can be translated into their corresponding proteins by the recipient cell, a process that is inhibited by heat inactivation or prolonged RNAse treatment of the EVs before culturing them with recipient cells (98).

The miRNA content of EVs is a prominent component of secreted RNAs and can strongly influence the phenotype of recipient cells by altering gene expression (20, 104). The precise mechanism by which miRNAs are selectively trafficked into EVs has yet to be confirmed. However, several recent findings have suggested that proteins that bind to miRNAs might be important for their recruitment to exosomes (105). A good example of this involves Argonaute 2 (Ago2), a component of the RNA-induced silencing complex (RISC). Ago2 is an essential component of the miRNA-mediated degradation of mRNA and has been detected in extracellular vesicles, specifically exosomes, while in complex with miRNA (106, 107). Ago2 associates with MVBs during the formation of intraluminal vesicles and aids in the sorting of miRNA into the endosome (108). Over activation of KRAS in cancer cells has been shown to increase Ago2 activation, altering the miRNA content of exosomes (97, 109, 110). Mutant KRAS was shown to act through MEK I/II by phosphorylating Ago2 on S387 to inhibit the association of Ago2-miRNA complexes with MVBs, and altering the miRNA content of exosomes (109).

Interestingly, RNA species found to be enriched in EVs relative to cellular RNA includes a large variety of small non-coding RNA species, long non-coding RNA, repeat sequences, structural RNAs, transfer RNA (tRNA), and Y-RNA (bound to ribonuclear complexes) (95). The enrichment of non-coding RNA in EVs introduces a wider range of biological effects that could be mediated by EV RNA than just transferring messages.

MV protein cargo sorting

Despite the advancements in our understanding of MV biogenesis, and how they contribute to various biological processes and disease states, there are still several major

questions regarding how MVs are loaded with cargo. There are a few cases where this question is starting to be addressed. For example, it has been demonstrated that for amoeboid-like invasive tumor cell lines, v-SNARE-vesicle associated membrane protein (VAMP3), potentially regulates the loading of cargo into MVs (111). VAMP3 is a SNARE protein known to play a role in intracellular membrane fusion and the subcellular localization of proteins such as matrix metalloproteases (MMPs), proteins critical for remodeling the extracellular matrix (112, 113). VAMP3 and a specific MMP known as MT1-MMP co-localize at sites of active MV formation, and can be detected in shed MVs. However, when VAMP3 is depleted from an invasive melanoma cell line, LOX, by shRNA, MT1-MMP is no longer detected at sites of MV formation, nor is it detected in the MVs that the cells release (111). Decreasing VAMP3 expression and subsequent loss of MT1-MMP as MV cargo, decreased the efficiency with which cells are able to migrate through the extracellular matrix. Interestingly, MVs isolated from ovarian cancer patients also contained VAMP3 and MT1-MMP, and were capable of matrix degradation. Thus, the inclusion of MMP in MVs generated by cancer cells appears to play an important role in their ability to migrate and invade through the tumor microenvironment.

Exosome protein cargo sorting

Incorporation of protein cargo into ESCRT-dependent exosomes is a slightly better understood event, and several of the complexes involved in the formation of exosomes are also involved in incorporating cargo. Classically, ubiquitylation of membrane proteins triggers their sorting into ILVs by binding to the ESCRT-0, I, and II complexes, which have several distinct ubiquitin-binding motifs (67, 114, 115). An additional mechanism involves the ESCRT-III adaptor protein Alix binding to the C terminus of Snf7; and loss of Alix affects cargo sorting

(116). Alix has also been shown to interact with syndecans and syntenin to segretate exosome cargo into ILVs; specifically, syntenin overexpression stimulated exosomal release of FGFRs (117).

Certain protein modifications can influence the localization of proteins to exosomes. Adding a membrane-targeting 10-amino acid acyl tag to the N-terminus of the yeast cytoplasmic protein TyA-GFP, targeted it to endosome-like domains of the plasma membrane and resulted in its efficient incorporation into endosomes (118). This also resulted in its enrichment in the exosomes secreted by these cells. A subset of early endosomes are thought to originate in lipid raft domains, areas of the plasma membrane enriched with cholesterol and glycosylphosphatidylinositol (GPI)-anchored proteins (119). Proteins with a GPI tag such as CD55 and CD59 are enriched within exosomes, and adding a GPI tag to proteins that do not normally have one increased their localization to exosomes (120).

Although addition of a membrane-targeting domain has been shown to increase the localization of proteins to exosomes, our laboratory and others have shown that many proteins lacking these membrane-targeting modifications can also be found in exosomes. For example, the small anti-apoptotic protein survivin is primarily expressed in the nucleus and mitochondria. However, exposing cancer cells to various stresses, for example, non-lethal doses of ionizing radiation, can lead to an increase in the levels of survivin detected in exosomes generated by the cells (121, 122). Additionally, I have discovered that the disruption of microtubule dynamics using the chemotherapeutic drugs nocodazole or paclitaxel leads to a significant enrichment of survivin in exosomes without changing the total survivin detected within the cells.

EVs interacting with recipient cells

Several different mechanisms have been suggested for how EVs interact with recipient cell including juxtacrine signaling, endocytosis, phagocytosis, or direct membrane fusion (Figure 1.7) (7, 123). This transfer event can be observed by labeling EVs with a fluorescent lipid membrane dye and detecting the fluorescent signal being distributed throughout the plasma membrane of a cell treated with labeled EVs (124). Many studies have shown that there is either a direct fusion of the EV membrane with the plasma membrane of the recipient cell, or that the EV is endocytosed and the EV fuses with the endosomal membrane to deposit cargo into the cytoplasm of the recipient cell (92).

The majority of experimental evidence suggests that EVs are taken up by cells via endocytosis and enclosed within endosomal compartments (125, 126). This is thought to be an active process, since it can be nearly entirely blocked if the recipient cells are incubated at 4°C, fixed with paraformaldehyde, or treated with Cytochalasin D to depolymerize actin filaments and inhibit endocytic pathways (127, 128). One form of endocytosis involves clathrin-coated vesicles. Clathrin is able to deform the membrane into a bud to form an intracellular vesicle which undergoes subsequent clathrin un-coating before fusing with the endosome and depositing its contents into the cytoplasm of the recipient cell (129). Clathrin-mediated endocytosis can be inhibited by treating cells with chlorpromazine, and a study has shown that treating ovarian cancer cells with this inhibitor reduces their ability to take up EVs (130, 131). Another form of endocytosis involves the formation of caveolae, cave-like pits on areas of the plasma membrane rich in cholesterol (132). Some studies suggest that caveolae inhibition will impair a cell's ability to uptake EVs; however, additional studies have shown that mouse embryonic fibroblasts

Figure 1.7. The mechanisms through which EVs are transferred to recipient cells.
(A) EVs fuse directly with the plasma membrane to transfer cargo to recipient cells, including mRNA sequences that can be translated into protein by the recipient cell. (B) EVs can be endocytosed by a recipient cell, and the EV can subsequently fuse with the endosomal membrane to release its cargo into the cytoplasm. (C) Contact-dependent signaling can occur when the EV presents ligands on is membrane that interact with receptors on the surface of the recipient cell.

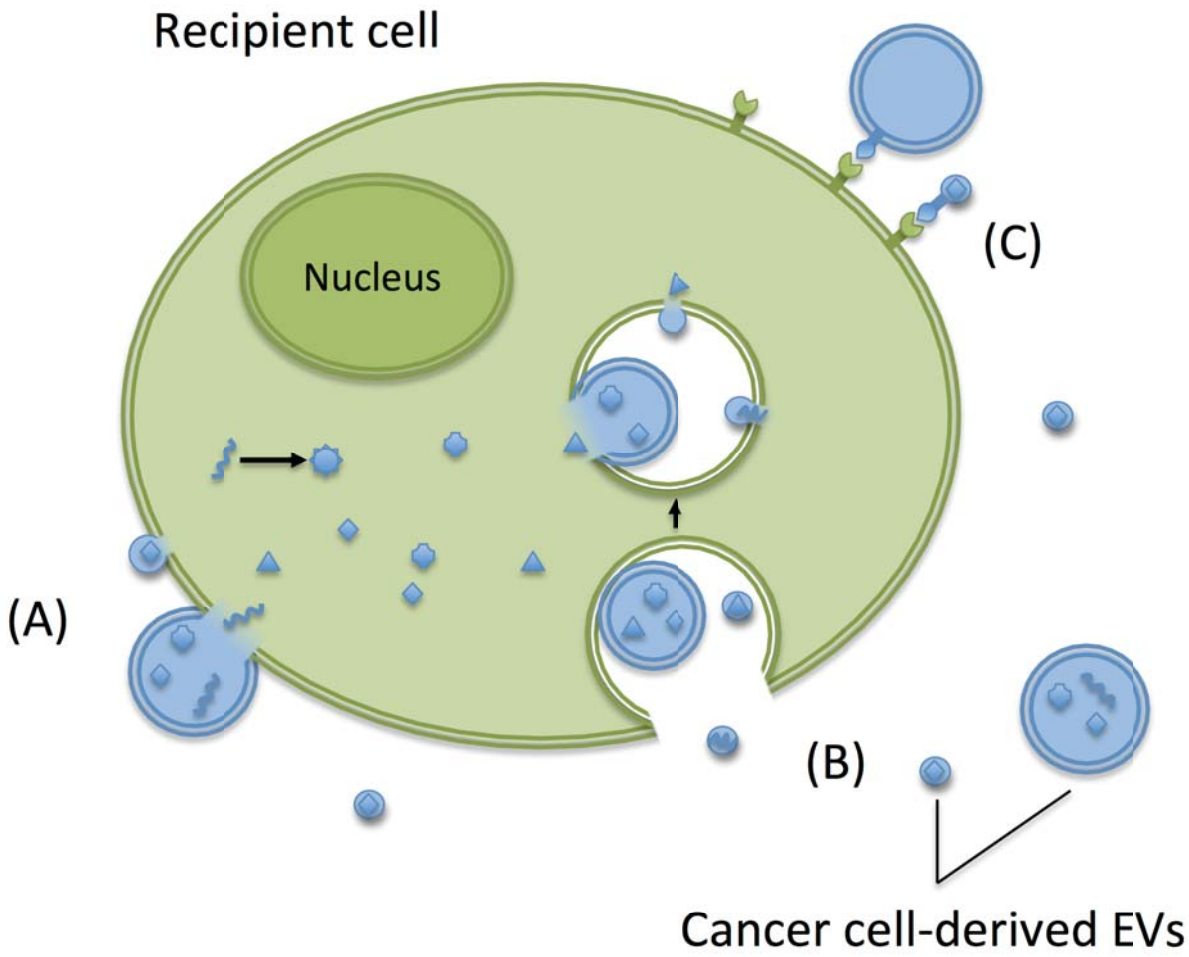
Recipient cell
Nucleus
(A)
(B)
(C)
Cancer cell-derived EVs

derived from CAV1 knock out animals lead to an increase in EV uptake, suggesting that different cell types may use distinct mechanisms to uptake EVs (126).

Another form of endocytosis is macropinocytosis and involves the formation of membrane ruffles that invaginate to internalize an area of extracellular fluid (132, 133). The GTPase Rac1 is a major regulator of macropinocytosis, however, actin and cholesterol are also required for this process to occur (134). It is generally thought that macropinocytosis is stimulated by the activation of phosphatidylinositol-3-kinase (PI3K), Ras, and c-Src activity (124, 132). Macropinocytosis does not require direct interaction between the plasma membrane and the internalized material (i.e. EVs); however, phagocytosis is a receptor-mediated internalization of material from the extracellular environment (132, 133, 135). Macrophages are well known for their ability to phagocytose, and frequently utilize this process to internalize larger particles. However, small exosomes derived from leukemia cells have been reported to be phagocytosed by macrophages in an actin- and PI3K-dependent mechanism (135). Interaction with EVs at the cell surface is necessary for their phagocytosis as proteinase K treatment of EVs significantly reduces their uptake (131).

The presentation of phosphatidylserine (PS) on the outer leaflet of EV membranes also plays a role in their uptake, especially by phagocytosis (136). A highly metastatic melanoma cell line, B16F10, produces large quantities of MVs with PS on their outer membrane. These MVs were found to be extremely potent in enhancing the metastatic potential of cells injected in mice, a phenomenon reversed by treating the EVs with annexin V (52). Annexin V is a phospholipid binding protein that specifically binds to PS. Thus, pretreatment of MVs with annexin V prevents a recipient cell from binding to PS on the EV membranes and triggering endocytosis of the EVs.

As a result of this finding, annexin V has become commonly used as a way to block EV uptake by recipient cells (19, 125, 135).

It is also possible for EVs to influence recipient cells without requiring internalization of the vesicles. Multiple studies have found that proteins expressed on the surface of EVs are sufficient to bind to receptors expressed on the recipient cells and activate signaling events. For example, exosomes shed by the cells making up the outer layer of a blastocyst-stage embryo called trophoblasts, can induce synthesis of pro-inflammatory cytokines by macrophages. Importantly, these effects were not blocked by inhibitors that prevented EV uptake (e.g. annexin V), suggesting the internalization of the exosomes was not required to influence the recipient cell. However the exosome-dependent signals were blocked by using an RGD peptide, which specifically inhibits the ability of the extracellular matrix protein fibronectin to function as a ligand and interact with and activate α5β1 integrin receptors expressed on the recipient macrophage. This signifies that the exosome docking at the plasma membrane of the recipient cell was sufficient to induce changes within the macrophage (137). Another study performed in our laboratory found that MVs shed by mouse embryonic stem (ES) cells were coated with both fibronectin and laminin, which binds to the integrins and laminin receptors on the surface of trophoblasts. These interactions activate JNK and FAK signaling in the trophoblast and promote their ability to migrate, an essential step for embryo implantation (90).

Another study from our laboratory highlighted the importance of MV-associated fibronectin in the context of cancer progression (94). MVs derived from the highly aggressive MDAMB-231 breast cancer cells and U87 glioma cells were shown to be capable of transiently transforming normal (non-transformed) fibroblasts due to the MV cargo tissue transglutaminase (tTG), a protein crosslinking enzyme, and fibronectin. The study found that tTG cross-links

fibronectin located on the surface of MVs. The cross-linked form of fibronectin was then able to engage integrins on recipient cells and strongly induce signaling events (i.e. activate JNK, PI3K, and ERK) that impacted their function.

EVs and tumor progression

Tumor initiation and progression requires continuous communication between cancer cells and the cells within the local microenvironment (138). EVs are now recognized as an important mediator of this cross-talk (139). Specifically, EVs derived from highly aggressive forms of cancer cells have been shown to activate fibroblasts, stimulate tumor angiogenesis, alter immune responses, and aid in the development of a pre-metastatic niche (Figure 1.8) (94, 140, 141).

The effects of EVs on cell growth and survival

As mentioned previously, the EV-mediated transfer of RNA species between cells has been demonstrated to play a major role in changing the behavior of recipient cells (16). In order to understand the ability of EVs derived from primary glioblastoma cell lines to manipulate surrounding cells, one study focused on the most abundant miRNA identified in EVs, miR-21 (142). Incubating mouse microglia cells with EVs derived from these glioblastoma cell lines alters the cytokine production to promote the growth and survival of the cancer cells. The researchers demonstrated the EV-dependent transfer of miR-21 from glioblastoma cells to recipient microglia cells. miR-21 has been shown to play a role in regulating cell survival, and in fact, there was a 40% increase in cell viability over the course of 7 days when microglia cells were incubated with EVs derived from glioblastoma cells.

Figure 1.8. Extracellular vesicles in the tumor microenvironment.
EVs shed by cancer cells can contribute to the propagation of the tumor phenotype in many ways including: chemotherapy resistance, cell proliferation, migration, recruitment of endothelial cells for blood vessel formation, cell survival, and establishment of a pre-metastatic niche.

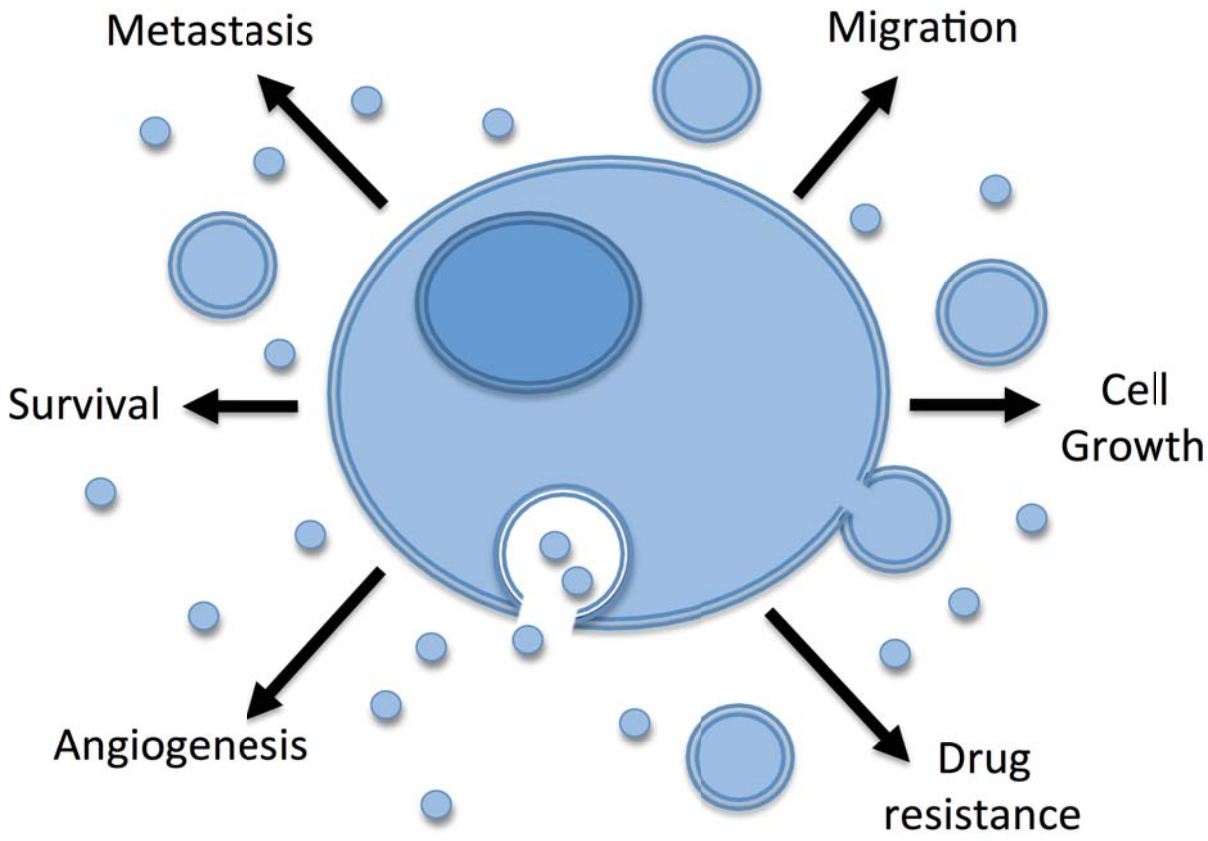
Metastasis
Migration
Survival
Cell
Growth
Angiogenesis
Drug
resistance

One of the original studies linking EVs to cancer progression investigated how EVs propagate the oncogenic phenotype exhibited by highly aggressive human brain tumors known as gliomas (19). These tumors were shown to shed EVs that contain a highly oncogenic form of the epidermal growth factor receptor (EGFR) called EGFR variant III (EGFRvIII). This mutant form of the receptor arises from an in-frame deletion event and activates signaling events (i.e. activation of ERK and PI3K) that simulate cell growth and survival.

EGFRvIII is only expressed in a low number of cells within a glioma tumor (143). However the influence of the mutant receptor within the tumor is pervasive, suggesting that EGFRvIII is shared between glioma cells by intercellular transfer via EVs. The researchers observed that when the glioma cell line U373 stably expressed EGFRvIII, these cells shed more EVs, and these EVs contained EGFRvIII. This may be because oncogenic receptors tend to localize within specific regions of the plasma membrane, like lipid rafts, from which MVs have been suggested to originate from (56). When injected into nude mice, the EGFRvIII expressing cells were readily able to form tumors unlike the parental control cells. Additionally the blood serum collected from EGFRvIII tumor-bearing mice contained vesicles that could be isolated and were found to contain the EGFRvIII mutant receptor, demonstrating the systemic release of EVs from a tumor.

The consequences of transferring MVs derived from EGFRvIII-expressing glioma cells to recipient parental U373 cells were examined (19). First, a GFP-tagged version of EGFRvIII was expressed in the donor cells to demonstrate the uptake of GFP-EGFRvIII-positive EVs by recipient cells. Indeed, the resulting fluorescent images taken of the cells treated with these EVs showed that the fluorescent signal could be detected along the plasma membrane of the recipient cells. The EV-mediated transfer of the EGFRvIII to the recipient glioma cells stimulated Erk1/2

and Akt activation and these signals could be blocked by treating the EVs with an EGFR inhibitor, or with annexin V to block EV uptake. The presence of EGFRvIII ultimately resulted in tumor growth and survival.

EVs and tumor angiogenesis

Tumor progression requires the recruitment and formation of new blood vessels for the tumor mass to grow beyond the diffusion limit of the existing vasculature. A potent mediator of angiogenesis is the vascular endothelial growth factor (VEGF). When VEGF is secreted it is recognized by VEGF receptors on vascular endothelial cells and leads to their activation for the formation of new blood vessels. As mentioned previously, there is an oncogenic form of the EGFR called EGFRvIII, and expression of this mutant receptor can lead to the increased secretion of vascular endothelial growth factor (VEGF) (144). In fact, when endothelial cells were cultured with EVs derived from EGFRvIII-expressing cells, the recipient cells exhibited a marked increase in the production of VEGF for the autocrine activation of angiogenesis (15).

Hypoxia is known to be a trigger for angiogenesis within a tumor microenvironment and one study found that hypoxia was sufficient to alter the cargo of EVs derived from an aggressive glioblastoma (GBM) brain tumor to a pro-angiogenic state (145). GBM cells grown in a hypoxic environment generate EVs that are enriched with factors related to tumor development including adrenomedullin (ADM), lysyl oxidase (LOX), IGF binding protein (IGFPB) 3, inhibitor of DNA binding 2, B-cell lymphoma (BCL)2/adenovirus E18 19-kDa interacting protein 3 (BNIP3), N-myelocytomatosis viral related oncogene (myc) downstream regulated 1 (NDRG1), procollagen-lysine 2-oxoglutarate 5-dioxygenase 2 (PLOD2), and plasminogen activator inhibitor-1 (PAI1). Endothelial cells readily take up GBM EVs, and when hypoxic GBM EVs were compared to

EVs isolated from GBM cells grown in normoxic conditions, they were more potent at inducing microvascular sprouting, and are able to induce tubulogenesis *in vitro*. To examine the differences *in vivo*, EVs derived from normoxic and hypoxic GBMs were injected in a mouse tumor xenograft model. Interestingly, after the tumors were grown for 5 weeks, there was a substantial increase in tumor vascularization and almost three-fold increase in tumor volume.

Migration

Tumor cell migration and invasion require a unique interaction between the cell and the microenvironment, and is essential for tumor cell dissemination and metastasis (146). The role of EVs in reshaping the tumor microenvironment in ways that promote migration and invasion have been attracting more and more attention (33, 53, 58, 147, 148).

As mentioned previously in this chapter, Arf6 can regulate the shedding (release) of the class of EVs known as MVs from cells. In this same study, the authors also found that these vesicles played a key role in the cancer cell's ability to degrade extracellular matrix and for generating paths for the cancer cells to migrate and invade (33). These MVs are dependent on RhoA activity and are selectively enriched with cargo that promotes invasive activities, including matrix metalloproteases (MMPs) that efficiently deform less rigid environments. The MV-mediated release of MMPs, such as MMP-2, and MMP-9 has been shown to be a critical event in migration and invasion, leading to higher rates of angiogenesis and metastasis (33, 44, 149).

The class of EVs known as exosomes has also been implicated in the directional migration of cancer cells. It had been shown previously that exosomes play a role in cell invasion and migration where detachment of adherent cells would induce a rapid release of exosomes that mediate adhesion to extracellular matrix proteins (150). A role for exosomes in the directional

migration of cancer cells *in vivo* has also recently been shown (151). Fluorescently labeled HT1080 fibrosarcoma cells were injected into chick embryos, which rapidly formed tumors that exhibited a significant amount of invasive activity. HT1080 cells were then treated with short hairpin RNAs (shRNAs) that specifically targeted synaptotagmin-7 (Syt7) or Rab27a, two proteins that regulate the fusion event between MVBs and the plasma membrane. Thus, the down regulation of Syt7 and Rab27a expression significantly impaired the ability of these cancer cells to shed exosomes. When HT1080 cells depleted of Syt7 and Rab27a were injected into chick embryos, they again formed tumors, similar to the control cells. However, these cells had significantly shorter invasive fronts, revealing that fewer cells had migrated away from the tumor compared to control cells. Time-lapse images collected from injected control HT1080 cells showed that they exhibited directional cell migration (i.e. away from the tumor). On the other hand, those HT1080 cells incapable of generating exosomes frequently stop and change direction, as well as move more slowly.

To investigate this phenomenon further, exosomes from the cancer cells were purified and then either added directly to the culture media, or were used to coat the surface of the dish. In both situations, migration of control HT1080 cells was increased further, however, the migration defect in the Rab27a-knock down cells was rescued only when the exosomes were coated to the surface of the culture plates. This suggests that the cells require exosomes at the site of adhesion formation in order to migrate properly through the matrix. Due to the fact that fibronectin was identified as a major exosomal cargo and is involved in the interaction between the cell and the extracellular matrix (137, 152, 153), the researchers went on to determine if fibronectin is involved in the observed exosome-mediated migratory effect. Tissue culture dishes were coated with either purified exosomes, or purified fibronectin, and both conditions were

sufficient to rescue the motility speed defect of Hrs-knock down HT1080 cells. To visualize exosomes in migrating cells, HT1080 cells expressing fluorescently-tagged forms of CD63 (an exosome marker) and paxillin (focal adhesion marker) were imaged by video microscopy. Interestingly, CD63 positive "trails" were seen behind migrating cells, and these deposits preceded adhesion formation. These exosomes present in the extracellular matrix are thought to act as pro-migratory tracks for the regulation of directional movement. In fact, recent studies in neutrophils have found that exosome trails laid down in the extracellular matrix also contain chemoattractants that lead to an increase in migration persistence and directionality while also recruiting neighboring neutrophils (154).

Metastasis

Most cancer fatalities occur when the primary tumor spreads or metastasizes to other sites in the body. The influence of EVs on the prerequisites for metastasis, including tumor angiogenesis and increased cancer cell migration, has already been discussed. However, EVs can also directly participate in establishing a secondary site of tumor growth (5, 29, 53). There have been multiple reports highlighting how EVs promote metastatic spread by contributing to the formation of the pre-metastatic niche, a specialized microenvironment that is established at a distant site and increases the chances that cancer cell will settle and grow at this site (155).

To investigate the role of EVs in metastasis, EVs derived from melanoma cells were injected into the tail vein of a mouse, tracked through the lymphatic system and were found to accumulate in the lymph nodes (156). The tumor-derived vesicles were more likely to localize to lymph nodes and recruit melanoma cells due to their pro-metastatic cargo including integrin αv, MAPK and TNF-α (157, 158). Using a similar melanoma model, it was shown that fluorescently

labeled exosomes derived from the highly malignant B16-F10 melanoma cell line could be detected throughout the blood stream of the animal within 5 minutes of being injected. Within 24 hours of injection, the exosomes were localized to the lungs, bone marrow, liver, and spleen of the mice (common sites of melanoma metastasis), but were no longer detected in the circulation (159). Gene expression profiling of lung tissue after a tail vein injection of EVs revealed 130 differentially expressed genes, many related to extracellular matrix remodeling, and heat-shock proteins *S100a8* and *S100a9*, which have been implicated in the formation of the pre-metastatic niche (160).

The metastatic effects of EVs derived from a subpopulation of human renal cell carcinomas were also studied (161). This cell line was shown to be a subset of cells with tumor-initiating properties expressing the mesenchymal stem cell marker CD105 (162). EVs collected from renal cancer cells sorted for CD105 were able to stimulate angiogenesis, apoptosis resistance, and the invasion of endothelial cells significantly more than CD105- renal cancer EVs. The EVs were then shown to play a role in priming the metastatic site. EVs were intravenously injected into mice for 5 days in a row, and on the sixth day, renal tumor cells were injected. Five weeks later, the liver, spleen, kidney, and lungs of the mice were recovered and analyzed for tumor formation. Metastases were detected only in the lungs isolated from mice injected with CD105+ EVs, while the mice injected with EV vehicle alone, with CD105- EVs, or with RNase-treated CD105+ EVs, lacked detectable metastases. The CD105+ EVs were shown to contain mRNA species for VEGFR1, VEGF, MMP9, and MMP2, and these EVs were capable of increasing expression of these proteins in lung endothelial cells. VEGF is a signaling factor that stimulates angiogenesis, while MMP proteins alter cell-cell and cell-extracellular matrix interactions necessary for recruiting of endothelial cells and establishing vasculature (163, 164).

The idea that tumor-derived EVs can promote metastasis has recently been expanded to the notion that these EVs can predict metastasis. Tumor-derived exosomes have been shown to localize to specific sites of organotropic metastasis, dependent on the type of primary tumor (140, 159, 165). To determine if exosomal cargo was helping direct organ specificity, proteomics were performed on exosomes derived from several different tumor models that are known to metastasize to specific sites (166). The study revealed that specific integrins expressed on tumor-derived exosomes, distinct from the tumor cell of origin, determined where the cancer metastasized. For example, exosomes carrying integrin αvβ5 specifically bound to Kupffer cells, mediating liver tropism, however, exosomes with integrin α6β4 and integrin α6β1 bound to lung fibroblasts and epithelial cells, governing lung tropism. Interestingly, the researchers were able to alter the site of metastasis of 1833-BoT, a MDAMB-231 cancer sub-line that metastasizes to the bone marrow by pre-injecting mice with exosomes derived from 4175-LuT, a MDAMB-231 sub-line that was selected for metastasizing to the lung, causing a significant increase in the presence of 1833-BoT metastasis in the lung. The data correlated with the integrin profiles of EVs collected from cancer patients, suggesting plasma-derived EVs could be useful in predicting the metastatic potential of patient tumors.

Chemotherapy resistance

The management of cancer includes surgery, radiotherapy, and chemotherapy. While advancements in patient care have been made, development of chemoresistance is a persistent problem faced by clinicians. The mechanisms behind therapy resistance are numerous and varied and can often be attributed to a small subpopulation of cancer cells that make up a tumor that are

inherently resistant to a given therapy. (167). In order to overcome resistance, a deeper understanding of the different mechanisms involved in drug resistance is needed.

EVs have been shown to contribute to chemotherapy resistance. For example, immunotherapy against the B-lymphocyte plasma membrane protein CD20 in malignant lymphoma has a wide range of responses in patients. It was determined that lymphoma cells were releasing exosomes that carried CD20, and binding the therapeutic anti-CD20 antibodies, decreased the effectiveness of the therapy (168). However, by combining the immunotherapy with pharmacological inhibition of exosome biogenesis targeting the lysosome-related organelle-associated ATP-binding cassette (ABC) transporter A3 (ABCA3), there was a significant increase in the amount of lymphoma cell death.

EVs can also decrease drug efficiency by acting as a mechanism to remove the drug from the cell, as seen in human ovarian carcinoma cells treated with cisplatin (169). The researchers showed that cisplatin-resistance correlated with increased expression of lysosome associated proteins 1 and 2 (LAMP1 and LAMP2) and vesicle trafficking proteins in the resistant cells, and increased levels of cisplatin export transporters in the exosomes. This response led to an increase in the amount of exosomes generated, and a subsequent decrease in the levels of cisplatin within the cells. Another study showed that the rate of EV shedding also correlated with doxorubicin insensitivity in various cancer cell lines (170). Twenty-four hours after treating the cancer cells with fluorescent doxorubicin, the drug went from having a predominantly nuclear localization to being present in extracellular vesicles loosely associated with the plasma membrane. Shed vesicles isolated from conditioned media of treated cells were isolated and shown to contain the labeled drug in as little as 2 hours after treatment.

Concluding remarks

EVs are being aggressively pursued as a diagnostic indicator. EVs collected from the bloodstream of cancer patients are a frequent source, however they have also been studied in the context of other diseases and collected from other biological fluids including urine, saliva, and cerebral spinal fluid (171-174). Considering the prevalence and accessibility of EVs in biological samples, and because EV cargo reflects the cell of origin, there is understandable enthusiasm for the use of EVs for diagnosis and indicators of disease progression. In fact, exosomes have been proposed as a non-invasive screening tool for pancreatic cancer, a disease notorious for being diagnosed in late stages. Glypican-1 was found to be specifically enriched in cancer cell-derived exosomes, and in the serum of patients with pancreatic cancer with high specificity and sensitivity (22). Furthermore, levels of glypican-1 were found to correlate with tumor burden and patient survival.

However, before we can rely on EVs for diagnosis, or take advantage of their dramatic influence of recipient cells, there must be rigorous assessment of EV cargo, and how the cargo correlates with disease progression. In the following chapters, I discuss several EV cargoes such as FAK, a MV cargo specific to oncogenic transformation, and survivin, a cargo specific to exosomes derived from chemotherapy treated cancer cells, and the contributions these EV cargoes make in influencing recipient cells.

REFERENCES

1. Singer, S. J. (1992) Intercellular communication and cell-cell adhesion. *Science*. **255**, 1671–1677

2. Lindsey, S., and Langhans, S. A. (2015) Epidermal growth factor signaling in transformed cells. *Int Rev Cell Mol Biol*. **314**, 1–41

3. Carrasco-Garcia, E., Saceda, M., and Martinez-Lacaci, I. (2014) Role of receptor tyrosine kinases and their ligands in glioblastoma. *Cells*. **3**, 199–235

4. Burdick, M. M., McCarty, O. J., Jadhav, S., and Konstantopoulos, K. (2001) Cell-cell interactions in inflammation and cancer metastasis. *IEEE Eng Med Biol Mag*. **20**, 86–91

5. Vader, P., Breakefield, X. O., and Wood, M. J. (2014) Extracellular vesicles: Emerging targets for cancer therapy. *Trends Mol Med*. **20**, 385–393

6. van der Pol, E., Boing, A. N., Harrison, P., Sturk, A., and Nieuwland, R. (2012) Classification, functions, and clinical relevance of extracellular vesicles. *Pharmacol Rev*. **64**, 676–705

7. Ogorevc, E., Kralj-Iglic, V., and Veranic, P. (2013) The role of extracellular vesicles in phenotypic cancer transformation. *Radiol Oncol*. **47**, 197–205

8. Antonyak, M. A., and Cerione, R. A. (2014) Microvesicles as mediators of intercellular communication in cancer. *Methods Mol Biol*. **1165**, 147–173

9. An, Q., Huckelhoven, R., Kogel, K.-H., and van Bel, A. J. E. (2006) Multivesicular bodies participate in a cell wall-associated defence response in barley leaves attacked by the pathogenic powdery mildew fungus. *Cell Microbiol*. **8**, 1009–1019

10. Biller, S. J., Schubotz, F., Roggensack, S. E., Thompson, A. W., Summons, R. E., and Chisholm, S. W. (2014) Bacterial vesicles in marine ecosystems. *Science*. **343**, 183–186

11. Tetta, C., Ghigo, E., Silengo, L., Deregibus, M. C., and Camussi, G. (2013) Extracellular vesicles as an emerging mechanism of cell-to-cell communication. *Endocrine*. **44**, 11–19

12. Cocucci, E., Racchetti, G., and Meldolesi, J. (2009) Shedding microvesicles: artefacts no more. *Trends Cell Biol*. **19**, 43–51

13. Azmi, A. S., Bao, B., and Sarkar, F. H. (2013) Exosomes in cancer development, metastasis, and drug resistance: a comprehensive review. *Cancer Metastasis Rev*. **32**, 623–642

14. Liu, Y., Zhao, L., Li, D., Yin, Y., Zhang, C.-Y., Li, J., and Zhang, Y. (2013) Microvesicle-delivery miR-150 promotes tumorigenesis by up-regulating VEGF, and the neutralization of miR-150 attenuate tumor development. *Protein Cell*. **4**, 932–941

15. Al-Nedawi, K., Meehan, B., Kerbel, R. S., Allison, A. C., and Rak, J. (2009) Endothelial expression of autocrine VEGF upon the uptake of tumor-derived microvesicles containing oncogenic EGFR. *Proc Natl Acad Sci U S A*. **106**, 3794–3799

16. Skog, J., Wurdinger, T., van Rijn, S., Meijer, D. H., Gainche, L., Sena-Esteves, M., Curry, W. T. J., Carter, B. S., Krichevsky, A. M., and Breakefield, X. O. (2008) Glioblastoma microvesicles transport RNA and proteins that promote tumour growth and provide diagnostic biomarkers. *Nat Cell Biol*. **10**, 1470–1476

17. Rak, J., and Guha, A. (2012) Extracellular vesicles - vehicles that spread cancer genes. *Bioessays*. **34**, 489–497

18. Chen, X., Liang, H., Zhang, J., Zen, K., and Zhang, C.-Y. (2012) Secreted microRNAs: a new form of intercellular communication. *Trends Cell Biol*. **22**, 125–132

19. Al-Nedawi, K., Meehan, B., Micallef, J., Lhotak, V., May, L., Guha, A., and Rak, J. (2008) Intercellular transfer of the oncogenic receptor EGFRvIII by microvesicles derived from tumour cells. *Nat Cell Biol*. **10**, 619–624

20. Valadi, H., Ekstrom, K., Bossios, A., Sjostrand, M., Lee, J. J., and Lotvall, J. O. (2007) Exosome-mediated transfer of mRNAs and microRNAs is a novel mechanism of genetic exchange between cells. *Nat Cell Biol*. **9**, 654–659

21. Taylor, D. D., and Gercel-Taylor, C. (2009) The origin, function, and diagnostic potential of RNA within extracellular vesicles present in human biological fluids. *J Cell Physiol*. **218**, 460–466

22. Melo, S. A., Luecke, L. B., Kahlert, C., Fernandez, A. F., Gammon, S. T., Kaye, J.,

LeBleu, V. S., Mittendorf, E. A., Weitz, J., Rahbari, N., Reissfelder, C., Pilarsky, C., Fraga, M. F., Piwnica-Worms, D., and Kalluri, R. (2015) Glypican-1 identifies cancer exosomes and detects early pancreatic cancer. *Nature*. **523**, 177–182

23. Cocucci, E., and Meldolesi, J. (2011) Ectosomes. *Curr Biol*. **21**, R940–1

24. Di Vizio, D., Kim, J., Hager, M. H., Morello, M., Yang, W., Lafargue, C. J., True, L. D., Rubin, M. A., Adam, R. M., Beroukhim, R., Demichelis, F., and Freeman, M. R. (2009) Oncosome Formation in Prostate Cancer: Association with a Region of Frequent Chromosomal Deletion in Metastatic Disease. *Cancer Res*. **69**, 5601–5609

25. Mezouar, S., Darbousset, R., Dignat-George, F., Panicot-Dubois, L., and Dubois, C. (2015) Inhibition of platelet activation prevents the P-selectin and integrin-dependent accumulation of cancer cell microparticles and reduces tumor growth and metastasis in vivo. *Int J Cancer*. **136**, 462–475

26. Desrochers, L. M., Antonyak, M. A., and Cerione, R. A. (2016) Extracellular Vesicles: Satellites of Information Transfer in Cancer and Stem Cell Biology. *Dev Cell*. **37**, 301–309

27. Raposo, G., and Stoorvogel, W. (2013) Extracellular vesicles: exosomes, microvesicles, and friends. *J Cell Biol*. **200**, 373–383

28. Ihara, T., Yamamoto, T., Sugamata, M., Okumura, H., and Ueno, Y. (1998) The process of ultrastructural changes from nuclei to apoptotic body. *Virchows Arch*. **433**, 443–447

29. Kahlert, C., and Kalluri, R. (2013) Exosomes in tumor microenvironment influence cancer progression and metastasis. *Journal of Molecular Medicine*. **91**, 431–437

30. Morita, E., and Sundquist, W. I. (2004) Retrovirus budding. *Annu Rev Cell Dev Biol*. **20**, 395–425

31. Schmidt, O., and Teis, D. (2012) The ESCRT machinery. *Curr Biol*. **22**, R116–20

32. B Li, MA Antonyak, Zhang, J., and RA Cerione (2012) RhoA triggers a specific signaling pathway that generates transforming microvesicles in cancer cells. *Oncogene*. 10.1038/onc.2011.636

33. Muralidharan-Chari, V., Clancy, J., Plou, C., Romao, M., Chavrier, P., Raposo, G., and D'Souza-Schorey, C. (2009) ARF6-regulated shedding of tumor cell-derived plasma membrane microvesicles. *Curr Biol*. **19**, 1875–1885

34. Roberts, P. J., and Der, C. J. (2007) Targeting the Raf-MEK-ERK mitogen-activated protein kinase cascade for the treatment of cancer. *Oncogene*. **26**, 3291–3310

35. Heasman, S. J., and Ridley, A. J. (2008) Mammalian Rho GTPases: new insights into their functions from in vivo studies. *Nat Rev Mol Cell Biol*. **9**, 690–701

36. Watanabe, N., Madaule, P., Reid, T., Ishizaki, T., Watanabe, G., Kakizuka, A., Saito, Y., Nakao, K., Jockusch, B. M., and Narumiya, S. (1997) p140mDia, a mammalian homolog of Drosophila diaphanous, is a target protein for Rho small GTPase and is a ligand for profilin. *EMBO J*. **16**, 3044–3056

37. Narumiya, S., Tanji, M., and Ishizaki, T. (2009) Rho signaling, ROCK and mDia1, in transformation, metastasis and invasion. *Cancer Metastasis Rev*. **28**, 65–76

38. Kimura, K., Ito, M., Amano, M., Chihara, K., Fukata, Y., Nakafuku, M., Yamamori, B., Feng, J., Nakano, T., Okawa, K., Iwamatsu, A., and Kaibuchi, K. (1996) Regulation of myosin phosphatase by Rho and Rho-associated kinase (Rho-kinase). *Science*. **273**, 245–248

39. Hill, C. S., Wynne, J., and Treisman, R. (1995) The Rho family GTPases RhoA, Rac1, and CDC42Hs regulate transcriptional activation by SRF. *Cell*. **81**, 1159–1170

40. Guo, Y., Kenney, S. R., Muller, C. Y., Adams, S., Rutledge, T., Romero, E., Murray-Krezan, C., Prekeris, R., Sklar, L. A., Hudson, L. G., and Wandinger-Ness, A. (2015) R-Ketorolac Targets Cdc42 and Rac1 and Alters Ovarian Cancer Cell Behaviors Critical for Invasion and Metastasis. *Mol Cancer Ther*. **14**, 2215–2227

41. Parri, M., and Chiarugi, P. (2010) Rac and Rho GTPases in cancer cell motility control. *Cell Communication and Signaling*. **8**, 1–14

42. Etienne-Manneville, S., and Hall, A. (2002) Rho GTPases in cell biology. *Nature*. 10.1038/nature01148

43. Maekawa, M., Ishizaki, T., Boku, S., Watanabe, N., Fujita, A., Iwamatsu, A., Obinata, T., Ohashi, K., Mizuno, K., and Narumiya, S. (1999) Signaling from Rho to the actin

cytoskeleton through protein kinases ROCK and LIM-kinase. *Science*. **285**, 895–898

44. D'Souza-Schorey, C., and Chavrier, P. (2006) ARF proteins: roles in membrane traffic and beyond. *Nat Rev Mol Cell Biol*. **7**, 347–358

45. Murphy, D. A., and Courtneidge, S. A. (2011) The 'ins' and “outs” of podosomes and invadopodia: characteristics, formation and function. *Nat Rev Mol Cell Biol*. **12**, 413–426

46. Santy, L. C., and Casanova, J. E. (2001) Activation of ARF6 by ARNO stimulates epithelial cell migration through downstream activation of both Rac1 and phospholipase D. *J Cell Biol*. **154**, 599–610

47. Tushir, J. S., and D'Souza-Schorey, C. (2007) ARF6-dependent activation of ERK and Rac1 modulates epithelial tubule development. *EMBO J*. **26**, 1806–1819

48. Filenko, A. M., Danilova, V. M., and Sobieszek, A. (1997) Smooth muscle myosin light chain kinase, supramolecular organization, modulation of activity, and related conformational changes. *Biophys J*. **73**, 1593–1606

49. Sobieszek, A., Strobl, A., Ortner, B., and Babiychuk, E. B. (1993) Ca(2+)-calmodulin-dependent modification of smooth-muscle myosin light-chain kinase leading to its co-operative activation by calmodulin. *Biochem J*. **295 (Pt 2)**, 405–411

50. Zwaal, R. F., and Schroit, A. J. (1997) Pathophysiologic implications of membrane phospholipid asymmetry in blood cells. *Blood*. **89**, 1121–1132

51. Daleke, D. L. (2003) Regulation of transbilayer plasma membrane phospholipid asymmetry. *J Lipid Res*. **44**, 233–242

52. Lima, L. G., Chammas, R., Monteiro, R. Q., Moreira, M. E. C., and Barcinski, M. A. (2009) Tumor-derived microvesicles modulate the establishment of metastatic melanoma in a phosphatidylserine-dependent manner. *Cancer Lett*. **283**, 168–175

53. Muralidharan-Chari, V., Clancy, J. W., Sedgwick, A., and D'Souza-Schorey, C. (2010) Microvesicles: mediators of extracellular communication during cancer progression. *J Cell Sci*. **123**, 1603–1611

54. Manno, S., Takakuwa, Y., and Mohandas, N. (2002) Identification of a functional role for lipid asymmetry in biological membranes: Phosphatidylserine-skeletal protein interactions modulate membrane stability. *Proc Natl Acad Sci U S A*. **99**, 1943–1948

55. Pike, L. J. (2009) The challenge of lipid rafts. *J Lipid Res*. **50 Suppl**, S323–8

56. Del Conde, I., Shrimpton, C. N., Thiagarajan, P., and Lopez, J. A. (2005) Tissue-factor-bearing microvesicles arise from lipid rafts and fuse with activated platelets to initiate coagulation. *Blood*. **106**, 1604–1611

57. Liu, M.-L., Scalia, R., Mehta, J. L., and Williams, K. J. (2012) Cholesterol-induced membrane microvesicles as novel carriers of damage-associated molecular patterns: mechanisms of formation, action, and detoxification. *Arterioscler Thromb Vasc Biol*. **32**, 2113–2121

58. Lee, T. H., D'Asti, E., Magnus, N., Al-Nedawi, K., Meehan, B., and Rak, J. (2011) Microvesicles as mediators of intercellular communication in cancer--the emerging science of cellular 'debris'. *Semin Immunopathol*. **33**, 455–467

59. Gangalum, R. K., Atanasov, I. C., Zhou, Z. H., and Bhat, S. P. (2011) AlphaB-crystallin is found in detergent-resistant membrane microdomains and is secreted via exosomes from human retinal pigment epithelial cells. *J Biol Chem*. **286**, 3261–3269

60. Yu, S., Cao, H., Shen, B., and Feng, J. (2015) Tumor-derived exosomes in cancer progression and treatment failure. *Oncotarget*. **6**, 37151–37168

61. Henne, W. M., Buchkovich, N. J., and Emr, S. D. (2011) The ESCRT Pathway. *Dev Cell*. **21**, 77–91

62. Raiborg, C., Bremnes, B., Mehlum, A., Gillooly, D. J., D'Arrigo, A., Stang, E., and Stenmark, H. (2001) FYVE and coiled-coil domains determine the specific localisation of Hrs to early endosomes. *J Cell Sci*. **114**, 2255–2263

63. Bache, K. G., Raiborg, C., Mehlum, A., and Stenmark, H. (2003) STAM and Hrs are subunits of a multivalent ubiquitin-binding complex on early endosomes. *J Biol Chem*. **278**, 12513–12521

64. Katzmann, D. J., Stefan, C. J., Babst, M., and Emr, S. D. (2003) Vps27 recruits ESCRT machinery to endosomes during MVB sorting. *J Cell Biol*. **162**, 413–423

65. Lu, Q., Hope, L. W., Brasch, M., Reinhard, C., and Cohen, S. N. (2003) TSG101 interaction with HRS mediates endosomal trafficking and receptor down-regulation. *Proc Natl Acad Sci U S A*. **100**, 7626–7631

66. Katzmann, D. J., Babst, M., and Emr, S. D. (2001) Ubiquitin-dependent sorting into the multivesicular body pathway requires the function of a conserved endosomal protein sorting complex, ESCRT-I. *Cell*. **106**, 145–155

67. Slagsvold, T., Aasland, R., Hirano, S., Bache, K. G., Raiborg, C., Trambaiolo, D., Wakatsuki, S., and Stenmark, H. (2005) Eap45 in mammalian ESCRT-II binds ubiquitin via a phosphoinositide-interacting GLUE domain. *J Biol Chem*. **280**, 19600–19606

68. Teo, H., Perisic, O., Gonzalez, B., and Williams, R. L. (2004) ESCRT-II, an endosome-associated complex required for protein sorting: crystal structure and interactions with ESCRT-III and membranes. *Dev Cell*. **7**, 559–569

69. Tang, S., Buchkovich, N. J., Henne, W. M., Banjade, S., Kim, Y. J., and Emr, S. D. (2016) ESCRT-III activation by parallel action of ESCRT-I/II and ESCRT-0/Bro1 during MVB biogenesis. *Elife*. 10.7554/eLife.15507

70. Babst, M., Katzmann, D. J., Estepa-Sabal, E. J., Meerloo, T., and Emr, S. D. (2002) Escrt-III: an endosome-associated heterooligomeric protein complex required for mvb sorting. *Dev Cell*. **3**, 271–282

71. Tang, S., Henne, W. M., Borbat, P. P., Buchkovich, N. J., Freed, J. H., Mao, Y., Fromme, J. C., and Emr, S. D. (2015) Structural basis for activation, assembly and membrane binding of ESCRT-III Snf7 filaments. *Elife*. 10.7554/eLife.12548

72. Adell, M. A. Y., Migliano, S. M., and Teis, D. (2016) ESCRT-III and Vps4: a dynamic multipurpose tool for membrane budding and scission. *FEBS J*. 10.1111/febs.13688

73. Luhtala, N., and Odorizzi, G. (2004) Bro1 coordinates deubiquitination in the multivesicular body pathway by recruiting Doa4 to endosomes. *J Cell Biol*. **166**, 717–729

74. Seabra, M. C., Mules, E. H., and Hume, A. N. (2002) Rab GTPases, intracellular traffic and disease. *Trends Mol Med*. **8**, 23–30

75. Ostrowski, M., Carmo, N. B., Krumeich, S., Fanget, I., Raposo, G., Savina, A., Moita,

C. F., Schauer, K., Hume, A. N., Freitas, R. P., Goud, B., Benaroch, P., Hacohen, N., Fukuda, M., Desnos, C., Seabra, M. C., Darchen, F., Amigorena, S., Moita, L. F., and Thery, C. (2010) Rab27a and Rab27b control different steps of the exosome secretion pathway. *Nat Cell Biol*. **12**, 19–30– sup pp 1–13

76. Hsu, C., Morohashi, Y., Yoshimura, S.-I., Manrique-Hoyos, N., Jung, S., Lauterbach, M. A., Bakhti, M., Gronborg, M., Mobius, W., Rhee, J., Barr, F. A., and Simons, M. (2010) Regulation of exosome secretion by Rab35 and its GTPase-activating proteins TBC1D10A-C. *J Cell Biol*. **189**, 223–232

77. Savina, A., Fader, C. M., Damiani, M. T., and Colombo, M. I. (2005) Rab11 promotes docking and fusion of multivesicular bodies in a calcium-dependent manner. *Traffic*. **6**, 131–143

78. Elmore, S. (2007) Apoptosis: a review of programmed cell death. *Toxicol Pathol*. **35**, 495–516

79. Taylor, R. C., Cullen, S. P., and Martin, S. J. (2008) Apoptosis: controlled demolition at the cellular level. *Nat Rev Mol Cell Biol*. **9**, 231–241

80. Savill, J., and Fadok, V. (2000) Corpse clearance defines the meaning of cell death. *Nature*. **407**, 784–788

81. Gallucci, S., Lolkema, M., and Matzinger, P. (1999) Natural adjuvants: endogenous activators of dendritic cells. *Nat Med*. **5**, 1249–1255

82. Shi, Y., Zheng, W., and Rock, K. L. (2000) Cell injury releases endogenous adjuvants that stimulate cytotoxic T cell responses. *Proc Natl Acad Sci U S A*. **97**, 14590–14595

83. Rood, I. M., Deegens, J. K. J., Merchant, M. L., Tamboer, W. P. M., Wilkey, D. W., Wetzels, J. F. M., and Klein, J. B. (2010) Comparison of three methods for isolation of urinary microvesicles to identify biomarkers of nephrotic syndrome. *Kidney Int*. **78**, 810–816

84. Chen, C., Skog, J., Hsu, C.-H., Lessard, R. T., Balaj, L., Wurdinger, T., Carter, B. S., Breakefield, X. O., Toner, M., and Irimia, D. (2010) Microfluidic isolation and transcriptome analysis of serum microvesicles. *Lab Chip*. **10**, 505–511

85. Sokolova, V., Ludwig, A.-K., Hornung, S., Rotan, O., Horn, P. A., Epple, M., and

Giebel, B. (2011) Characterisation of exosomes derived from human cells by nanoparticle tracking analysis and scanning electron microscopy. *Colloids Surf B Biointerfaces*. **87**, 146–150

86. Witwer, K. W., Buzas, E. I., Bemis, L. T., Bora, A., Lasser, C., Lotvall, J., Nolte-'t Hoen, E. N., Piper, M. G., Sivaraman, S., Skog, J., Thery, C., Wauben, M. H., and Hochberg, F. (2013) Standardization of sample collection, isolation and analysis methods in extracellular vesicle research. *J Extracell Vesicles*

87. Iverius, P. H., and Laurent, T. C. (1967) Precipitation of some plasma proteins by the addition of dextran or polyethylene glycol. *Biochim Biophys Acta*. **133**, 371–373

88. Yuana, Y., Levels, J., Grootemaat, A., Sturk, A., and Nieuwland, R. (2014) Co-isolation of extracellular vesicles and high-density lipoproteins using density gradient ultracentrifugation. *J Extracell Vesicles*

89. Cvjetkovic, A., Lotvall, J., and Lasser, C. (2014) The influence of rotor type and centrifugation time on the yield and purity of extracellular vesicles. *J Extracell Vesicles*

90. Desrochers, L. M., Bordeleau, F., Reinhart-King, C. A., Cerione, R. A., and Antonyak, M. A. (2016) Microvesicles provide a mechanism for intercellular communication by embryonic stem cells during embryo implantation. *Nat Commun*. **7**, 11958

91. Shelke, G. V., Lasser, C., Gho, Y. S., and Lotvall, J. (2014) Importance of exosome depletion protocols to eliminate functional and RNA-containing extracellular vesicles from fetal bovine serum. *J Extracell Vesicles*

92. Montecalvo, A., Larregina, A. T., Shufesky, W. J., Stolz, D. B., Sullivan, M. L. G., Karlsson, J. M., Baty, C. J., Gibson, G. A., Erdos, G., Wang, Z., Milosevic, J., Tkacheva, O. A., Divito, S. J., Jordan, R., Lyons-Weiler, J., Watkins, S. C., and Morelli, A. E. (2012) Mechanism of transfer of functional microRNAs between mouse dendritic cells via exosomes. *Blood*. **119**, 756–766

93. Temchura, V. V., Tenbusch, M., Nchinda, G., Nabi, G., Tippler, B., Zelenyuk, M., Wildner, O., Uberla, K., and Kuate, S. (2008) Enhancement of immunostimulatory properties of exosomal vaccines by incorporation of fusion-competent G protein of vesicular stomatitis virus. *Vaccine*. **26**, 3662–3672

94. Antonyak, M. A., Li, B., Boroughs, L. K., Johnson, J. L., Druso, J. E., Bryant, K. L., Holowka, D. A., and Cerione, R. A. (2011) Cancer cell-derived microvesicles induce

transformation by transferring tissue transglutaminase and fibronectin to recipient cells. *Proc Natl Acad Sci U S A*. **108**, 4852–4857

95. Nolte-'t Hoen, E. N. M., Buermans, H. P. J., Waasdorp, M., Stoorvogel, W., Wauben, M. H. M., and 't Hoen, P. A. C. (2012) Deep sequencing of RNA from immune cell-derived vesicles uncovers the selective incorporation of small non-coding RNA biotypes with potential regulatory functions. *Nucleic Acids Res*. **40**, 9272–9285

96. D'Souza-Schorey, C., and Clancy, J. W. (2012) Tumor-derived microvesicles: shedding light on novel microenvironment modulators and prospective cancer biomarkers. *Genes Dev*. **26**, 1287–1299

97. Demory Beckler, M., Higginbotham, J. N., Franklin, J. L., Ham, A.-J., Halvey, P. J., Imasuen, I. E., Whitwell, C., Li, M., Liebler, D. C., and Coffey, R. J. (2013) Proteomic analysis of exosomes from mutant KRAS colon cancer cells identifies intercellular transfer of mutant KRAS. *Mol Cell Proteomics*. **12**, 343–355

98. Ratajczak, J., Miekus, K., Kucia, M., Zhang, J., Reca, R., Dvorak, P., and Ratajczak, M. Z. (2006) Embryonic stem cell-derived microvesicles reprogram hematopoietic progenitors: evidence for horizontal transfer of mRNA and protein delivery. *Leukemia*. **20**, 847–856

99. Waldenstrom, A., Genneback, N., Hellman, U., and Ronquist, G. (2012) Cardiomyocyte microvesicles contain DNA/RNA and convey biological messages to target cells. *PLoS One*. **7**, e34653

100. Laurent, L. C., Abdel-Mageed, A. B., Adelson, P. D., Arango, J., Balaj, L., Breakefield, X., Carlson, E., Carter, B. S., Majem, B., Chen, C. C., Cocucci, E., Danielson, K., Courtright, A., Das, S., Abd Elmageed, Z. Y., Enderle, D., Ezrin, A., Ferrer, M., Freedman, J., Galas, D., Gandhi, R., Huentelman, M. J., Van Keuren-Jensen, K., Kalani, Y., Kim, Y., Krichevsky, A. M., Lai, C., Lal-Nag, M., Laurent, C. D., Leonardo, T., Li, F., Malenica, I., Mondal, D., Nejad, P., Patel, T., Raffai, R. L., Rubio, R., Skog, J., Spetzler, R., Sun, J., Tanriverdi, K., Vickers, K., Wang, L., Wang, Y., Wei, Z., Weiner, H. L., Wong, D., Yan, I. K., Yeri, A., and Gould, S. (2015) Meeting report: discussions and preliminary findings on extracellular RNA measurement methods from laboratories in the NIH Extracellular RNA Communication Consortium. *J Extracell Vesicles*. **4**, 26533

101. Hill, A. F., Pegtel, D. M., Lambertz, U., Leonardi, T., O'Driscoll, L., Pluchino, S., Ter-Ovanesyan, D., and Nolte-'t Hoen, E. N. M. (2013) ISEV position paper: extracellular vesicle RNA analysis and bioinformatics. *J Extracell Vesicles*

102. Batagov, A. O., Kuznetsov, V. A., and Kurochkin, I. V. (2011) Identification of nucleotide patterns enriched in secreted RNAs as putative cis-acting elements targeting them to exosome nano-vesicles. *BMC Genomics*. **12 Suppl 3**, S18

103. Bolukbasi, M. F., Mizrak, A., Ozdener, G. B., Madlener, S., Strobel, T., Erkan, E. P., Fan, J.-B., Breakefield, X. O., and Saydam, O. (2012) miR-1289 and "Zipcode-"like Sequence Enrich mRNAs in Microvesicles. *Mol Ther Nucleic Acids*. **1**, e10

104. Patton, J. G., Franklin, J. L., Weaver, A. M., Vickers, K., Zhang, B., Coffey, R. J., Ansel, K. M., Blelloch, R., Goga, A., Huang, B., L'Etoille, N., Raffai, R. L., Lai, C. P., Krichevsky, A. M., Mateescu, B., Greiner, V. J., Hunter, C., Voinnet, O., and McManus, M. T. (2015) Biogenesis, delivery, and function of extracellular RNA. *J Extracell Vesicles*. **4**, 27494

105. Villarroya-Beltri, C., Gutierrez-Vazquez, C., Sanchez-Cabo, F., Perez-Hernandez, D., Vazquez, J., Martin-Cofreces, N., Martinez-Herrera, D. J., Pascual-Montano, A., Mittelbrunn, M., and Sanchez-Madrid, F. (2013) Sumoylated hnRNPA2B1 controls the sorting of miRNAs into exosomes through binding to specific motifs. *Nat Commun*. **4**, 2980

106. Meister, G. (2013) Argonaute proteins: functional insights and emerging roles. *Nat Rev Genet*. **14**, 447–459

107. Melo, S. A., Sugimoto, H., O'Connell, J. T., Kato, N., Villanueva, A., Vidal, A., Qiu, L., Vitkin, E., Perelman, L. T., Melo, C. A., Lucci, A., Ivan, C., Calin, G. A., and Kalluri, R. (2014) Cancer exosomes perform cell-independent microRNA biogenesis and promote tumorigenesis. *Cancer Cell*. **26**, 707–721

108. Gibbings, D. J., Ciaudo, C., Erhardt, M., and Voinnet, O. (2009) Multivesicular bodies associate with components of miRNA effector complexes and modulate miRNA activity. *Nat Cell Biol*. **11**, 1143–1149

109. McKenzie, A. J., Hoshino, D., Hong, N. H., Cha, D. J., Franklin, J. L., Coffey, R. J., Patton, J. G., and Weaver, A. M. (2016) KRAS-MEK Signaling Controls Ago2 Sorting into Exosomes. *Cell Rep*. **15**, 978–987

110. Cha, D. J., Franklin, J. L., Dou, Y., Liu, Q., Higginbotham, J. N., Demory Beckler, M., Weaver, A. M., Vickers, K., Prasad, N., Levy, S., Zhang, B., Coffey, R. J., and Patton, J. G. (2015) KRAS-dependent sorting of miRNA to exosomes. *Elife*. **4**, e07197

111. Clancy, J. W., Sedgwick, A., Rosse, C., Muralidharan-Chari, V., Raposo, G., Method, M., Chavrier, P., and D'Souza-Schorey, C. (2015) Regulated delivery of molecular cargo to invasive tumour-derived microvesicles. *Nat Commun*. **6**, 6919

112. Rothman, J. E. (1994) Mechanisms of intracellular protein transport. *Nature*. **372**, 55–63

113. Steffen, A., Le Dez, G., Poincloux, R., Recchi, C., Nassoy, P., Rottner, K., Galli, T., and Chavrier, P. (2008) MT1-MMP-dependent invasion is regulated by TI-VAMP/VAMP7. *Curr Biol*. **18**, 926–931

114. Bilodeau, P. S., Urbanowski, J. L., Winistorfer, S. C., and Piper, R. C. (2002) The Vps27p Hse1p complex binds ubiquitin and mediates endosomal protein sorting. *Nat Cell Biol*. **4**, 534–539

115. Shields, S. B., Oestreich, A. J., Winistorfer, S., Nguyen, D., Payne, J. A., Katzmann, D. J., and Piper, R. (2009) ESCRT ubiquitin-binding domains function cooperatively during MVB cargo sorting. *J Cell Biol*. **185**, 213–224

116. Odorizzi, G., Katzmann, D. J., Babst, M., Audhya, A., and Emr, S. D. (2003) Bro1 is an endosome-associated protein that functions in the MVB pathway in Saccharomyces cerevisiae. *J Cell Sci*. **116**, 1893–1903

117. Baietti, M. F., Zhang, Z., Mortier, E., Melchior, A., Degeest, G., Geeraerts, A., Ivarsson, Y., Depoortere, F., Coomans, C., Vermeiren, E., Zimmermann, P., and David, G. (2012) Syndecan-syntenin-ALIX regulates the biogenesis of exosomes. *Nat Cell Biol*. **14**, 677–685

118. Fang, Y., Wu, N., Gan, X., Yan, W., Morrell, J. C., and Gould, S. J. (2007) Higher-order oligomerization targets plasma membrane proteins and HIV gag to exosomes. *PLoS Biol*. **5**, e158

119. Harder, T., Scheiffele, P., Verkade, P., and Simons, K. (1998) Lipid domain structure of the plasma membrane revealed by patching of membrane components. *J Cell Biol*. **141**, 929–942

120. de Gassart, A., Geminard, C., Fevrier, B., Raposo, G., and Vidal, M. (2003) Lipid raft-associated protein sorting in exosomes. *Blood*. **102**, 4336–4344

121. Khan, S., Jutzy, J. M. S., Aspe, J. R., McGregor, D. W., Neidigh, J. W., and Wall, N. R.

(2011) Survivin is released from cancer cells via exosomes. *Apoptosis*. **16**, 1–12

122. Khan, S., Bennit, H. F., and Wall, N. R. (2015) The emerging role of exosomes in survivin secretion. *Histol Histopathol*. **30**, 43–50

123. Mulcahy, L. A., Pink, R. C., and Carter, D. R. F. (2014) Routes and mechanisms of extracellular vesicle uptake. *J Extracell Vesicles*

124. Franzen, C. A., Simms, P. E., Van Huis, A. F., Foreman, K. E., Kuo, P. C., and Gupta, G. N. (2014) Characterization of uptake and internalization of exosomes by bladder cancer cells. *Biomed Res Int*. **2014**, 619829

125. Morelli, A. E., Larregina, A. T., Shufesky, W. J., Sullivan, M. L. G., Stolz, D. B., Papworth, G. D., Zahorchak, A. F., Logar, A. J., Wang, Z., Watkins, S. C., Falo, L. D. J., and Thomson, A. W. (2004) Endocytosis, intracellular sorting, and processing of exosomes by dendritic cells. *Blood*. **104**, 3257–3266

126. Svensson, K. J., Christianson, H. C., Wittrup, A., Bourseau-Guilmain, E., Lindqvist, E., Svensson, L. M., Mörgelin, M., and Belting, M. (2013) Exosome Uptake Depends on ERK1/2-Heat Shock Protein 27 Signaling and Lipid Raft-mediated Endocytosis Negatively Regulated by Caveolin-1. *J Biol Chem*. **288**, 17713–17724

127. Tian, T., Zhu, Y.-L., Hu, F.-H., Wang, Y.-Y., Huang, N.-P., and Xiao, Z.-D. (2013) Dynamics of exosome internalization and trafficking. *J Cell Physiol*. **228**, 1487–1495

128. Lamaze, C., Fujimoto, L. M., Yin, H. L., and Schmid, S. L. (1997) The actin cytoskeleton is required for receptor-mediated endocytosis in mammalian cells. *J Biol Chem*. **272**, 20332–20335

129. Kirchhausen, T. (2000) Clathrin. *Annu Rev Biochem*. **69**, 699–727

130. Wang, L. H., Rothberg, K. G., and Anderson, R. G. (1993) Mis-assembly of clathrin lattices on endosomes reveals a regulatory switch for coated pit formation. *J Cell Biol*. **123**, 1107–1117

131. Escrevente, C., Keller, S., Altevogt, P., and Costa, J. (2011) Interaction and uptake of exosomes by ovarian cancer cells. *BMC Cancer*. **11**, 108

132. Doherty, G. J., and McMahon, H. T. (2009) Mechanisms of endocytosis. *Annu Rev Biochem*. **78**, 857–902

133. Swanson, J. A. (2008) Shaping cups into phagosomes and macropinosomes. *Nat Rev Mol Cell Biol*. **9**, 639–649

134. Kerr, M. C., and Teasdale, R. D. (2009) Defining macropinocytosis. *Traffic*. **10**, 364–371

135. Feng, D., Zhao, W.-L., Ye, Y.-Y., Bai, X.-C., Liu, R.-Q., Chang, L.-F., Zhou, Q., and Sui, S.-F. (2010) Cellular internalization of exosomes occurs through phagocytosis. *Traffic*. **11**, 675–687

136. Fadok, V. A., Voelker, D. R., Campbell, P. A., Cohen, J. J., Bratton, D. L., and Henson, P. M. (1992) Exposure of phosphatidylserine on the surface of apoptotic lymphocytes triggers specific recognition and removal by macrophages. *J Immunol*. **148**, 2207–2216

137. Atay, S., Gercel-Taylor, C., and Taylor, D. D. (2011) Human trophoblast-derived exosomal fibronectin induces pro-inflammatory IL-1beta production by macrophages. *Am J Reprod Immunol*. **66**, 259–269

138. Billottet, C., and Jouanneau, J. (2008) [Tumor-stroma interactions]. *Bull Cancer*. **95**, 51–56

139. Kalluri, R., and Zeisberg, M. (2006) Fibroblasts in cancer. *Nat Rev Cancer*. **6**, 392–401

140. Costa-Silva, B., Aiello, N. M., Ocean, A. J., Singh, S., Zhang, H., Thakur, B. K., Becker, A., Hoshino, A., Mark, M. T., Molina, H., Xiang, J., Zhang, T., Theilen, T.-M., Garcia-Santos, G., Williams, C., Ararso, Y., Huang, Y., Rodrigues, G., Shen, T.-L., Labori, K. J., Lothe, I. M. B., Kure, E. H., Hernandez, J., Doussot, A., Ebbesen, S. H., Grandgenett, P. M., Hollingsworth, M. A., Jain, M., Mallya, K., Batra, S. K., Jarnagin, W. R., Schwartz, R. E., Matei, I., Peinado, H., Stanger, B. Z., Bromberg, J., and Lyden, D. (2015) Pancreatic cancer exosomes initiate pre-metastatic niche formation in the liver. *Nat Cell Biol*. **17**, 816–826

141. Zhang, X., Pei, Z., Chen, J., Ji, C., Xu, J., Zhang, X., and Wang, J. (2016) Exosomes for Immunoregulation and Therapeutic Intervention in Cancer. *J Cancer*. **7**, 1081–1087

142. van der Vos, K. E., Abels, E. R., Zhang, X., Lai, C., Carrizosa, E., Oakley, D.,

Prabhakar, S., Mardini, O., Crommentuijn, M. H. W., Skog, J., Krichevsky, A. M., Stemmer-Rachamimov, A., Mempel, T. R., Khoury, El, J., Hickman, S. E., and Breakefield, X. O. (2016) Directly visualized glioblastoma-derived extracellular vesicles transfer RNA to microglia/macrophages in the brain. *Neuro Oncol*. **18**, 58–69

143. Biernat, W., Huang, H., Yokoo, H., Kleihues, P., and Ohgaki, H. (2004) Predominant expression of mutant EGFR (EGFRvIII) is rare in primary glioblastomas. *Brain Pathol*. **14**, 131–136

144. Petit, A. M., Rak, J., Hung, M. C., Rockwell, P., Goldstein, N., Fendly, B., and Kerbel, R. S. (1997) Neutralizing antibodies against epidermal growth factor and ErbB-2/neu receptor tyrosine kinases down-regulate vascular endothelial growth factor production by tumor cells in vitro and in vivo: angiogenic implications for signal transduction therapy of solid tumors. *Am J Pathol*. **151**, 1523–1530

145. Kucharzewska, P., Christianson, H. C., Welch, J. E., Svensson, K. J., Fredlund, E., Ringner, M., Mörgelin, M., Bourseau-Guilmain, E., Bengzon, J., and Belting, M. (2013) Exosomes reflect the hypoxic status of glioma cells and mediate hypoxia-dependent activation of vascular cells during tumor development. *Proc Natl Acad Sci U S A*. **110**, 7312–7317

146. Chaffer, C. L., and Weinberg, R. A. (2011) A perspective on cancer cell metastasis. *Science*. **331**, 1559–1564

147. Wang, Y., Yi, J., Chen, X., Zhang, Y., Xu, M., and Yang, Z. (2016) The regulation of cancer cell migration by lung cancer cell-derived exosomes through TGF-beta and IL-10. *Oncol Lett*. **11**, 1527–1530

148. Liao, J., Liu, R., Shi, Y.-J., Yin, L.-H., and Pu, Y.-P. (2016) Exosome-shuttling microRNA-21 promotes cell migration and invasion-targeting PDCD4 in esophageal cancer. *Int J Oncol*. **48**, 2567–2579

149. Taraboletti, G., D'Ascenzo, S., Borsotti, P., Giavazzi, R., Pavan, A., and Dolo, V. (2002) Shedding of the matrix metalloproteinases MMP-2, MMP-9, and MT1-MMP as membrane vesicle-associated components by endothelial cells. *Am J Pathol*. **160**, 673–680

150. Koumangoye, R. B., Sakwe, A. M., Goodwin, J. S., Patel, T., and Ochieng, J. (2011) Detachment of breast tumor cells induces rapid secretion of exosomes which subsequently mediate cellular adhesion and spreading. *PLoS One*. **6**, e24234

151. Sung, B. H., Ketova, T., Hoshino, D., Zijlstra, A., and Weaver, A. M. Directional cell movement through tissues is controlled by exosome secretion. *Nat Commun*. 10.1038/ncomms8164

152. Deng, Z., Cheng, Z., Xiang, X., Yan, J., Zhuang, X., Liu, C., Jiang, H., Ju, S., Zhang, L., Grizzle, W., Mobley, J., Roman, J., Miller, D., and Zhang, H.-G. (2012) Tumor cell cross talk with tumor-associated leukocytes leads to induction of tumor exosomal fibronectin and promotes tumor progression. *Am J Pathol*. **180**, 390–398

153. Lobert, V. H., Brech, A., Pedersen, N. M., Wesche, J., Oppelt, A., Malerod, L., and Stenmark, H. (2010) Ubiquitination of alpha 5 beta 1 integrin controls fibroblast migration through lysosomal degradation of fibronectin-integrin complexes. *Dev Cell*. **19**, 148–159

154. Majumdar, R., Tavakoli Tameh, A., and Parent, C. A. (2016) Exosomes Mediate LTB4 Release during Neutrophil Chemotaxis. *PLoS Biol*. **14**, e1002336

155. Psaila, B., and Lyden, D. (2009) The metastatic niche: adapting the foreign soil. *Nat Rev Cancer*. **9**, 285–293

156. Hood, J. L., San, R. S., and Wickline, S. A. (2011) Exosomes released by melanoma cells prepare sentinel lymph nodes for tumor metastasis. *Cancer Res*. **71**, 3792–3801

157. Nip, J., Shibata, H., Loskutoff, D. J., Cheresh, D. A., and Brodt, P. (1992) Human melanoma cells derived from lymphatic metastases use integrin alpha v beta 3 to adhere to lymph node vitronectin. *J Clin Invest*. **90**, 1406–1413

158. Montero, L., and Nagamine, Y. (1999) Regulation by p38 mitogen-activated protein kinase of adenylate- and uridylate-rich element-mediated urokinase-type plasminogen activator (uPA) messenger RNA stability and uPA-dependent in vitro cell invasion. *Cancer Res*. **59**, 5286–5293

159. Peinado, H., Aleckovic, M., Lavotshkin, S., Matei, I., Costa-Silva, B., Moreno-Bueno, G., Hergueta-Redondo, M., Williams, C., Garcia-Santos, G., Ghajar, C., Nitadori-Hoshino, A., Hoffman, C., Badal, K., Garcia, B. A., Callahan, M. K., Yuan, J., Martins, V. R., Skog, J., Kaplan, R. N., Brady, M. S., Wolchok, J. D., Chapman, P. B., Kang, Y., Bromberg, J., and Lyden, D. (2012) Melanoma exosomes educate bone marrow progenitor cells toward a pro-metastatic phenotype through MET. *Nat Med*. **18**, 883–891

160. Hiratsuka, S., Watanabe, A., Sakurai, Y., Akashi-Takamura, S., Ishibashi, S., Miyake,

K., Shibuya, M., Akira, S., Aburatani, H., and Maru, Y. (2008) The S100A8-serum amyloid A3-TLR4 paracrine cascade establishes a pre-metastatic phase. *Nat Cell Biol*. **10**, 1349–1355

161. Grange, C., Tapparo, M., Collino, F., Vitillo, L., Damasco, C., Deregibus, M. C., Tetta, C., Bussolati, B., and Camussi, G. (2011) Microvesicles released from human renal cancer stem cells stimulate angiogenesis and formation of lung premetastatic niche. *Cancer Res*. **71**, 5346–5356

162. Bussolati, B., Bruno, S., Grange, C., Ferrando, U., and Camussi, G. (2008) Identification of a tumor-initiating stem cell population in human renal carcinomas. *FASEB J*. **22**, 3696–3705

163. Hicklin, D. J., and Ellis, L. M. (2005) Role of the vascular endothelial growth factor pathway in tumor growth and angiogenesis. *J Clin Oncol*. **23**, 1011–1027

164. Gialeli, C., Theocharis, A. D., and Karamanos, N. K. (2011) Roles of matrix metalloproteinases in cancer progression and their pharmacological targeting. *FEBS J*. **278**, 16–27

165. Hart, I. R., and Fidler, I. J. (1980) Role of organ selectivity in the determination of metastatic patterns of B16 melanoma. *Cancer Res*. **40**, 2281–2287

166. Hoshino, A., Costa-Silva, B., Shen, T.-L., Rodrigues, G., Hashimoto, A., Tesic Mark, M., Molina, H., Kohsaka, S., Di Giannatale, A., Ceder, S., Singh, S., Williams, C., Soplop, N., Uryu, K., Pharmer, L., King, T., Bojmar, L., Davies, A. E., Ararso, Y., Zhang, T., Zhang, H., Hernandez, J., Weiss, J. M., Dumont-Cole, V. D., Kramer, K., Wexler, L. H., Narendran, A., Schwartz, G. K., Healey, J. H., Sandstrom, P., Labori, K. J., Kure, E. H., Grandgenett, P. M., Hollingsworth, M. A., de Sousa, M., Kaur, S., Jain, M., Mallya, K., Batra, S. K., Jarnagin, W. R., Brady, M. S., Fodstad, O., Muller, V., Pantel, K., Minn, A. J., Bissell, M. J., Garcia, B. A., Kang, Y., Rajasekhar, V. K., Ghajar, C. M., Matei, I., Peinado, H., Bromberg, J., and Lyden, D. (2015) Tumour exosome integrins determine organotropic metastasis. *Nature*. **527**, 329–335

167. Luqmani, Y. A. (2005) Mechanisms of drug resistance in cancer chemotherapy. *Med Princ Pract*. **14 Suppl 1**, 35–48

168. Aung, T., Chapuy, B., Vogel, D., Wenzel, D., Oppermann, M., Lahmann, M., Weinhage, T., Menck, K., Hupfeld, T., Koch, R., Trumper, L., and Wulf, G. G. (2011) Exosomal evasion of humoral immunotherapy in aggressive B-cell lymphoma modulated by ATP-binding cassette transporter A3. *Proc Natl Acad Sci U S A*. **108**, 15336–15341

169. Safaei, R., Larson, B. J., Cheng, T. C., Gibson, M. A., Otani, S., Naerdemann, W., and Howell, S. B. (2005) Abnormal lysosomal trafficking and enhanced exosomal export of cisplatin in drug-resistant human ovarian carcinoma cells. *Mol Cancer Ther*. **4**, 1595–1604

170. Shedden, K., Xie, X. T., Chandaroy, P., Chang, Y.-T., and Rosania, G. R. (2003) Expulsion of small molecules in vesicles shed by cancer cells: association with gene expression and chemosensitivity profiles. *Cancer Res*. **63**, 4331–4337

171. Gallo, A., Tandon, M., Alevizos, I., and Illei, G. G. (2012) The majority of microRNAs detectable in serum and saliva is concentrated in exosomes. *PLoS One*. **7**, e30679

172. Erdbrugger, U., and Le, T. H. (2016) Extracellular Vesicles in Renal Diseases: More than Novel Biomarkers? *J Am Soc Nephrol*. **27**, 12–26

173. Batiz, L. F., Castro, M. A., Burgos, P. V., Velasquez, Z. D., Munoz, R. I., Lafourcade, C. A., Troncoso-Escudero, P., and Wyneken, U. (2015) Exosomes as Novel Regulators of Adult Neurogenic Niches. *Front Cell Neurosci*. **9**, 501

174. Coleman, B. M., and Hill, A. F. (2015) Extracellular vesicles--Their role in the packaging and spread of misfolded proteins associated with neurodegenerative diseases. *Semin Cell Dev Biol*. **40**, 89–96

CHAPTER 2

[1]Microvesicle Cargo and Function Changes Upon the Induction of Cellular Transformation

Extracellular vesicles (EVs), including exosomes and microvesicles (MVs), have emerged as a major form of intercellular communication, playing important roles in several physiological processes and diseases including cancer. EVs generated by cancer cells contain a variety of proteins and RNA species that can be transferred between cancer cells, as well as between cancer and non-transformed (normal) cells, thereby impacting a number of aspects of cancer progression. Here we show how oncogenic transformation influences the biogenesis and function of EVs using a mouse embryonic fibroblast (MEF) cell line that can be induced to express an oncogenic form of Dbl (for diffuse B cell lymphoma). While MEFs induced to express onco-Dbl generated a similar amount of MVs as the uninduced control cells, we found that MVs isolated from onco-Dbl-transformed cells contain a unique signaling protein, the ubiquitously expressed non-receptor tyrosine kinase, focal adhesion kinase (FAK). The addition of MVs isolated from MEFs expressing onco-Dbl to cultures of fibroblasts strongly promoted their survival and induced their ability to grow under anchorage-independent conditions, outcomes that could be reversed by knocking-down FAK and depleting it from the MVs, or by inhibiting its kinase activity using a specific inhibitor. We then showed the same to be true for MVs isolated from aggressive MDAMB231 breast cancer cells. Together, these findings demonstrate that the induction of oncogenic transformation gives rise to MVs, which uniquely contain a

[1]Currently in press as a manuscript by Bridget T. Kreger, Andrew L. Dougherty, Kai Su Greene, Richard A. Cerione, and Marc A. Antonyak in the *Journal of Biological Chemistry*.

signaling protein kinase that helps propagate the transformed phenotype, and thus may offer a specific diagnostic marker of malignant disease

Introduction

Classical intercellular signaling involves the secretion of growth factors, pro-inflammatory cytokines, and extracellular matrix proteins, by a cell into its local environment (1, 2). These soluble factors then bind to their corresponding receptors expressed in a neighboring cell and induce the activation of intracellular signaling events that determine whether a cell grows, differentiates, migrates, or dies (3). These types of paracrine signaling activities are required throughout development and for tissue homeostasis, while de-regulation of these events often leads to developmental abnormalities and the onset of diseases.

The generation of EVs by cells has quickly become appreciated as another major form of intercellular communication with important consequences in biology (4-7). Cells generate two distinct types of EVs, MVs and exosomes. MVs typically range in size from 0.2-2.0μm in diameter, and are formed via the budding and release (shedding) of membrane-enclosed packages from plasma membranes. Exosomes represent the second major class of EVs. They are significantly smaller than MVs, averaging only 0.03-0.1μm in size, and are formed through a distinct mechanism. Specifically, exosomes are generated as a result of the endosomal sorting complex required for transport (ESCRT)- and Rab-dependent re-routing of multivesicular bodies (MVBs) containing endosomes from the lysosome, where they would be degraded, to the cell surface. The MVBs then fuse with the plasma membrane and release their contents (i.e. endosomes) into the extracellular environment, at which point they are referred to as exosomes.

One of the main reasons that MVs and exosomes have been attracting a good deal of attention has to do with the cargo they contain, which includes cell surface receptors, cytosolic signaling proteins, metabolic enzymes, and even nuclear proteins, as well as RNA transcripts and micro RNAs (1, 2, 6, 7). Once released from a cell, EVs can function in a paracrine or endocrine manner through the transfer of their cargo to a recipient cell (3, 4). This cargo is then used by the cell to elicit specific cellular processes or outcomes.

Although it is beginning to be appreciated that both normal cell types and cancer cells generate MVs and exosomes, EVs have been most often studied in the context of cancer, where they have been shown to play important roles in the progression of the disease (4-9). For example, MVs generated by highly aggressive human cancer cells are capable of stimulating tumor angiogenesis, reorganizing the stroma to establish the tumor microenvironment, as well as promote tumor growth and chemoresistance (10-12). The role of MVs in cancer progression was exemplified in a study showing that a highly oncogenic form of the epidermal growth factor receptor (EGFR), known as the EGFR variant type III (EGFRvIII), is present in MVs generated by glioma cells engineered to express this truncated EGFR. When MVs from these glioma cells were isolated and then added to EGFRvIII-negative glioma cells, the EGFRvIII was transferred from the MVs to the cells where it triggered oncogenic signaling events that promoted cell growth and survival (8).

Increasing evidence suggests that cancer cell-derived MVs also impact the behavior of normal cell types that can be found bordering a tumor (13, 14). For example, our laboratory has shown that MVs generated by the highly aggressive MDAMB231 breast cancer cell line are capable of conferring a transformed-like phenotype onto normal mammary epithelial cells and fibroblasts, including the ability to grow under serum-limiting, or anchorage-independent

conditions. We further showed that an important aspect of the mechanism underlying the ability of MVs to mediate such phenotypic changes involved the crosslinking of the extracellular matrix protein fibronectin, which is associated with MVs, through the acyl transferase activity of another MV-associated protein, tissue transglutaminase. This enabled the MVs to dock onto normal epithelial cells and fibroblasts through the binding of the MV-associated cross-linked fibronectin to integrins on the surfaces of theses cells (6).

In addition to EVs acting locally to promote tumor growth, they can also impact cells at distant sites, through their ability to enter the bloodstream and circulate throughout the body. Thus, the isolation of EVs from blood samples is being actively pursued as a potential source of diagnostic information (15). Many lines of evidence have shown that high grade/highly aggressive cancer cells shed considerably more EVs than lower grade cancer cells and normal cells (16). In one such study, patients with malignant melanoma were found to have nearly twice the amount of EVs in their blood serum compared to normal patients (17). Moreover, a study conducted on glioblastoma patients found that the amount of EVs in the circulation increased proportionally to tumor volume (18). Collectively, these findings suggest that the levels of circulating EVs, and/or the cancer-specific cargo contained within these vesicles, could be used as potential diagnostic indicators.

Given the importance of EVs in cancer progression, we set out to better understand the key differences between MVs generated by normal and transformed cells, as this information would shed additional light on how cancer cell-derived MVs impact recipient cells, as well as further examine their potential as diagnostic markers. Here, using an inducible model of cellular transformation, we show that the amount of MVs shed by non-transformed MEFs is comparable to that generated by MEFs transformed by inducing the expression of onco-Dbl (19), a truncated

nucleotide exchange factor (GEF) that constitutively activates members of the Rho family of small GTPases. However, we found that MVs from transformed MEFs were specifically enriched in the non-receptor tyrosine kinase FAK, despite this kinase being expressed at similar levels in both the non-transformed and transformed MEFs. We went on to determine that FAK is also preferentially expressed in MVs derived from several highly aggressive breast cancer cell lines. Moreover, we found that the presence of FAK in the MVs from the transformed MEFs, as well as the highly aggressive MDAMB231 breast cancer cells, has important functional consequences, namely, it enables MVs to promote cell survival and anchorage-independent growth. Overall, the findings reported here highlight that specific cargo is recruited to MVs upon oncogenic transformation, thus conferring these vesicles with unique functional capabilities.

Results

Onco-Dbl expression in MEFs induces cellular transformation

The formation and shedding of MVs by cells is now appreciated as a form of intercellular communication with important roles in human cancer progression. These vesicles are also being aggressively pursued as a novel source of diagnostic information. However, there still remains a gap in our understanding of how cancer cell-derived MVs mediate their effects and how we might best utilize their unique properties for diagnostic purposes. Therefore, we took advantage of a well-defined, inducible system of oncogenic transformation to compare the cargo and functional properties of MVs isolated from transformed cells and their non-transformed counterparts. Specifically, this system involves MEFs that stably express a doxycycline-regulated form of onco-Dbl, a truncated GEF that activates the small GTPases Rho and Cdc42 (20-22).

When cultured in the presence of doxycycline, the expression of HA-tagged onco-Dbl in MEFs is inhibited (Figure 2.1A, top panel, first lane). However, 24 hours after placing the MEFs in medium lacking doxycycline, HA-tagged onco-Dbl is readily detected in lysates derived from these cells (compare the first and third lanes), with maximal expression occurring within 48 hours (compare the third-fifth lanes). Thus, for all the experiments where MEFs expressing onco-Dbl are used, we first induced its expression for 48 hours prior to beginning the assays.

As previously reported (19), marked actin cytoskeletal rearrangements accompanied the expression of onco-Dbl and its activation of the small GTPases Cdc42 and Rho. Figure 2.1B shows an example of an uninduced control MEF stained with an HA antibody and rhodamine-conjugated phalloidin to label filamentous actin (F-actin). The uninduced control MEFs, which lacked onco-Dbl expression (top left panel), showed a typical fibroblast-like morphology (top right panel). However, upon the induction of HA-tagged onco-Dbl expression (Figure 2.1B, bottom left panel), there was a significant increase in the number and size of F-actin stress fibers (bottom right panel).

We then subjected the uninduced control and onco-Dbl-expressing MEFs to soft agar and cell death assays. Soft agar assays determine the ability of cells to grow and form colonies under anchorage-independent conditions, an *in vitro* measure of tumorigenicity. Figure 2.1C shows that after 14 days in culture, the control MEFs remained as single cells (top panel). In contrast, the induction of HA-tagged onco-Dbl expression resulted in the formation of large colonies of cells (Figure 2.1C, bottom panel and Figure 2.1D). In order to examine how onco-Dbl expression influenced MEF viability, we then cultured uninduced control MEFs, as well as MEFs induced to express HA-tagged onco-Dbl, in medium lacking or containing serum for 48 hours. The cells were then collected, stained with DAPI to label their nuclei, and analyzed by fluorescent

Figure 2.1. The induction of onco-Dbl expression in MEFs leads to cellular transformation.

(**A**) Western blot analysis using HA and actin antibodies was performed on lysates of MEFs stably expressing an inducible form of HA-tagged onco-Dbl after the removal of doxycycline (Dox) from the culturing medium for the indicated lengths of time. Molecular weight markers (in kDa) have been included along the right side of each blot. (**B**) Immunofluorescence using an HA antibody was performed on uninduced control MEFs and on MEFs induced to express onco-Dbl (onco-Dbl induced) for 48 hours (left panels). The cells were also stained with rhodamine-conjugated phalloidin to detect F-actin (right panels). (**C**) and (**D**) Soft agar assays were carried out on control MEFs (uninduced) and MEFs expressing onco-Dbl. Representative bright field images of the assays are shown in (C), while (D) shows the number of colonies that formed for each condition. (**E**) Cell death assays were performed on uninduced MEFs, and MEFs expressing onco-Dbl, by culturing them in serum-free medium supplemented without or with 2% serum, as indicated. Approximately 48 hours later, the cells were collected and stained with DAPI to identify condensed or blebbed (apoptotic) nuclei. The experiments in (A-E) were performed a minimum of 3 separate times, with each experiment yielding similar results. The data shown (in D and E) represents the mean ± standard deviation (SD). Student t-tests were performed. ***$p<0.001$.

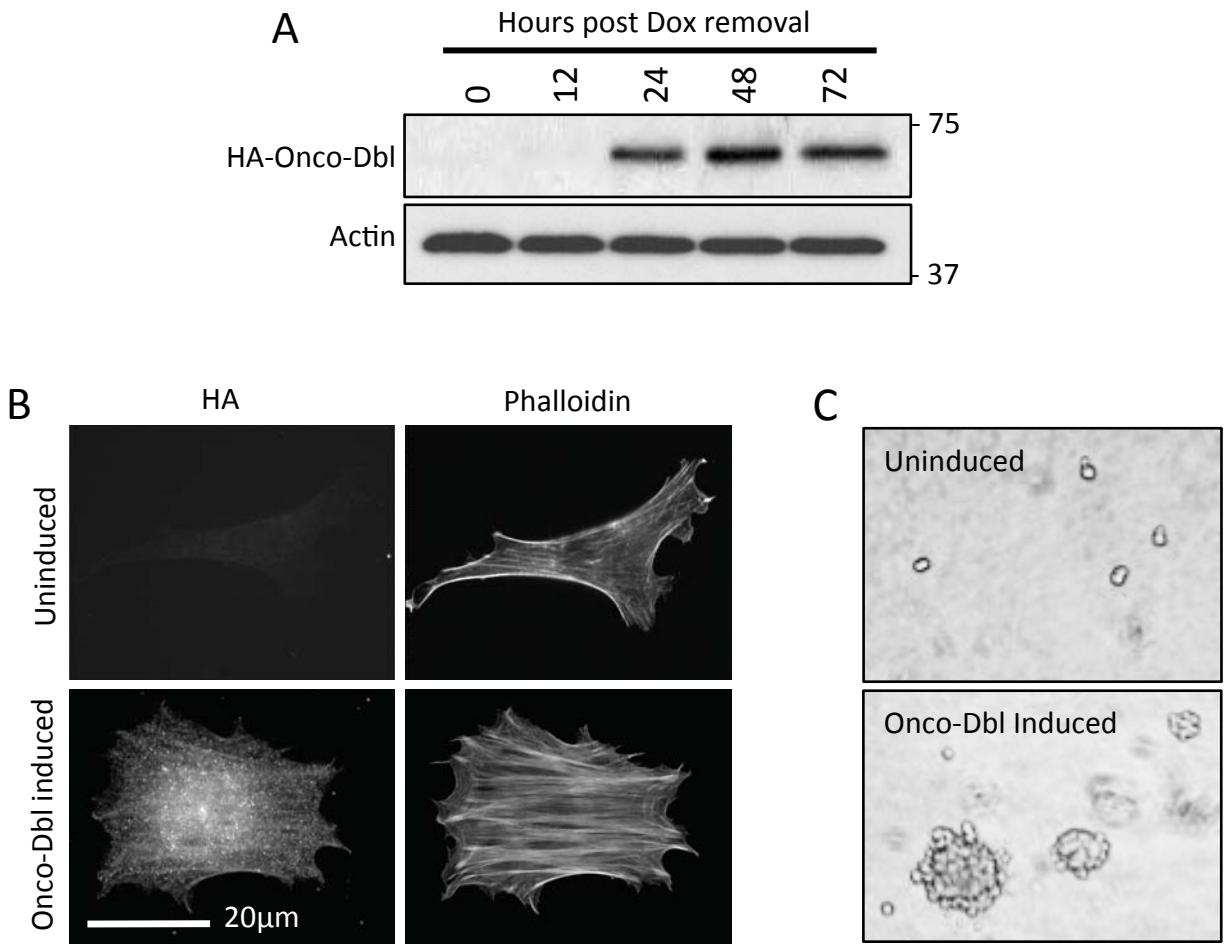
A
Hours post Dox removal
0
12
24
48
72
HA-Onco-Dbl
Actin
75
37
B
HA
Phalloidin
Uninduced
Onco-Dbl induced
20µm
C
Uninduced
Onco-Dbl Induced
D
***
number of colonies
350
300
250
200
150
100
50
0
Uninduced
Onco-Dbl induced
E
***
***
Relative cell death (fold changes)
20
15
10
5
0
Onco-Dbl Induction:
Serum:
- - + +
+ - + -

microscopy for the appearance of condensed or blebbed nuclei, a hallmark of apoptosis. There was a nearly 18-fold increase in the number of control MEFs that died when cultured in serum free medium, compared to MEFs cultured in 2% serum (Figure 2.1E, compare the first two bars). However, onco-Dbl expression reduced the amount of cell death caused by serum-starvation to a similar extent as culturing the control MEFs in 2% serum (Figure 2.1E, compare the first and fourth bars).

Comparison of MVs from control versus onco-Dbl-transformed MEFs

We next used the inducible model of cellular transformation to determine how MVs generated by normal (non-transformed) cells differ from those generated by transformed cells. Given that various studies have suggested that high-grade and highly aggressive cancer cells generate more EVs compared to either lower grade cancer cells or their normal cellular counterparts (16, 18), we asked whether uninduced control MEFs generated less MVs than MEFs expressing onco-Dbl. Control MEFs and MEFs expressing HA-tagged onco-Dbl were treated with the fluorescent membrane dye FM1-43FX and visualized using fluorescent microscopy. Figure 2.2A shows that MVs could be detected along the surfaces of cells from both of these cultures. The MVs were then isolated from the conditioned media collected from an equivalent number of serum-starved control MEFs, or MEFs expressing onco-Dbl, using a method that involved a series of centrifugations to remove cells and cell debris, followed by a filtration step using a 0.22μm filter (Figure 2.2B). This approach allows for the separation of MVs from the population of smaller sized EVs known as exosomes. Transmission electron microscopy (TEM) performed on the MV preparations revealed that EVs averaging ~300-400 nm in diameter could indeed be routinely isolated from each of these cell cultures (Figure

Figure 2.2. Control and onco-Dbl-transformed MEFs generate MVs.
(**A**) Control MEFs (uninduced), and MEFs expressing onco-Dbl (onco-Dbl induced), were stained with the fluorescent membrane dye FM1-43FX to visualize MVs on their surfaces. Some of the MVs are indicated with arrows and the insets are magnifications of the boxed areas. Scale bar = 20μm. (**B**) Schematic of the MV isolation procedure used to prepare MVs lysates for Western blot analysis, or for use in biological assays. (**C**) TEM images of MVs isolated from the different MEF cultures. Scale bars = 500nm. (**D**) Western blot analysis using an anti-HA antibody to detect onco-Dbl expression, an IκBα antibody as a cytoplasmic marker, a flotillin-2 antibody as a MV marker, and an actin antibody as a loading control was performed on control MEFs (uninduced) and MEFs expressing onco-Dbl (lanes labeled whole cell lysates; WCL), as well as on the MVs that these cells generated (lanes labeled MVs). Molecular weight markers (in kDa) have been included along the right side of each blot. (**E**) NTA was performed on MVs isolated from an equivalent number of control MEFs and MEFs expressing onco-Dbl. The experiments (in A and C-E) were performed a minimum of 3 separate times, with each experiment yielding similar results.

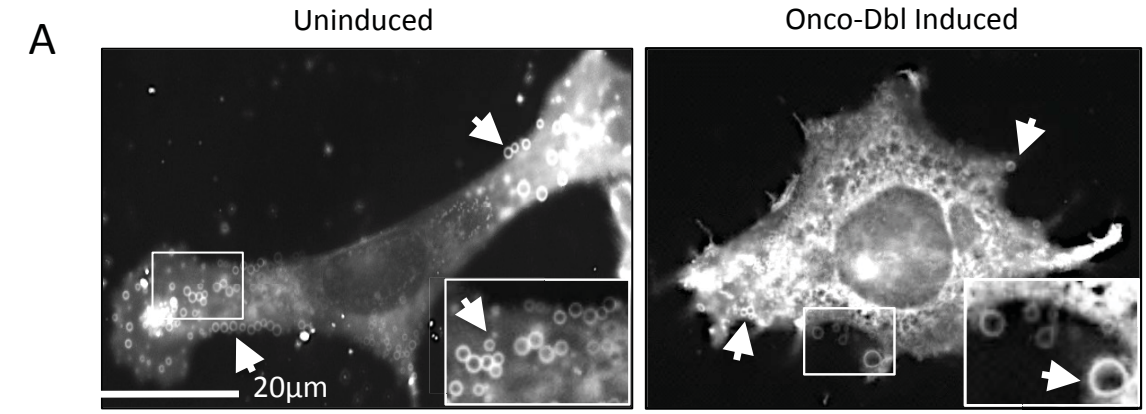
A
Uninduced
Onco-Dbl Induced
20µm

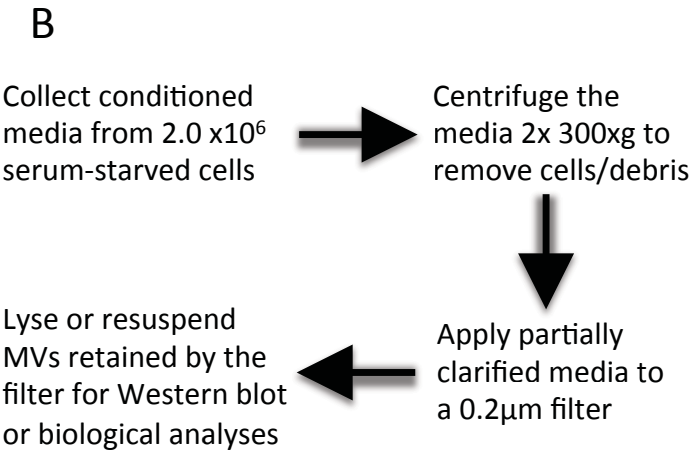
B
Collect conditioned media from 2.0 x10^6 serum-starved cells
Centrifuge the media 2x 300xg to remove cells/debris
Apply partially clarified media to a 0.2µm filter
Lyse or resuspend MVs retained by the filter for Western blot or biological analyses

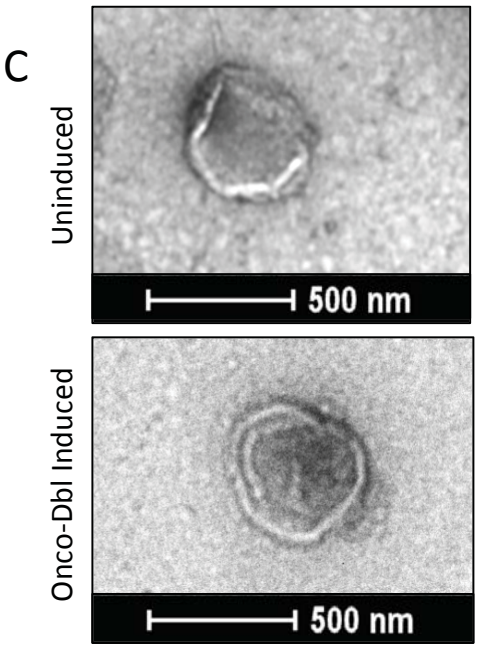
C
Uninduced
500 nm
Onco-Dbl Induced
500 nm

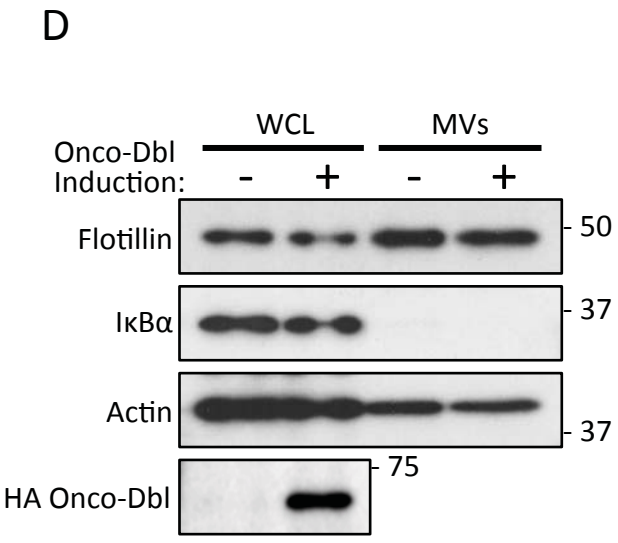
D
WCL
MVs
Onco-Dbl Induction:
- + - +
Flotillin
50
IκBα
37
Actin
37
HA Onco-Dbl
75

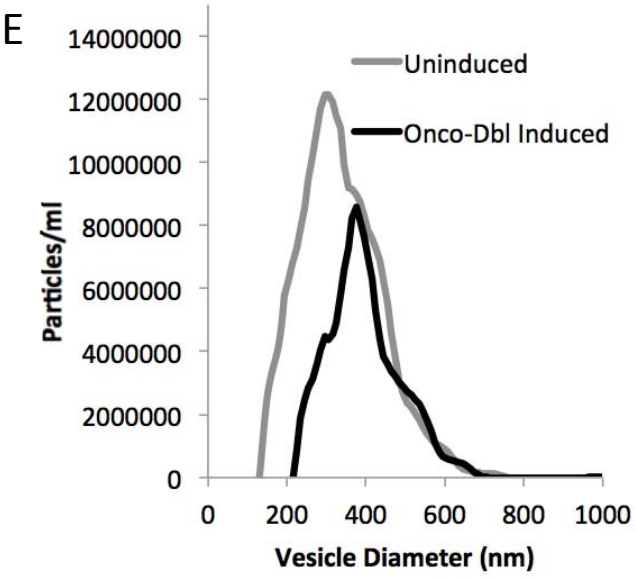
E
Uninduced
Onco-Dbl Induced
Particles/ml
14000000
12000000
10000000
8000000
6000000
4000000
2000000
0
0
200
400
600
800
1000
Vesicle Diameter (nm)

2.2C). A portion of these MV preparations were also lysed and analyzed by Western blot to detect the MV marker protein flotillin. Figure 2.2D shows that flotillin is readily detectable in the MVs isolated from both control MEFs and from cells expressing onco-Dbl (top panel, lanes labeled MVs). Importantly, the cytosolic signaling protein IkBa was only detected in the whole cell lysates (second panel, lanes labeled WCL), indicating that the MV preparations were devoid of cytosolic contaminants.

These same MV preparations were also subjected to nanoparticle tracking analysis (NTA) to determine the size and amount of MVs in each sample. Consistent with our TEM results, NTA showed that the MVs generated by these cells range in size from ~200-700 nm, with most of them averaging ~300-400 nm (Figure 2.2E). Interestingly, this analysis also showed that the uninduced control MEFs actually shed slightly more MVs into their culturing medium than the MEFs expressing onco-Dbl (Figure 2.2E), indicating that non-transferred cells are capable of generating equivalent, if not slightly greater, amounts of MVs than their transformed counterparts.

MVs generated by MEFs expressing onco-Dbl promote the survival and anchorage-independent growth of cells

We then set out to determine whether MVs generated by non-transformed MEFs, versus MVs from MEFs transformed by onco-Dbl, exhibit distinct functional capabilities. Thus, MVs generated by each of these cell types were isolated, quantified using NTA, and normalized based on MV number. The MVs were then added to cultures of serum-starved NIH-3T3 cells for 48 hours (Figure 2.3A), at which point the amount of cell death for each condition was determined by staining the cells with DAPI to identify condensed or blebbed (apoptotic) nuclei.

Figure 2.3. Onco-Dbl-transformed MEFs generate MVs capable of strongly promoting cell survival and inducing cellular transformation.
(**A**), Schematic of the cell death and soft agar assays performed. For the cell death assay, serum starved plates of NIH-3T3 cells were incubated without (serum starved) or with an equivalent amount of MVs derived from either control MEFs (Uninduced MVs) or MEFs induced to express onco-Dbl (Onco-Dbl Induced MVs). The MVs from the control MEFs were also added at twice the concentration (2x Unind. MVs). As a positive control, a plate of NIH-3T3 cells were maintained in medium supplemented with serum (2% serum). Approximately 48 hours later, the cells were analyzed for apoptotic nuclei. (**B**) The results of the cell death assay described in (A). Soft agar assays were carried out on NIH-3T3 fibroblasts that were either left untreated (No MVs), or treated with MVs derived from control MEFs (Uninduced MVs) and MEFs expressing onco-Dbl (Onco-Dbl induced MVs). Representative bright field images of the soft agar assays are shown in (**C**), while (**D**) shows the number of colonies that formed for each condition. The experiments performed in (B-D) were performed a minimum of 3 separate times, with each experiment yielding similar results. The data shown in (B and D) represents the mean ± the SD. Student t-tests were performed. *$p<0.05$; ***$p<0.001$; n.s., not significant.

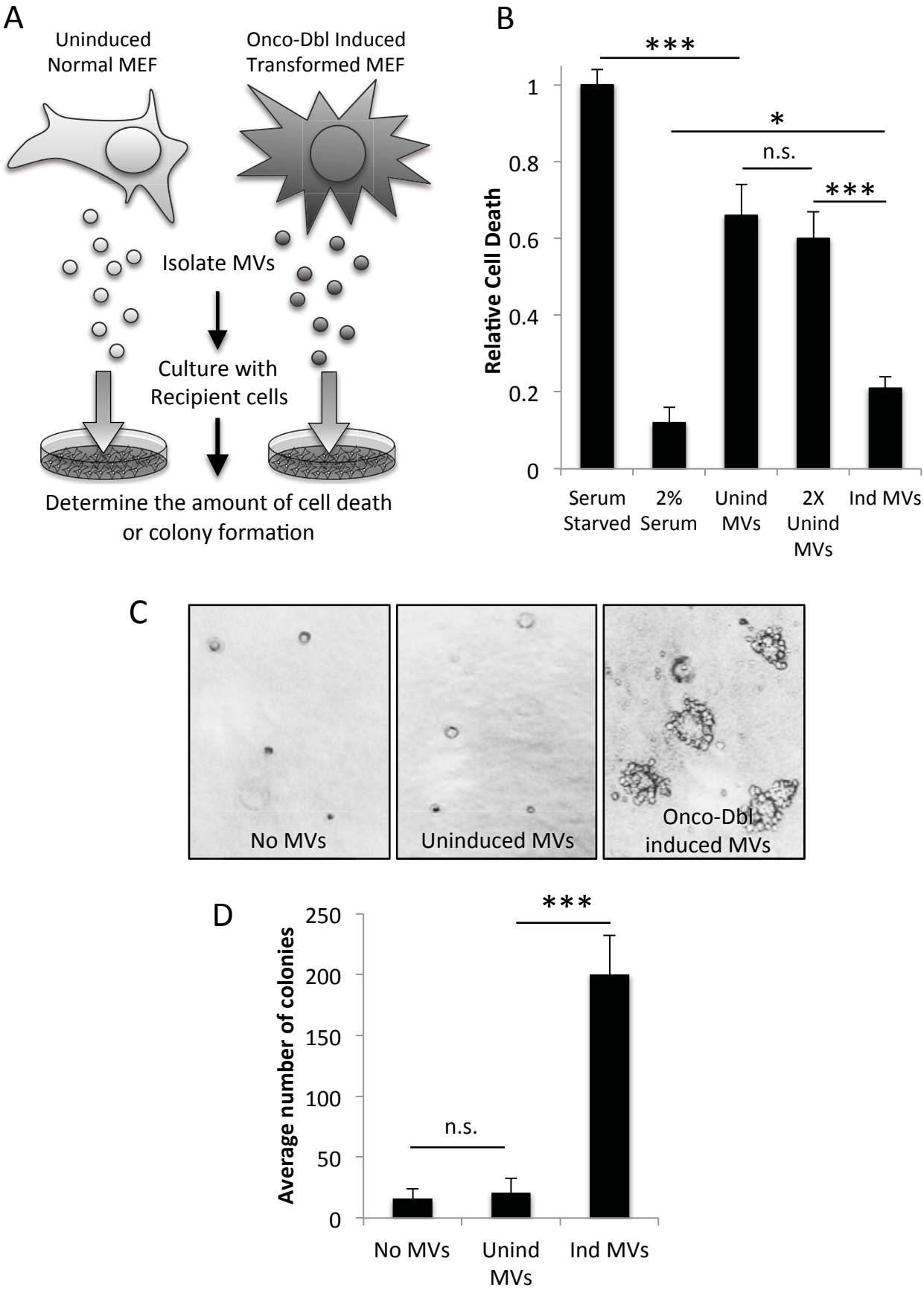
A
Uninduced
Normal MEF
Onco-Dbl Induced
Transformed MEF
Isolate MVs
Culture with
Recipient cells
Determine the amount of cell death
or colony formation
B
***
*
n.s.
***
Relative Cell Death
1
0.8
0.6
0.4
0.2
0
Serum
Starved
2%
Serum
Unind
MVs
2X
Unind
MVs
Ind MVs
C
No MVs
Uninduced MVs
Onco-Dbl
induced MVs
D
***
Average number of colonies
250
200
150
100
50
0
n.s.
No MVs
Unind
MVs
Ind MVs

Approximately 60-70% of the NIH-3T3 cells cultured in serum-free medium underwent cell death (Figure 2.3B, first bar). When NIH-3T3 cells were cultured in serum-free media supplemented with MVs derived from uninduced control MEFs, a modest reduction (~30%) in cell death was observed (Figure 2.3B, compare the first and third bars). Doubling the amount of these MVs did not reduce the extent of cell death further (compare the third and fourth bars), suggesting a maximal MV dose for conferring a survival advantage had been achieved in these experiments. However, when NIH-3T3 cells were cultured in serum-free medium supplemented with MVs from MEFs expressing onco-Dbl, the apoptotic rate was dramatically reduced and approached the extent of protection from cell death that was provided when culturing cells in 2% serum (Figure 2.3B, compare the second and fifth bars).

The ability of MVs derived from MEFs expressing onco-Dbl to induce the anchorage-independent growth (i.e. colony formation in soft agar) of the non-transformed NIH-3T3 cell line was also determined (Figure 2.3A). As expected, NIH-3T3 cells either left untreated (no MVs), or treated with MVs from the uninduced control MEFs for 14 days, remained primarily as single cells (Figure 2.3C, first two panels). However, when the same cells were treated with MVs derived from the transformed MEFs they began to form colonies (Figure 2.3C, last panel, and Figure 2.3D, compare the first two bars and the third bar), similar to what was observed with MVs isolated from highly aggressive brain and breast cancer cells (6).

These findings suggested that MVs generated by transformed cells may contain distinct cargo that enables them to promote the anchorage-independent growth and survival of cells to a much greater degree compared to MVs isolated from non-transformed MEFs. To identify such cargo, lysates prepared from control and transformed cells, as well as the lysates of the MVs shed by these cells, were subjected to Western blot analysis to detect proteins linked to cell

survival. We examined MV lysates for the presence of a number of signaling proteins linked to cell survival. One that stood-out was FAK, a non-receptor tyrosine kinase that is overexpressed and/or hyper-active in many different cancer cell types, where it has been shown to participate in the maintenance of the transformed phenotype, including the evasion of apoptosis and promotion of anchorage independent growth (23-27). In fact, targeting FAK for inactivation is currently being used as a strategy to treat several different types of human cancer (28, 29). Figure 2.4A shows that FAK is expressed at similar levels in control MEFs and MEFs expressing onco-Dbl (top panel; lanes labeled WCL). However, while FAK was only barely detectable in the MVs derived from control MEFs, a significantly greater amount of FAK was present in MVs derived from cells induced to express onco-Dbl (top panel, lanes labeled MVs). Quantifying the levels of FAK in MVs isolated from control MEFs, versus MVs obtained from MEFs expressing onco-Dbl, indicated that there was ~12-fold more FAK in MVs generated by transformed cells (Figure 2.4B).

We then determined whether the non-receptor tyrosine kinase c-Src and the protein scaffold paxillin, two proteins that cooperate with FAK and mediate cell growth and survival (30, 31), are also enriched in MVs generated by the transformed MEFs. While similar amounts of c-Src were detected in MVs from the uninduced control MEFs and MEFs expressing onco-Dbl (Figure 2.4A, second panel, lanes labeled MVs), paxillin was absent from both of these MV preparations (third panel, lanes labeled MVs). These findings further underscore that FAK is uniquely enriched in MVs generated by transformed MEFs.

To determine if FAK was present in the smaller class of EVs referred to as exosomes, the total EVs shed by non-transformed and onco-Dbl-transformed MEFs were separated by collecting the MVs on a 0.22μm filter and comparing their protein contents to those of exosomes

Figure 2.4. MVs generated by transformed MEFs and aggressive breast cancer cells contain FAK.

(**A**) Western blot analysis using FAK, Src, Paxillin, IκBα, and flotillin antibodies was performed on control MEFs and MEFs expressing onco-Dbl (lanes labeled WCL), as well as on the MVs that these cells generated (lanes labeled MVs). Note that FAK is uniquely enriched in MVs derived from the MEFs expressing onco-Dbl. (**B**) The relative amounts of FAK detected in MVs generated by control (uninduced) MEFs and MEFs expressing onco-Dbl (onco-Dbl induced) was determined across several experiments. The data represents the mean ± SD. Student t-tests were performed. ***$p<0.001$. (**C**) Western Blot analysis using FAK, IκBα, and flotillin antibodies was performed on uninduced MEFs and MEFs expressing onco-Dbl (lanes labeled WCL), as well as on the exosomes (lanes labeled Exosomes) and MVs (lanes labeled MVs) these cells generated. The blots were also probed with a CD-63 antibody, an exosome-specific marker. The vertical lines placed through the blots indicate where a small portion of each blot was deleted. Note that FAK is present only in the MVs from MEFs expressing onco-Dbl. (**D**) Western Blot analysis using FAK, IκBα, HA, and flotillin antibodies was performed on normal MCF-10A mammary epithelial cells and MDAMB231, BT-549, and Hs-578T breast cancer cells (lanes labeled WCL), as well as on the MVs that these various cell lines generated (lanes labeled MVs). The experiments in *(A-D)* were performed a minimum of 3 separate times and molecular weight markers (in kDa) have been included along the right side of the blots shown in (A, C, and D).

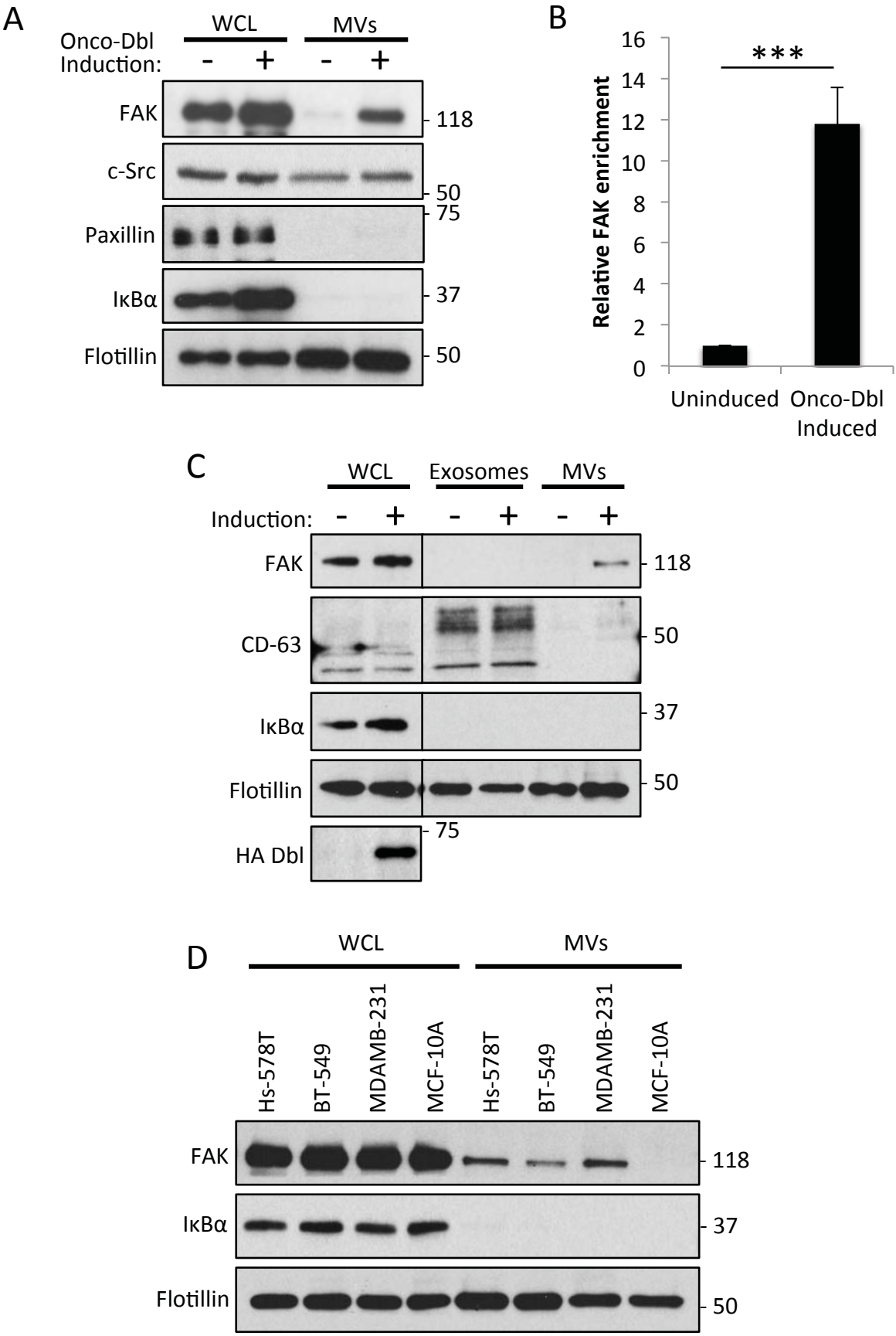
A
WCL
MVs
Onco-Dbl Induction:
- + - +
FAK
c-Src
Paxillin
IκBα
Flotillin
118
50
75
37
50
B
***
Relative FAK enrichment
16
14
12
10
8
6
4
2
0
Uninduced
Onco-Dbl Induced
C
WCL
Exosomes
MVs
Induction:
- + - + - +
FAK
CD-63
IκBα
Flotillin
HA Dbl
118
50
37
50
75
D
WCL
MVs
Hs-578T
BT-549
MDAMB-231
MCF-10A
Hs-578T
BT-549
MDAMB-231
MCF-10A
FAK
IκBα
Flotillin
118
37
50

collected from the flow-through following centrifugation at 100,000xg. Figure 2.4C shows that the exosome preparation contains the specific exosomal marker CD-63, whereas the MV fraction does not (second panel, compare the lanes labeled Exosomes and MVs). It should be noted that FAK is only present in whole cell lysates (WCLs), and lysates collected from MVs derived from transformed MEFs (top panel).

We then examined whether the levels of FAK were similarly increased in MVs generated by human breast cancer cells. The non-malignant mammary epithelial MCF-10A cell line, together with several highly aggressive, triple-negative breast cancer cell lines including MDAMB231, BT-549, and Hs-578T cells, were cultured and the MVs shed by each of these cell lines were isolated. Figure 2.4D shows that each of these cell lines expressed comparable levels of FAK (top panel, lanes labeled WCL). However, while FAK was absent in MVs isolated from the normal mammary MCF-10A cell line, its expression was readily detectable in the MVs derived from each of the breast cancer cell lines (top panel, compare the lanes labeled MVs).

FAK plays an important role in the ability of MVs from transformed cells to promote cell growth and survival

We set out to determine whether FAK in the MVs from the MEFs expressing onco-Dbl was necessary for their strong cell survival and anchorage-independent growth promoting capabilities. As a first step toward addressing this question, we collected MVs generated by control MEFs and MEFs expressing onco-Dbl, and confirmed that FAK is preferentially loaded in MVs isolated from cells expressing onco-Dbl (Figure 2.5A, second panel, compare lanes labeled MVs). Interestingly, we found that activated FAK, as well as the activated form of its major binding partner, c-Src (32), were both present in these MVs, as detected by Western

Figure 2.5. The FAK associated with MVs can be transferred to recipient cells and activate intracellular signaling events.
(**A**) Lysates of control MEFs (uninduced) and MEFs induced to express onco-Dbl (lanes labeled WCL), as well as lysates of the MVs that these cells generated (lanes labeled MVs) were subjected to Western blot analysis using an antibody that recognizes FAK when it is phosphorylated on tyrosine 397 (P-FAK^{Tyr397}). The blot was also probed with FAK, P-c-Src^{Tyr416}, IκBα, and flotillin antibodies. (**B**) and (**C**) Multiple sets of MEFs expressing onco-Dbl were either mock transfected, or transfected with an HA-tagged form of FAK (HA-FAK). (B) One set of the transfectants (lanes labeled WCL), and the MVs that they generated (lanes labeled MVs) were subjected to Western blot analysis using HA and flotillin antibodies. (C) the MVs generated by another set of transfectants was collected and then incubated with NIH-3T3 fibroblasts for 2 hours, at which point immunofluorescence using an HA antibody was carried out on the cells. The cells were also stained with phalloidin to label F-actin. Note that the HA-FAK can be detected as puncta on the surface of the cells treated with MVs expressing HA-FAK (arrows). (**D**) Serum starved cultures of NIH-3T3 fibroblasts were treated without (time=0) or with an equivalent amount of MVs isolated from either control MEFs (lanes labeled treatment with MVs from uninduced MEFs) or MEFs expressing onco-Dbl (lanes labeled treatment with MVs from onco-Dbl induced MEFs) for the indicated length of time and lysed. Western blot analysis was performed on the cell lysates using P-FAK^{Tyr397}, FAK, P-AKT, AKT, P-ERK 1/2, and ERK 1/2 antibodies. The experiments in (A-D) were performed a minimum of 3 separate times, with each experiment yielding similar results. Molecular weight markers (in kDa) have been included along the right side of each of the blots shown in (A, B, and D).

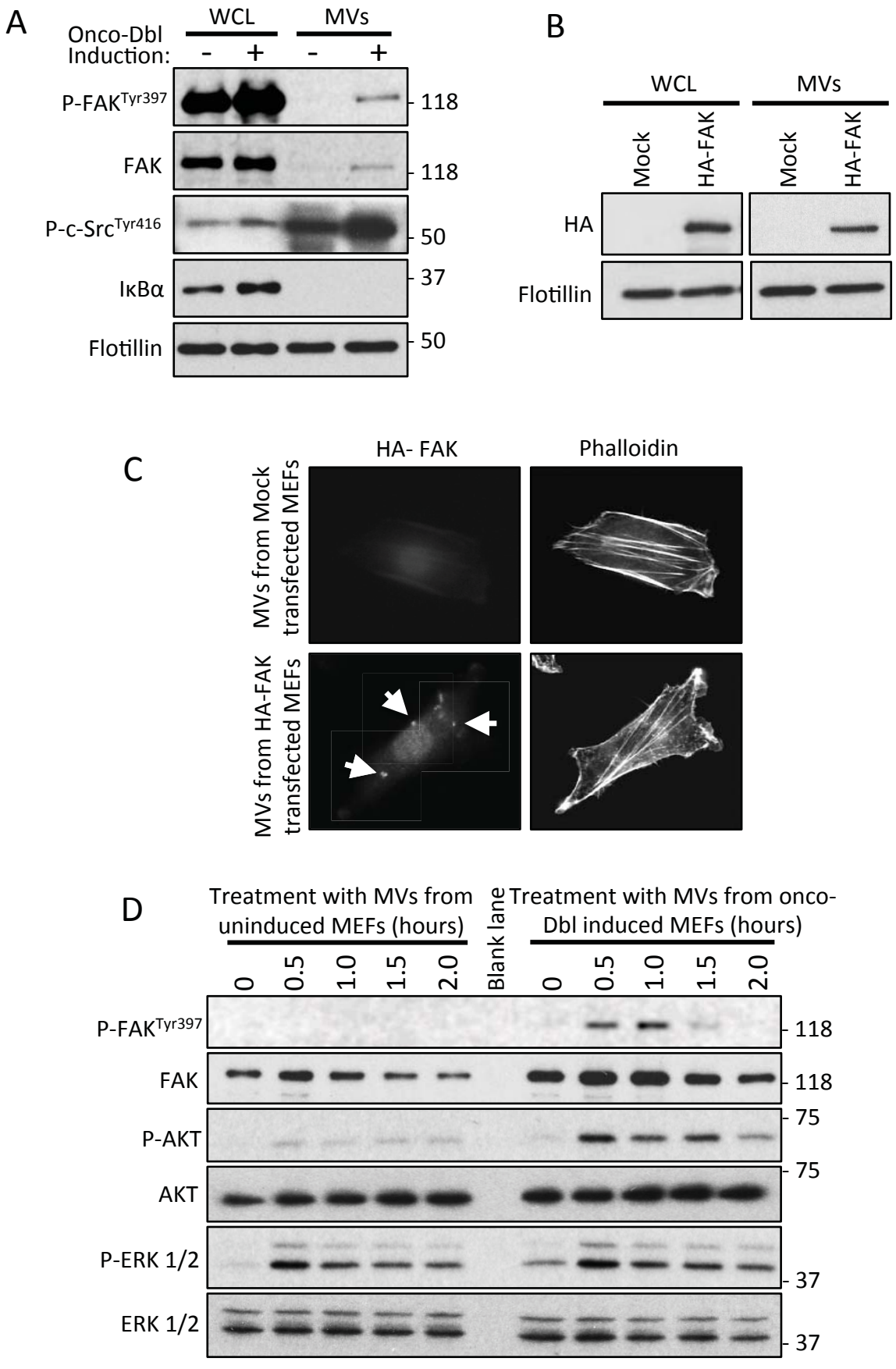
A
WCL
MVs
Onco-Dbl Induction:
- + - +
P-FAK Tyr397
FAK
P-c-Src Tyr416
IκBα
Flotillin
118
118
50
37
50
B
WCL
MVs
Mock
HA-FAK
Mock
HA-FAK
HA
Flotillin
C
HA- FAK
Phalloidin
MVs from Mock transfected MEFs
MVs from HA-FAK transfected MEFs
D
Treatment with MVs from uninduced MEFs (hours)
Blank lane
Treatment with MVs from onco-Dbl induced MEFs (hours)
0 0.5 1.0 1.5 2.0
0 0.5 1.0 1.5 2.0
P-FAK Tyr397
FAK
P-AKT
AKT
P-ERK 1/2
ERK 1/2
118
118
75
75
37
37

blotting MV lysates with antibodies that detect FAK phosphorylated at tyrosine 397 (P-FAK^{Tyr397}) and c-Src phosphorylated at tyrosine 416 (P-Src^{Tyr416}) (Figure 2.5A, top two panels, fourth lane). These findings raise the interesting possibility that FAK and c-Src may form a complex in MVs that is capable of strongly activating downstream signaling events (33, 34).

To demonstrate that the FAK present in the MVs can be transferred to recipient cells, we took advantage of the fact that transformed MEFs transiently transfected with a HA-tagged form of FAK (Figure 2.5B, top panel, lanes labeled WCL), generate MVs that contain the ectopically expressed protein (top panel, lanes labeled MVs). We then prepared MVs derived from onco-Dbl-expressing MEFs that had been either mock transfected, or transfected with HA-tagged FAK, and incubated these preparations with cultures of NIH-3T3 fibroblasts for 2 hours, at which time the cells were washed extensively, fixed, and then stained with an HA-antibody and rhodamine-conjugated phalloidin to label F-actin. Figure 2.5C shows that the NIH-3T3 fibroblasts treated with MVs from the mock-transfected cells lacked any detectable HA-FAK expression (upper left panel). On the other hand, HA-FAK could be detected as small puncta along the surfaces of cells treated with MVs collected from transformed MEFs ectopically expressing the FAK construct (lower left panel, see arrows).

We then examined whether the activated FAK present in MVs can induce signaling events in recipient cells. MVs collected from either control MEFs or MEFs expressing onco-Dbl were added to cultures of serum-starved NIH-3T3 fibroblasts for increasing lengths of time. Figure 2.5D shows that within 0.5 hours of treating cells with MVs from MEFs expressing onco-Dbl, an increase in the level of phosphorylated FAK could be detected, with maximal phosphorylation occurring at 1 hour (top panel, lanes labeled treatment with MVs from onco-Dbl induced MEFs). This increase in FAK phosphorylation was not observed in NIH-3T3 cells treated with MVs

isolated from control MEFs (top panel, lanes labeled treatment with MVs from uninduced MEFs). Because the MVs expressing HA-tagged FAK appear to remain primarily on the surface of recipient cells for up to 2 hours, we suspect that the FAK associated with MVs generated by transformed cells is most likely sending signals from the cell surface. Consistent with this idea, we have found that the phosphorylation level of AKT, a downstream effector of FAK (35), is preferentially activated in a time-dependent fashion by MVs from transformed cells (Figure 2.5D, third panel). It is worth mentioning that this appears to be a specific signaling outcome, as the MVs isolated from both uninduced and onco-Dbl expressing MEFs were able to stimulate ERK activation to similar extents (Figure 2.5D, fifth panel).

We then set out to build upon this finding by directly assaying whether the MV-mediated transfer of FAK to recipient cells accounted for the ability of MVs from MEFs expressing onco-Dbl to strongly promote cell survival, by performing two sets of experiments. In the first set, we obtained conditioned medium from cultures of control MEFs, or MEFs expressing onco-Dbl, and treated them without or with the FAK III inhibitor, a small molecule that undergoes a covalent interaction with FAK and blocks its activation (36). MVs were then isolated from the conditioned medium using a 0.22μm filter to remove any unbound (freely soluble) inhibitor. A portion of the isolated MVs was lysed and Western blotted using phospho-FAK^{Tyr397} and total FAK antibodies. While the MVs from the transformed MEFs treated with the FAK III inhibitor still contained FAK (Figure 2.6A, middle panel, compare the fifth and sixth lanes), the extent of its phosphorylation was greatly diminished (Figure 2.6A, top panel, compare the fifth and sixth lanes). These MVs were then added to cultures of NIH-3T3 cells that were being serum-starved. Two days later, the cells were collected and the amount of cell death for each condition was determined. Figure 2.6B shows that the relative ability of MVs from transformed cells to

Figure 2.6. The activated FAK associated with MVs from transformed MEFs is important for their cell growth and survival promoting capabilities.
(**A-C**). MVs isolated from control MEFs (uninduced), or MEFs expressing onco-Dbl, were treated without or with 5μM of the FAK III inhibitor for 2 hours, at which point any unbound inhibitor was removed by filtration using a 0.22μm filter and extensive rinsing with PBS. (**A**) One set of the MV preparations (lanes labeled MVs), as well as the cells that generated the MVs (lanes labeled WCL), were lysed and subjected to Western blot analysis using P-FAK^{Tyr397}, FAK, and flotillin antibodies. Molecular weight markers (in kDa) have been included along the right side of the blot. (**B**) Another set of the MV preparations was added to serum starved NIH-3T3 fibroblasts. Approximately 48 hours later the cells were collected and stained with DAPI to identify condensed/blebbed (apoptotic) nuclei. (**C**) Anchorage-independent growth assays were performed on NIH-3T3 fibroblasts supplemented without (no MVs) or with another set of the MV preparations. The experiments in (A-C) were carried out a minimum of 4 separate times, each time yielding similar results. The data shown in (B and C) represents the mean ± SD. Student t-tests were performed. **$p<0.01$; ***$p<0.001$; n.s., not significant.

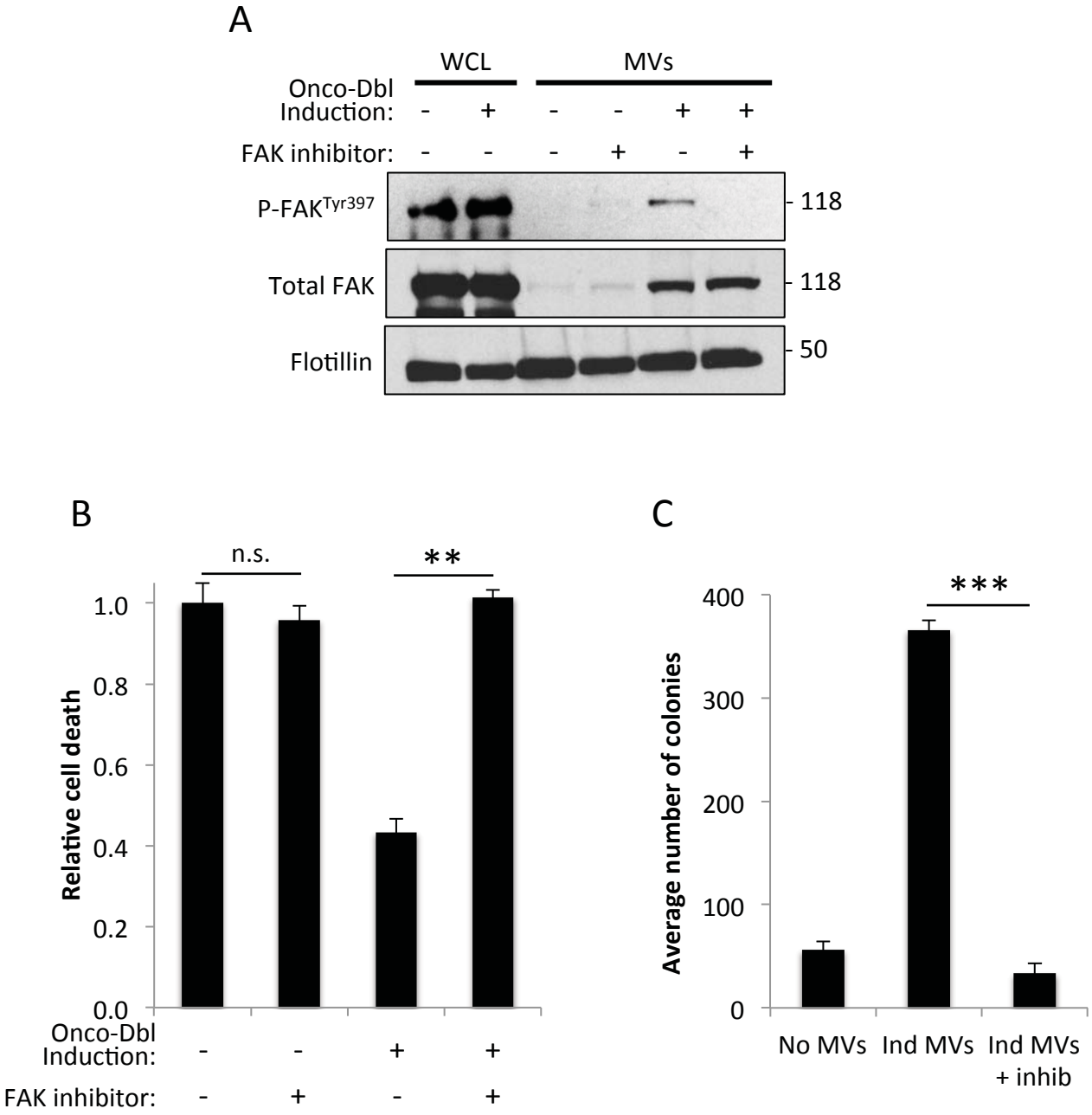
A
WCL
MVs
Onco-Dbl Induction:
- + - - + +
FAK inhibitor:
- - - + - +
P-FAK Tyr397
Total FAK
Flotillin
118
118
50
B
n.s.
**
Relative cell death
1.0
0.8
0.6
0.4
0.2
0.0
Onco-Dbl Induction:
- - + +
FAK inhibitor:
- + - +
C
***
Average number of colonies
400
300
200
100
0
No MVs
Ind MVs
Ind MVs + inhib

promote cell survival is completely lost under conditions where the activity of FAK associated with the MVs was inhibited, prior to adding the MVs to the serum-starved cells (compare the third and fourth bars). As a control, we verified that the relative extent of cell death for NIH-3T3 cells incubated with MVs from control MEFs was unaffected by the FAK inhibitor (Figure 2.6B, compare first and second bars). Moreover, the ability of the MVs isolated from onco-Dbl expressing MEFs to induce the anchorage-independent growth of NIH-3T3 cells was also blocked by inhibiting the FAK activity associated with these MVs (using the FAK inhibitor) prior to adding them to the NIH-3T3 cells (Figure 2.6C, compare second and third bars).

As a complimentary approach, we knocked down FAK in control and onco-Dbl expressing MEFs. The FAK-targeting siRNA reduced endogenous FAK expression by at least 85% in the control MEFs, and ~70% in the MEFs expressing onco-Dbl (Figure 2.7A, top panel, lanes labeled WCL). Knocking-down FAK in the transformed MEFs also effectively decreased FAK levels in their MVs (Figure 2.7A, top panel, lanes labeled MVs). Using NTA to determine the concentration of MVs in each of the various MV preparations, we normalized them and then compared the ability of an equivalent number of MVs isolated from control MEFs, or MEFs expressing onco-Dbl, that had been transfected with either control or FAK-targeting siRNAs, to promote cell survival. Figure 2.7B shows again that MVs from the MEFs expressing onco-Dbl are capable of promoting the survival of serum-starved NIH-3T3 cells (compare first and third bars). However, this advantage was lost when FAK levels in the MVs were reduced as a result of depleting FAK expression in the cells (Figure 2.7B, compare third and fourth bars).

These experiments were expanded to determine whether FAK expressed in MVs derived from the highly aggressive MDBMB231 breast cancer cell line also promoted cell survival. Cultures of MDAMB231 cells were transfected with either control or FAK-targeting siRNA and

Figure 2.7. Knocking-down FAK expression in MEFs expressing onco-Dbl decreases the survival-promoting capabilities of their MVs.
(**A**) Control MEFs, or MEFs induced to express onco-Dbl, were transfected with either control or FAK-targeting siRNA. Western blot analysis using a FAK antibody was performed on the cells (lanes labeled WCL) and the MVs that these cells generated (lanes labeled MVs). The blots were also probed with flotillin, actin, and IκBα antibodies. (**B**) NIH-3T3 cells were placed in serum free medium without or with an equivalent amount of MVs generated by each of the cells described in (A). About 48 hours later, the cells were stained with DAPI to identify the condensed/blebbed (apoptotic) nuclei. Note the amount of cell death seen for each condition is relative to the level of cell death observed in cells cultured with MVs from uninduced MEFs. (**C**) MDAMB231 breast cancer cells were transfected with either control or FAK-targeting siRNA. Western blot analysis using a FAK antibody was performed on the cells (lanes labeled WCL) and the MVs that these cells generated (lanes labeled MVs). (**D**) NIH-3T3 cells were cultured in serum free medium without or with an equivalent amount of MVs generated by the cells described in (C). About 48 hours later, the cells were stained with DAPI to identify condensed or blebbed (apoptotic) nuclei. The experiments in (A-D) were performed 3 separate times, each time yielding similar results. Molecular weight markers (in kDa) have been included along the right side of each blot shown in (A and C). The data shown in (B and D) represents the mean ± SD. Student t-tests were performed. *$p<0.05$; **$p<0.01$; ***$p<0.001$.

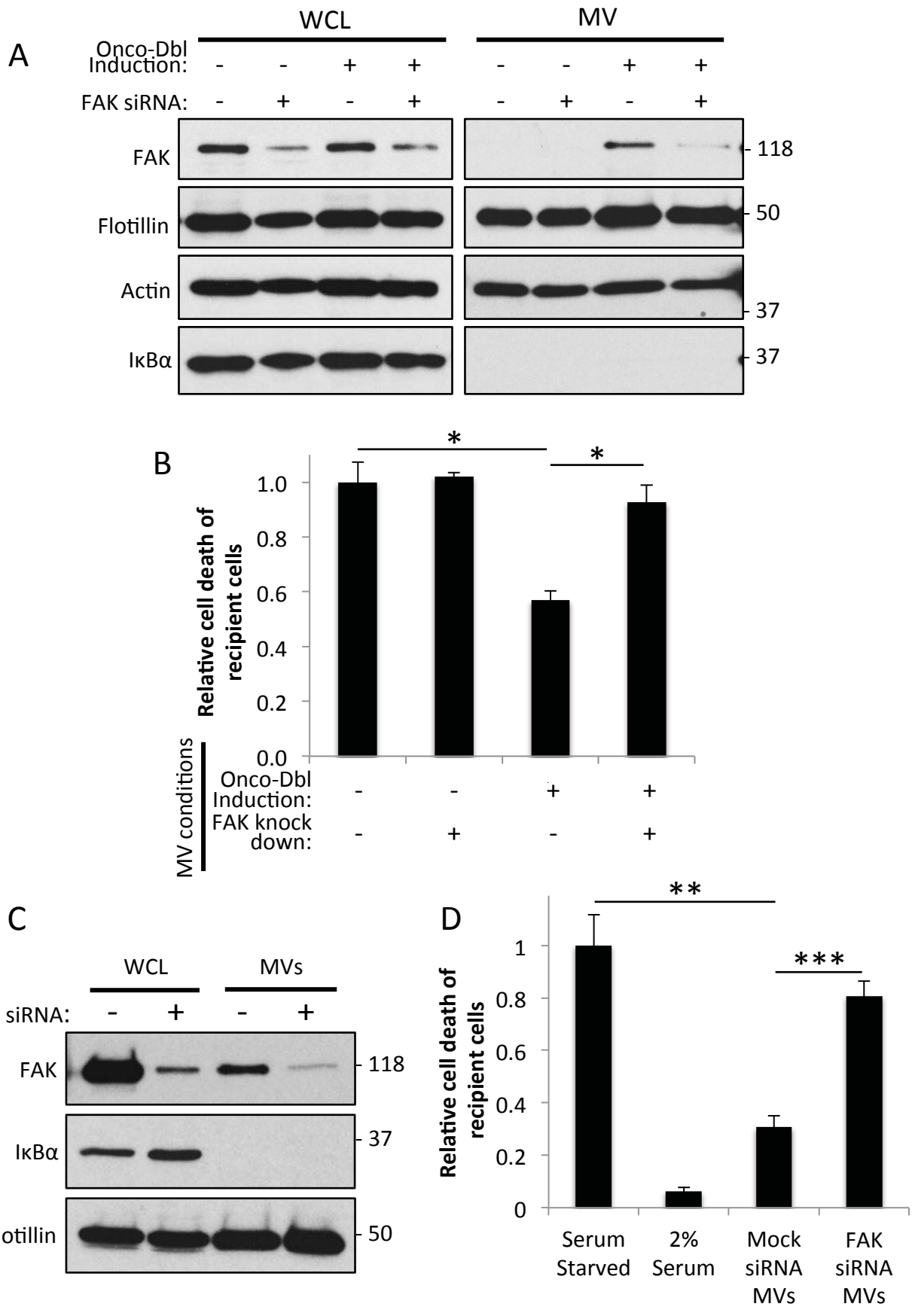
A
WCL
MV
Onco-Dbl Induction:
FAK siRNA:
FAK
Flotillin
Actin
IκBα
118
50
37
37
B
Relative cell death of recipient cells
1.0
0.8
0.6
0.4
0.2
0.0
MV conditions
Onco-Dbl Induction:
FAK knock down:
C
WCL
MVs
FAK siRNA:
FAK
IκBα
Flotillin
118
37
50
D
Relative cell death of recipient cells
1
0.8
0.6
0.4
0.2
0
Serum Starved
2% Serum
Mock siRNA MVs
FAK siRNA MVs

the levels of FAK in these cells, or in the MVs generated by the MDAMB231 cells, were determined. Figure 2.7C shows that the FAK-targeting siRNA decreased FAK expression in the cells, and also in the MVs from these cells, by ~75%. We then performed NTA on the MVs collected from MDAMB231 cells in order to normalize the MV preparations, so as to assess the function of an equivalent number of vesicles isolated from MDAMB231 cells that had been transfected with either control or FAK-targeting siRNAs. Figure 2.7D shows that the MVs isolated from MDAMB231 cells are able to confer a survival advantage upon serum-starved NIH-3T3 cells (compare first and third bars). However, this advantage is significantly reduced upon knocking-down FAK expression in the donor cells (Figure 2.7D, compare bars 3 and 4).

Ectopically expressing a kinase-dead form of FAK in MVs derived from transformed MEFs reduces their cell survival promoting capabilities

To further demonstrate the importance of FAK in the ability of MVs derived from transformed/cancer cells to promote cell survival, we ectopically expressed HA-tagged forms of wild-type FAK (FAK WT) and a kinase-dead form of FAK (FAK KD) that was generated by mutating an essential lysine residue (lysine 454) to arginine (37), in MEFs induced to express onco-Dbl. Figure 2.8A shows that both forms of FAK can be detected in the cells (panels labeled Donor MEFs), as well as in the MVs derived from the cells (panels labeled MVs from Donor MEFs). Thus, the kinase activity of FAK is not required for its incorporation into MVs. Interestingly, the ectopic expression of kinase-dead FAK in the MEFs expressing onco-Dbl led to a reduction in the overall levels of FAK activity in the MEFs (panels labeled Donor MEFS), as well as the MVs they generated (panels labeled MVs from Donor MEFs). The remaining portion of the isolated MVs were incubated with NIH-3T3 fibroblasts for 2 hours, and lysed. Western

blot analysis of these NIH-3T3 cell lysates revealed that the ectopically expressed HA-tagged forms of WT FAK and FAK KD could be detected in the cells (Figure 2.8A, panels labeled Recipient Fibroblasts).

Survival assays were then carried out on serum-starved NIH-3T3 fibroblasts that were treated without (just serum-starved) or with MVs derived from onco-Dbl transformed MEFs, which had been mock transfected or transfected with either HA-FAK WT or HA-FAK KD. The ability of the ectopically expressed HA-FAK WT to become incorporated into MVs derived from the transformed MEFs did not change their ability to promote cell survival, compared to MVs from the mock transfected cells (Figure 2.8B, compare the second and third bars). On the other hand, MVs from the transformed MEFs containing the kinase-dead form of FAK significantly reduced their survival-promoting capabilities (compare the second and fourth bars). These findings, combined with those showing that transiently expressing HA-tagged FAK WT, but not FAK KD in NIH-3T3 fibroblasts (Figure 2.8C, top panel), is sufficient to promote cell survival (Figure 2.8D), supports the conclusion that activated FAK contained in the MV derived from transformed or cancer cells plays a key role in mediating their survival promoting capabilities.

Discussion

Only a short time ago, EVs were considered to be nothing more than cell debris. Now, however, EVs are recognized as a genuine form of cell-cell communication that has far reaching implications in physiological processes and disease progression (4, 38, 39). This has been perhaps best studied in the context of human cancer, where EVs have been linked to a number of stages of cancer progression including the shaping of the tumor microenvironment, angiogenesis, and the creation of the pre-metastatic niche at secondary sites of tumor colony formation (10, 40,

Figure 2.8. Ectopically expressing a kinase-dead form of FAK in MVs derived from transformed MEFs reduces their cell survival promoting capabilities.
(**A**) MEFs induced to express onco-Dbl were mock transfected, or transfected with HA-tagged forms of either FAK WT or FAK KD, and lysed. The MVs generated by these cells were also collected and a portion of them were directly lysed, while the rest of the isolated MVs were added to cultures of NIH-3T3 fibroblasts for 2 hours, before the cells were lysed. Western blot analysis using HA, P-FAK^{Tyr397}, FAK, and actin antibodies was performed on the transfected MEFs (panels labeled Donor MEFs), the MVs that the cells generated (panels labeled MVs from Donor MEFs), as well as on the NIH-3T3 cells that were treated without (no MVs added) or with the various MV preparations (panels labeled Recipient Fibroblasts). (**B**) NIH-3T3 cells were cultured in serum-free medium supplemented without (serum starved) or with MVs collected from onco-Dbl transformed MEFs that had been mock transfected, or transfected with HA-tagged forms of either FAK WT or FAK KD. Approximately 48 hours later, the cells were stained with DAPI to identify the condensed/ blebbed (apoptotic) nuclei. (**C**) Western blot analysis using HA, FAK, and actin antibodies was performed on NIH-3T3 cells that had been mock transfected, or transfected with either HA-tagged forms of FAK WT or FAK KD. (**D**) NIH-3T3 cells that had been mock transfected, or were ectopically expressing HA-tagged FAK WT or HA-tagged FAK KD, were serum starved for ~48 hours, at which point the cells were stained with an HA antibody to identify the transfectants and DAPI to identify condensed/blebbed (apoptotic) nuclei. The experiments in (A-D) were performed 3 separate times, each time yielding similar results. Molecular weight markers (in kDa) have been including along the right side of each blot shown in (A and C). The data shown in (B and D) represents the mean ± SD. Student t-tests were performed. *$p<0.05$; ***$p<0.001$; n.s., not significant.

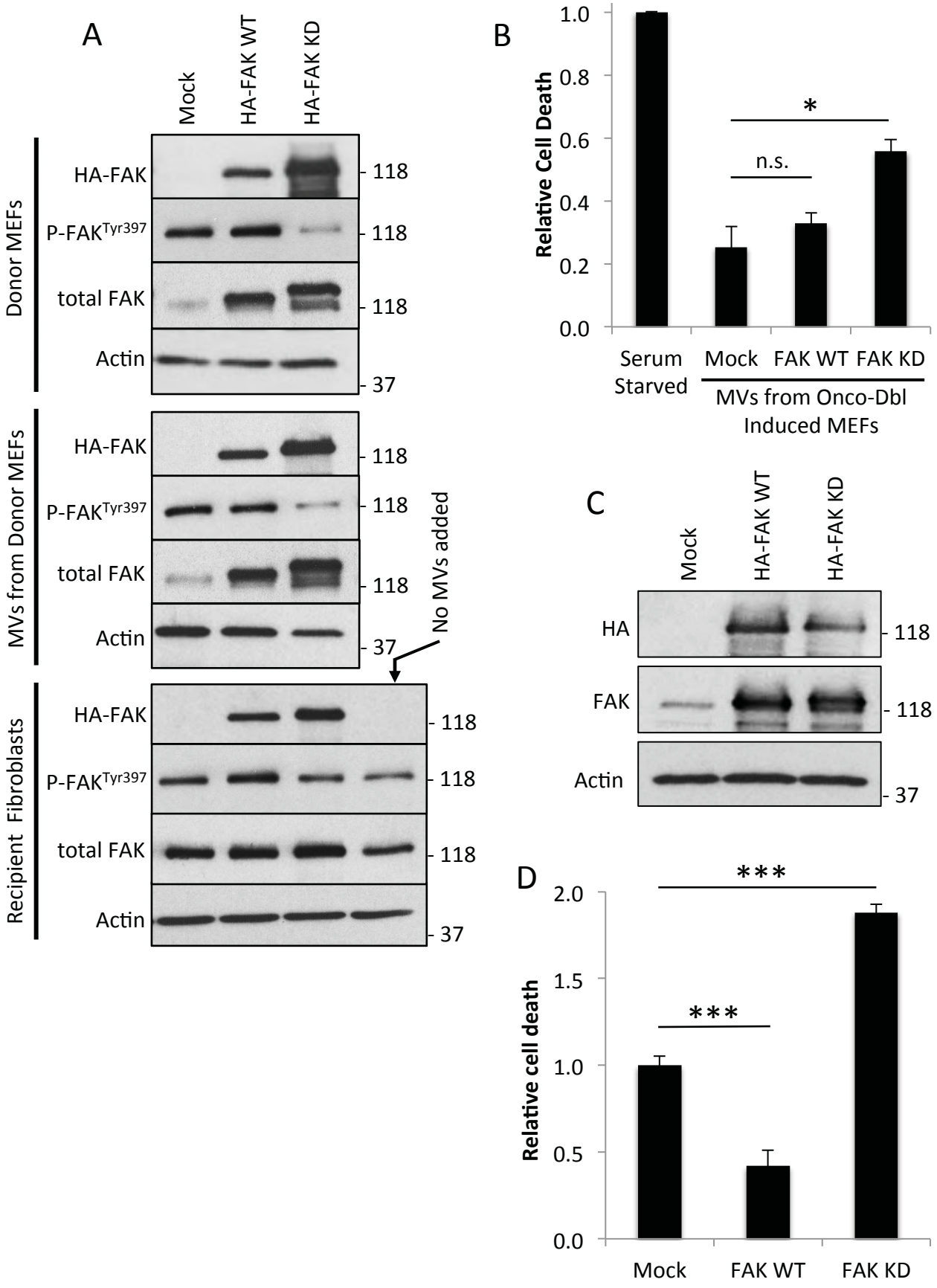
A
Mock
HA-FAK WT
HA-FAK KD
Donor MEFs
HA-FAK
P-FAK^Tyr397
total FAK
Actin
118
118
118
37
MVs from Donor MEFs
HA-FAK
P-FAK^Tyr397
total FAK
Actin
118
118
118
37
No MVs added
Recipient Fibroblasts
HA-FAK
P-FAK^Tyr397
total FAK
Actin
118
118
118
37
B
Relative Cell Death
1.0
0.8
0.6
0.4
0.2
0.0
*
n.s.
Serum Starved
Mock
FAK WT
FAK KD
MVs from Onco-Dbl Induced MEFs
C
Mock
HA-FAK WT
HA-FAK KD
HA
FAK
Actin
118
118
37
D
***
***
Relative cell death
2.0
1.5
1.0
0.5
0.0
Mock
FAK WT
FAK KD

41). The group of larger EVs, MVs, have been especially linked to changes in the tumor microenvironment, as demonstrated in studies showing that MVs isolated from the highly aggressive MDAMB231 breast cancer cell line and the U87 glioblastoma cell line, caused normal (non-transformed) cell lineages to acquire the ability to grow under serum-limiting condition, and survive apoptotic-inducing stresses (6).

MVs have also caught the attention of clinical researchers and pharmaceutical companies, largely because of the realization that cancer cell derived EVs can be isolated from the blood samples of patients suffering from a number of types of cancer including brain, breast, prostate, kidney, and pancreatic (16, 42, 43). This has raised the exciting possibility that MVs, which, given their size, might be the more readily detectable EVs in plasma and tissue fluids, offer a novel and non-invasive source of diagnostic information. However, in order to realize such a possibility, it will be important to establish that MVs shed by transformed/cancer cells in fact contain unique cargo that is not present within their normal cellular counterparts.

Here we set out to establish whether there might be differences both in the number of MVs generated by transformed/cancer cells, versus their non-transformed (non-cancerous) counterparts, as well as in the protein cargo that they contain. We started by using a well-defined system that allows for the inducible expression of the oncogenic Dbl protein in MEFs, resulting in the activation of Rho GTPases and giving rise to a number of transformed phenotypes. Somewhat surprisingly, in the light of the suggestions from some reports that the amount of EVs present in the bloodstream of a cancer patient can be correlated with the aggressiveness and/or grade of a particular tumor, we found that the amount of MVs generated by these cells did not increase upon the induction of oncogenic transformation. However, importantly, we did detect a specific change in the MV cargo from transformed cells. Specifically, we found that only MVs

generated by transformed cells contained the non-receptor tyrosine kinase FAK. Not only was FAK missing from MVs generated by non-transformed (normal) cells, it was also absent from exosomes isolated from either transformed or non-transformed MEFs. We then went on to demonstrate that the same is true in a number of human breast cancer cell lines, i.e. they shed MVs that specifically contained this important signaling kinase.

The presence of FAK within MVs derived from transformed/cancer cells had important functional consequences. Indeed, we found that the ability of these MVs to specifically impart increased survival and anchorage-independent growth capabilities upon non-transformed cells was absolutely dependent upon the vesicles containing FAK. A particularly interesting aspect of these findings concerns how the MV-mediated transfer of FAK to recipient cells, that already contain endogenous levels of this protein kinase, is able to elicit a significant functional outcome. The answer may lie in our findings that the FAK in the MVs from transformed/cancer cells is already activated, and that these microvesicles also contain the major FAK signaling partner c-Src. Thus, it is plausible that the MV-mediated transfer of just activated FAK, or an activated FAK-c-Src signaling complex, to recipient cells may provide a significant boost to the necessary signaling events within the cells to provide growth and survival benefits.

It now appears clear that MVs derived from transformed or cancer cells can drive the recipient cells that they target to undergo marked phenotypic changes, as an outcome of the specific protein cargo that they contain and independent of any changes in total vesicle numbers. The finding that FAK is a unique cargo of these MVs is particularly significant due to the major role that this tyrosine kinase plays in cell migration, metastasis, and inhibition of apoptosis. In particular, FAK is able to activate downstream signaling pathways that ultimately prevent apoptosis by inhibiting the caspase-3 cascade (25). Cancer cells take advantage of this

capability, often by over-expressing FAK (44), and therefore the ability of their MVs to transfer this important signaling kinase to surrounding recipient cells can obviously have important consequences for the microenvironment and tumorigenesis.

Among the important questions for the future will be to better understand how MVs from transformed/cancer cells are loaded with their unique cargo, i.e. what are the mechanisms by which certain key proteins are recruited to the maturing MV while others are excluded. Although, there is a good deal that we still need to learn, it is becoming increasingly clear that the generation of MVs with specific cargo will not only have important implications for cancer progression, but also in the development of new therapeutic strategies to block the spread of disease. Moreover, by taking advantage of the presence of specific cargo such as FAK in cancer cell-derived MVs, new opportunities will emerge for the development of diagnostic disease markers.

Materials and Methods

Cell culture and transfections

The tetracycline-off inducible onco-Dbl MEF cell line was generated as described previously (19). The cells were maintained in DMEM supplemented with 10% Tet system-approved fetal bovine serum (FBS) (Clontech), 100 μg/mL G418 (Gibco), and 1 μg/mL doxycycline (Sigma). To induce onco-Dbl expression, the cells were trypsinized and then plated in doxycycline-free culturing medium, where any residual doxycycline remaining in the cultures was removed by replacing the medium 6 hours after plating the cells. NIH-3T3 cells were maintained in DMEM supplemented with 10% calf serum (Clontech), while the normal mammary MCF10A epithelial cell line, as well as the MDAMB231, BT-549, and Hs-578T breast cancer cell lines, were grown

in RPMI 1640 supplemented with 10% FBS. Expression constructs encoding HA-tagged forms of either wild-type FAK (HA-FAK WT), or a kinase dead form of FAK (HA-FAK KD) that was generated by mutating lysine 454 to arginine (37), were transfected into cells using Lipofectamine (Invitrogen). Control and FAK-targeting siRNAs (Cell Signaling) were introduced into cells with Lipofectamine 2000 (Invitrogen).

Fluorescent Microscopy

Cells grown on glass coverslips were either transfected without or with the indicated expression constructs and siRNAs, or were treated with MVs isolated from MEFs expressing onco-Dbl and HA-tagged FAK WT, and then cultured as indicated. The cells were fixed with 3.7% formaldehyde, permeabilized with phosphate buffered saline (PBS) containing 0.1% Triton-X100, and blocked with 10% bovine serum albumin diluted in PBS. The cells were stained with a HA rabbit polyclonal antibody (Covance) at a dilution of 1:500, followed by incubation with an Oregon green 488-conjugated secondary antibody (Molecular Probes). Rhodamine-conjugated phalloidin (Life Technologies) and 4',6-diamidino-2- phenylindole (DAPI) (Sigma) were used to label actin filaments and nuclei, respectively. To detect MVs on the surfaces of cells, cultures of cells were incubated with the fluorescent membrane dye FM1-43FX (Invitrogen) diluted to 5 μg/ml in PBS for 1 minute, and fixed on ice for 20 minutes. All cells were visualized using a Zeiss Axioscope with a 63X oil objective lens. Digital images of the cells were taken using a Sensicam qe camera (Cooke Company) and processed using IPLABS software (BD Biosciences).

Isolation of MVs and exosomes

For the experiments involving MVs, the conditioned media collected from $2.0x10^6$ serum starved cells was subjected to two consecutive centrifugations at 300×g to clarify the media of cells and cell debris. The partially clarified media was filtered using a Steriflip PVDF filter with a 0.22µm pore size (Millipore) and rinsed 3 times with PBS to remove soluble factors. For cell-based assays, the MVs retained by the filter (vesicles larger than 0.22µm in diameter) were resuspended in serum-free medium. To generate MV lysates, the MVs retained by the filter were lysed using 200 ml of lysis buffer (25 mM Tris, 100 mM NaCl, 1% Triton X-100, 1 mM EDTA, 1 mM DTT, 1 mM $NaVO_4$, 1 mM b-glycerol phosphate, and 1 µg/mL each of aprotinin and leupeptin). Whole cell lysates (WCLs) were prepared by rinsing dishes of cells with PBS, adding 1 mL of lysis buffer, and scraping the cells off the plate. Exosomes were isolated from the conditioned medium that flowed-through the 0.22µm Steriflip filter (i.e. vesicles smaller than 220nm) by centrifugation at 100,000xg for 2 hours. The pelleted exosomes were then lysed with 200µl lysis buffer. The resulting MV, exosome, and cell lysates were centrifuged at 13,000 rpm for 10 minutes and the supernatants were then analyzed.

Immunoblot Analysis

The protein concentrations of the cell lysates, as well as the MV and exosome lysates, were determined using the Bio-Rad DC protein assay (Bio-Rad). The lysates were normalized by protein concentration, resolved by SDS-PAGE, and then the proteins were transferred to PVDF membranes. The membranes were incubated with various primary antibodies including beta-actin (Sigma, 5316), FAK (Cell Signaling, 3285S), flotillin-2 (Cell Signaling, 3436S), phospho-FAK^{Tyr397} (Cell Signaling, 3283S), phospho-src (Cell Signaling, 2101S), Src (Cell Signaling,

2123P), paxillin (BD, 612405), HA (Biolegend, 901503), IκBα (Cell Signaling, 9242), CD63 (ThermoFisher, 10628D), phospho-ERK (Cell Signaling, 9106), ERK (Cell Signaling, 9102), phospho-AKT (Cell Signaling, 2965S), AKT (Cell Signaling, 9272S), diluted 1:1000 in 20 mM Tris, 135 mM NaCl, and 0.02% Tween 20 (TBST). The primary antibodies were detected with HRP-conjugated secondary antibodies (Cell Signaling) followed by exposure to ECL reagent (Pierce).

Anchorage-independent Growth Assay

Control MEFs, MEFs expressing onco-Dbl, or Parental NIH-3T3 cells were plated at a density of 8×10^3 cells/mL in growth medium containing 0.3% agarose, with or without MVs as indicated, onto a base layer composed of growth medium containing 0.6% agarose in 6-well dishes. The soft-agar cultures were re-fed every third day, including the addition of freshly prepared MVs where indicated. After 14 days, the number of colonies that formed for each condition was counted. Each of the assays was preformed a minimum of three times and the results were averaged.

Cell Death Assays

Parental NIH-3T3 cells, or NIH-3T3 cells transfected with the indicated constructs, were plated in each well of a 6-well dish and then cultured in medium containing 2% calf serum or serum-free medium supplemented without or with 1×10^7 MVs derived from control MEFs, MEFs expressing onco-Dbl, or MDAMB231 cells. Twenty-four hours later, the cells were treated with an additional dose of freshly prepared MVs. Forty-eight hours from the start of the assay, the cells were stained with DAPI for viewing by fluorescent microscopy. Cells undergoing apoptosis

were identified by nuclear condensation or blebbing and the percentage of cell death was determined by calculating the ratio of apoptotic cells to total cells for each condition examined.

Nanoparticle Tracking Analysis (NTA)

The sizes and concentrations of EVs in a given sample were determined using a NanoSight NS300 (Malvern). The samples were diluted in PBS made from ultra-pure water and passed through the beam path to detect EVs as points of diffracted light moving rapidly under Brownian motion. Five 60-second digital videos of each sample were taken, analyzed to determine the concentration and size of the individual EVs based on their movement, and then results were averaged together.

Transmission Electron Microscopy (TEM)

Five µl of a MV preparation resuspended in PBS were added to a carbon-coated, 300-mesh copper grid and then stained with 1.75% uranyl acetate. Once dry, the samples were imaged using the FEI T12 Spirit 120 kV field emission TEM at Cornell's Center for Materials Research (CCMR), supported by NSF MRSEC award number: NSF DMR-1120296.

REFERENCES

1. Taylor, D. D., and Gercel-Taylor, C. (2009) The origin, function, and diagnostic potential of RNA within extracellular vesicles present in human biological fluids. *J Cell Physiol*. **218**, 460–466

2. Nickerson, N. K., Mill, C. P., Wu, H.-J., Riese, D. J., and Foley, J. (2013) Autocrine-Derived Epidermal Growth Factor Receptor Ligands Contribute to Recruitment of Tumor-Associated Macrophage and Growth of Basal Breast Cancer Cells In Vivo. *Oncology research*. **20**, 303–317

3. Hopkins, S., Linderoth, E., Hantschel, O., Suarez-Henriques, P., Pilia, G., Kendrick, H., Smalley, M. J., Superti-Furga, G., and Ferby, I. (2012) Mig6 Is a Sensor of EGF Receptor Inactivation that Directly Activates c-Abl to Induce Apoptosis during Epithelial Homeostasis. *Dev Cell*. **23**, 547–559

4. Antonyak, M. A., and Cerione, R. A. (2014) Microvesicles as mediators of intercellular communication in cancer. *Methods Mol Biol*. **1165**, 147–173

5. Santana, S. M., Antonyak, M. A., Cerione, R. A., and Kirby, B. J. (2014) Cancerous epithelial cell lines shed extracellular vesicles with a bimodal size distribution that is sensitive to glutamine inhibition. *Phys Biol*. **11**, 065001

6. Antonyak, M. A., Li, B., Boroughs, L. K., Johnson, J. L., Druso, J. E., Bryant, K. L., Holowka, D. A., and Cerione, R. A. (2011) Cancer cell-derived microvesicles induce transformation by transferring tissue transglutaminase and fibronectin to recipient cells. *Proc Natl Acad Sci U S A*. **108**, 4852–4857

7. Rak, J., and Guha, A. (2012) Extracellular vesicles - vehicles that spread cancer genes. *Bioessays*. **34**, 489–497

8. Al-Nedawi, K., Meehan, B., Micallef, J., Lhotak, V., May, L., Guha, A., and Rak, J. (2008) Intercellular transfer of the oncogenic receptor EGFRvIII by microvesicles derived from tumour cells. *Nat Cell Biol*. **10**, 619–624

9. Fujita, Y., Araya, J., Ito, S., Kobayashi, K., Kosaka, N., Yoshioka, Y., Kadota, T., Hara, H., Kuwano, K., and Ochiya, T. (2015) Suppression of autophagy by extracellular vesicles promotes myofibroblast differentiation in COPD pathogenesis. *J Extracell Vesicles*. **4**, 28388

10. Liu, Y., Zhao, L., Li, D., Yin, Y., Zhang, C.-Y., Li, J., and Zhang, Y. (2013) Microvesicle-delivery miR-150 promotes tumorigenesis by up-regulating VEGF, and the neutralization of miR-150 attenuate tumor development. *Protein Cell*. **4**, 932–941

11. Bordeleau, F., Chan, B., Antonyak, M. A., Lampi, M. C., Cerione, R. A., and Reinhart-King, C. A. (2015) Microvesicles released from tumor cells disrupt epithelial cell morphology and contractility. *J Biomech*. 10.1016/j.jbiomech.2015.10.003

12. Khan, S., Jutzy, J. M. S., Aspe, J. R., McGregor, D. W., Neidigh, J. W., and Wall, N. R. (2011) Survivin is released from cancer cells via exosomes. *Apoptosis*. **16**, 1–12

13. Heneberg, P. (2016) Paracrine tumor signaling induces transdifferentiation of surrounding fibroblasts. *Crit Rev Oncol Hematol*. **97**, 303–311

14. Zhao, X.-P., Wang, M., Song, Y., Song, K., Yan, T.-L., Wang, L., Liu, K., and Shang, Z.-J. (2015) Membrane microvesicles as mediators for melanoma-fibroblasts communication: roles of the VCAM-1/VLA-4 axis and the ERK1/2 signal pathway. *Cancer Lett*. **360**, 125–133

15. Skog, J., Wurdinger, T., van Rijn, S., Meijer, D. H., Gainche, L., Sena-Esteves, M., Curry, W. T. J., Carter, B. S., Krichevsky, A. M., and Breakefield, X. O. (2008) Glioblastoma microvesicles transport RNA and proteins that promote tumour growth and provide diagnostic biomarkers. *Nat Cell Biol*. **10**, 1470–1476

16. Di Vizio, D., Morello, M., Dudley, A. C., Schow, P. W., Adam, R. M., Morley, S., Mulholland, D., Rotinen, M., Hager, M. H., Insabato, L., Moses, M. A., Demichelis, F., Lisanti, M. P., Wu, H., Klagsbrun, M., Bhowmick, N. A., Rubin, M. A., D'Souza-Schorey, C., and Freeman, M. R. (2012) Large oncosomes in human prostate cancer tissues and in the circulation of mice with metastatic disease. *Am J Pathol*. **181**, 1573–1584

17. Logozzi, M., De Milito, A., Lugini, L., Borghi, M., Calabro, L., Spada, M., Perdicchio, M., Marino, M. L., Federici, C., Iessi, E., Brambilla, D., Venturi, G., Lozupone, F., Santinami, M., Huber, V., Maio, M., Rivoltini, L., and Fais, S. (2009) High levels of exosomes expressing CD63 and caveolin-1 in plasma of melanoma patients. *PLoS One*. **4**, e5219

18. Shao, H., Chung, J., Balaj, L., Charest, A., Bigner, D. D., Carter, B. S., Hochberg, F. H., Breakefield, X. O., Weissleder, R., and Lee, H. (2012) Protein typing of circulating microvesicles allows real-time monitoring of glioblastoma therapy. *Nat Med*. **18**, 1835–1840

19. Stalnecker, C. A., Ulrich, S. M., Li, Y., Ramachandran, S., McBrayer, M. K., DeBerardinis, R. J., Cerione, R. A., and Erickson, J. W. (2015) Mechanism by which a recently discovered allosteric inhibitor blocks glutamine metabolism in transformed cells. *Proc Natl Acad Sci U S A*. **112**, 394–399

20. Hoffman, G. R., and Cerione, R. A. (2002) Signaling to the Rho GTPases: networking with the DH domain. *FEBS Lett*. **513**, 85–91

21. Olivo, C., Vanni, C., Mancini, P., Silengo, L., Torrisi, M. R., Tarone, G., Defilippi, P., and Eva, A. (2000) Distinct involvement of cdc42 and RhoA GTPases in actin organization and cell shape in untransformed and Dbl oncogene transformed NIH3T3 cells. *Oncogene*. **19**, 1428–1436

22. Lin, R., Cerione, R. A., and Manor, D. (1999) Specific contributions of the small GTPases Rho, Rac, and Cdc42 to Dbl transformation. *J Biol Chem*. **274**, 23633–23641

23. Shibue, T., and Weinberg, R. A. (2009) Integrin beta1-focal adhesion kinase signaling directs the proliferation of metastatic cancer cells disseminated in the lungs. *Proc Natl Acad Sci U S A*. **106**, 10290–10295

24. Takahashi, R., Sonoda, Y., Ichikawa, D., Yoshida, N., Eriko, A.-Y., and Tadashi, K. (2007) Focal adhesion kinase determines the fate of death or survival of cells in response to TNFalpha in the presence of actinomycin D. *Biochim Biophys Acta*. **1770**, 518–526

25. Sonoda, Y., Matsumoto, Y., Funakoshi, M., Yamamoto, D., Hanks, S. K., and Kasahara, T. (2000) Anti-apoptotic role of focal adhesion kinase (FAK). Induction of inhibitor-of-apoptosis proteins and apoptosis suppression by the overexpression of FAK in a human leukemic cell line, HL-60. *J Biol Chem*. **275**, 16309–16315

26. Garces, C. A., Kurenova, E. V., Golubovskaya, V. M., and Cance, W. G. (2006) Vascular endothelial growth factor receptor-3 and focal adhesion kinase bind and suppress apoptosis in breast cancer cells. *Cancer Res*. **66**, 1446–1454

27. Ward, K. K., Tancioni, I., Lawson, C., Miller, N. L. G., Jean, C., Chen, X. L., Uryu, S., Kim, J., Tarin, D., Stupack, D. G., Plaxe, S. C., and Schlaepfer, D. D. (2013) Inhibition of focal adhesion kinase (FAK) activity prevents anchorage-independent ovarian carcinoma cell growth and tumor progression. *Clin Exp Metastasis*. **30**, 579–594

28. Serrels, A., Lund, T., Serrels, B., Byron, A., McPherson, R. C., Kriegsheim, von, A., Gomez-Cuadrado, L., Canel, M., Muir, M., Ring, J. E., Maniati, E., Sims, A. H., Pachter,

J. A., Brunton, V. G., Gilbert, N., Anderton, S. M., Nibbs, R. J. B., and Frame, M. C. (2015) Nuclear FAK controls chemokine transcription, Tregs, and evasion of anti-tumor immunity. *Cell*. **163**, 160–173

29. Chatzizacharias, N. A., Kouraklis, G. P., and Theocharis, S. E. (2007) Focal adhesion kinase: a promising target for anticancer therapy. *Expert Opin Ther Targets*. **11**, 1315–1328

30. Zhang, X. H.-F., Wang, Q., Gerald, W., Hudis, C. A., Norton, L., Smid, M., Foekens, J. A., and Massague, J. (2009) Latent bone metastasis in breast cancer tied to Src-dependent survival signals. *Cancer Cell*. **16**, 67–78

31. Deakin, N. O., Pignatelli, J., and Turner, C. E. (2012) Diverse Roles for the Paxillin Family of Proteins in Cancer. *Genes Cancer*. **3**, 362–370

32. Mitra, S. K., Hanson, D. A., and Schlaepfer, D. D. (2005) Focal adhesion kinase: in command and control of cell motility. *Nat Rev Mol Cell Biol*. **6**, 56–68

33. Bolós, V., Gasent, J. M., López-Tarruella, S., and Grande, E. (2010) The dual kinase complex FAK-Src as a promising therapeutic target in cancer. *Onco Targets Ther*. **3**, 83–97

34. Mitra, S. K., and Schlaepfer, D. D. (2006) Integrin-regulated FAK-Src signaling in normal and cancer cells. *Curr Opin Cell Biol*. **18**, 516–523

35. Liu, Z., Zhang, H. M., Yuan, J., Lim, T., Sall, A., Taylor, G. A., and Yang, D. (2008) Focal adhesion kinase mediates the IGTP-induced PI3K/Akt survival pathway and further initiates a positive feedback loop of NF-κB activation. *Cell Microbiol*. **10**, 1787–1800

36. Tomita, N., Hayashi, Y., Suzuki, S., Oomori, Y., Aramaki, Y., Matsushita, Y., Iwatani, M., Iwata, H., Okabe, A., Awazu, Y., Isono, O., Skene, R. J., Hosfield, D. J., Miki, H., Kawamoto, T., Hori, A., and Baba, A. (2013) Structure-based discovery of cellular-active allosteric inhibitors of FAK. *Bioorg Med Chem Lett*. **23**, 1779–1785

37. Chen, H. C., Appeddu, P. A., Parsons, J. T., Hildebrand, J. D., Schaller, M. D., and Guan, J. L. (1995) Interaction of focal adhesion kinase with cytoskeletal protein talin. *J Biol Chem*. **270**, 16995–16999

38. Cicero, Lo, A., Stahl, P. D., and Raposo, G. (2015) Extracellular vesicles shuffling

intercellular messages: for good or for bad. *Curr Opin Cell Biol*. **35**, 69–77

39. Andaloussi, El, S., Mager, I., Breakefield, X. O., and Wood, M. J. A. (2013) Extracellular vesicles: biology and emerging therapeutic opportunities. *Nat Rev Drug Discov*. **12**, 347–357

40. Minciacchi, V. R., Freeman, M. R., and Di Vizio, D. (2015) Extracellular vesicles in cancer: exosomes, microvesicles and the emerging role of large oncosomes. *Semin Cell Dev Biol*. **40**, 41–51

41. Al-Nedawi, K., Meehan, B., Kerbel, R. S., Allison, A. C., and Rak, J. (2009) Endothelial expression of autocrine VEGF upon the uptake of tumor-derived microvesicles containing oncogenic EGFR. *Proc Natl Acad Sci U S A*. **106**, 3794–3799

42. Mahmoudi, K., Ezrin, A., and Hadjipanayis, C. (2015) Small extracellular vesicles as tumor biomarkers for glioblastoma. *Mol Aspects Med*. **45**, 97–102

43. Grange, C., Tapparo, M., Collino, F., Vitillo, L., Damasco, C., Deregibus, M. C., Tetta, C., Bussolati, B., and Camussi, G. (2011) Microvesicles released from human renal cancer stem cells stimulate angiogenesis and formation of lung premetastatic niche. *Cancer Res*. **71**, 5346–5356

44. Owens, L. V., Xu, L., Craven, R. J., Dent, G. A., Weiner, T. M., Kornberg, L., Liu, E. T., and Cance, W. G. (1995) Overexpression of the focal adhesion kinase (p125FAK) in invasive human tumors. *Cancer Res*. **55**, 2752–2755

CHAPTER 3

Survivin is enriched in cancer cell-derived exosomes upon treatment with Paclitaxel

The generation of extracellular vesicles (EVs), including exosomes and microvesicles (MVs), by cancer cells plays important roles in promoting several aspects of cancer progression, including chemoresistance. EVs mediate their effects by transferring their cargo to target cells, which includes a specific set of signaling proteins, RNA transcripts, and cytoskeletal components. However, how cargo is selectively trafficked to EVs is unclear. We have discovered that treating MDAMB231 breast cancer cells with the chemotherapy paclitaxel, which functions by stabilizing microtubules, significantly increases the amount of survivin in the EVs shed by these cells. We then go on to show that survivin is specifically enriched in the class of EVs known as exosomes. Exosomes collected from MDAMB-231 cancer cells treated with paclitaxel promoted the survival of recipient fibroblasts and other breast cancer cells (e.g. SKBR3 cells) exposed to serum-starvation and paclitaxel treatment, an effect that was lost when survivin was depleted from these exosomes by siRNA. Overall, these results highlight how a specific protein (e.g. survivin) is selectively packaged into exosomes, as well as shed light on a potential mechanism underlying paclitaxel resistance.

Introduction

Breast cancer remains one of the most prevalent forms of cancer, with 1 in 8 women being diagnosed with invasive breast cancer in their lifetime (1). Treatment regiments for these patients typically include irradiation, surgery, and chemotherapy treatment. However, as is the case with many cancer therapies, resistance and tumor recurrence are common and often result in patient death. Thus there is an overriding need to better understand the mechanisms underlying therapy resistance.

There are several mechanisms through which cancer cells can overcome the cytotoxic effects of chemotherapeutic agents. One such mechanism that is attracting a good deal of attention involves the generation of EVs by cancer cells (2, 3). EVs have the ability to act in both endocrine and paracrine fashions through the transfer of cargo to a recipient cell (4, 5). The cargo contained within EVs includes a variety of cell surface receptors, cytosolic signal proteins, metabolic enzymes, cytoskeletal proteins, and even nuclear proteins (6-8). Moreover, they also contain RNA transcripts and micro RNAs that are known to influence growth and survival responses (9-11). EVs derived from highly aggressive cancer cells have been shown to promote cell migration, tumor angiogenesis, tumor growth, and cell survival, making them an attractive target for therapy (12-14).

Exosomes are considered one of the major classes of EVs and they range in size from 30-100nm (15, 16). Exosomes are formed by a re-routing of the multivesicular bodies (MVBs) in the endosomal pathway from the lysosome (where they would typically be degraded) to the cell surface (17). The MVB then fuses with the plasma membrane and releases its contents (termed exosomes) into the extracellular space. Microvesicles (MVs) represent a distinct class of EVs that have the propensity to be much larger than exosomes, ranging in size between 200nm-2μm

(15). MVs also differ from exosomes on how they are generated, as they bud and are released (shed) directly from the plasma membrane (13).

Although there are several potential treatment options for breast cancer patients, taxanes have emerged as a frontline treatment against malignancies of not only the breast, but also the lung and ovaries (18). Taxanes, including paclitaxel (also known as taxol), function by disrupting the normal dynamic properties of microtubules (19). Microtubules normally go through cycles of polymerization and disassembly, which is especially important for cell division. Paclitaxel functions by binding to the beta subunit of microtubules and prevents the formation of a proper mitotic apparatus. Thus, paclitaxel blocks cells from progressing through the G2/M phase of cell cycle, leading to cell cycle arrest and eventually cell death (20).

Survivin is a protein characterized by its ability to prevent cell death, with its expression is normally being restricted to early embryo development and is absent in terminally differentiated cells (21). However, it is frequently expressed in cancer cells (22). Survivin expression is associated with poor patient prognosis, chemotherapy resistance, and increased tumor recurrence (23-26). This has caused survivin to be proposed as a marker of oncogenic transformation, and it is also being targeted as a potential therapy to treat cancer (27).

Survivin regulates cell cycle progression by interacting with aurora B kinase as a member of the chromosomal passenger complex responsible for the cell cycle checkpoint of faithful separation of sister chromatids into daughter cells (28). It has been shown that its interaction with microtubules in cell cycle progression is sufficient to control microtubule stability and facilitate checkpoint evasion, and to promote resistance to paclitaxel chemotherapy by preserving the integrity of the mitotic apparatus (29, 30). Survivin overexpression in cancer has been shown to overcome the apoptotic checkpoint at G2/M and favor abnormal progression of transformed cells

through mitosis even after paclitaxel treatment. Survivin is also a member of the "inhibitor of apoptosis" family and blocks cell death by inhibiting the activation of caspases. There are several mechanisms proposed by which survivin protects cells from apoptosis. The most studied model is based on survivin's ability to bind to the proapoptosis protein Smac/Diablo, sequestering it from blocking the activity of X-linked inhibitor of apoptosis protein (XIAP). XIAP is then free to directly bind caspase-3, caspase-7, and caspase-9, thereby preventing cell death (31, 32). The less frequently supported mechanism involves the direct binding of survivin to caspase-3 and caspase-7 (33).

In this study, we propose a novel mechanism by which breast cancer cells might become resistant to paclitaxel. Specifically, we found that treating MDAMB-231 breast cancer cells with paclitaxel causes them to generate exosomes that are enriched with survivin, a protein known to promote cell survival and drug resistance (34). These exosomes are able to transfer survivin to fibroblasts, as well as to other cancer cells, and promote their survival under conditions of serum deprivation and after treatment.

Results

Cancer cells shed exosomes that promote survival

EVs, including exosomes and MVs, have emerged as a major form of intercellular communication that play significant roles in cancer progression, including promoting drug resistance (2, 35, 36). The specific cargo contained within these EVs is vital for their biological function. However, whether chemotherapy treatments alter the cargo and function of exosomes generated by cancer cells is not clear.

To investigate this question, we first determined the amounts and sizes of exosomes that were generated by the triple negative breast cancer cell line, MDAMB-231. The conditioned medium from cultures of serum-starved MDAMB-231 cells was collected and the exosomes in the medium isolated using an approach developed in the laboratory that involves various centrifugation and filtration steps (Figure 3.1A). This approach effectively separates the exosomes from cells and cell debris, as well as from the larger class of EVs referred to as MVs. Lysates were subjected to Western blot analysis and the exosomal marker CD-63 was detected in the exosomal fraction (Exos), the total EVs (EVs), and the cells (WCL), but was not detected in the MVs (MVs) (Figure 3.1B, top panel). Importantly, the cytosolic signaling protein IκBα was only detected in the whole cell lysates (third panel, lanes labeled WCL), indicating that the MV preparations were devoid of cytosolic contaminants. The exosome preparations were then analyzed by electron microscopy (Figure 3.1C) to determine the sizes of the vesicles. Figure 3.1D is a histogram generated by analysis of TEM images and shows that most of the EVs detected were between ~30-40nm in diameter, consistent with the known size of exosomes.

We then determined whether the exosomes derived from the MDAMB-231 cells were capable of promoting cell survival. The removal of serum from NIH-3T3 fibroblasts in culture for extended periods of time strongly induces cell death, compared to cells maintained in medium containing 2% serum, (Figure 3.1E, compare bars 1 and 2). However, when fibroblasts were cultured in serum-free medium supplemented with exosomes from MDAMB-231 cells, there was an approximately 30% decrease in the number of cells that died after 48 hours (Figure 3.1E, compare bars 1 and 3).

Figure 3.1. MDAMB-231 breast cancer cells shed exosomes that can promote survival. (**A**) Outline of procedure used for collecting exosomes for Western blot analysis, or use in biological assays. (**B**) Western blot analysis using CD-63, IκBα, and actin was performed on MDAMB-231 cells (lane labeled WCL), as well as on the exosomes (lane labeled Exos) and MVs (lane labeled MVs), and the total EVs (lane labeled EVs) these cells generated. (**C**) TEM images of exosomes isolated from MDAMB-231 cells. Scale bars = 50nm. (**D**) Histogram of the diameter of exosomes collected from MDAMB-231 cells determined by analysis of TEM images. (**E**) Cell death assays were performed on NIH-3T3 fibroblasts cultured in serum-free media, media containing 2% serum, or serum-free media containing exosomes derived from MDAMB-231 cells to assess the survival-promoting capabilities of the exosomes. The experiments were performed a minimum of 3 separate times. The data shown represents the mean ± SD.

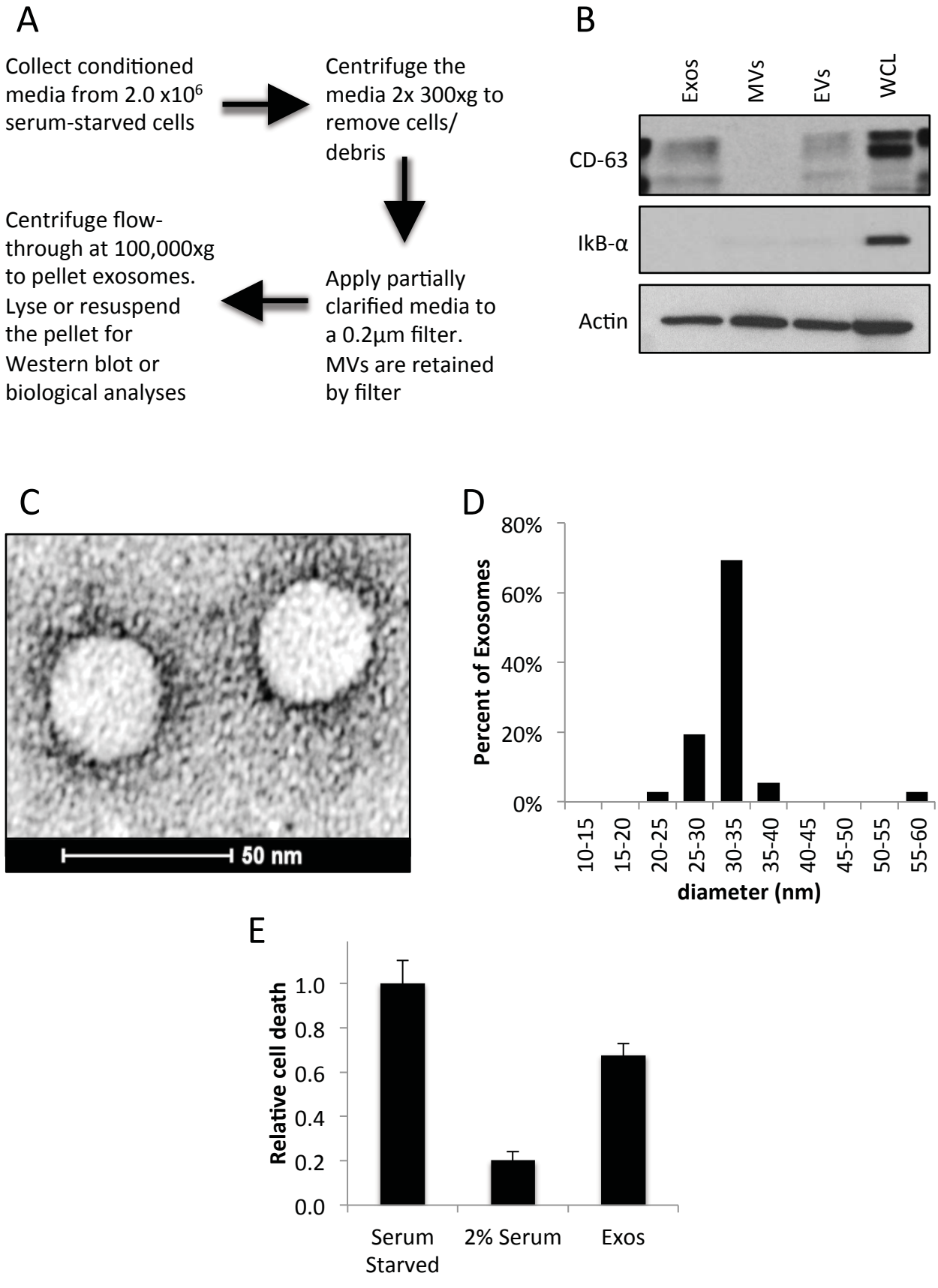
A
Collect conditioned media from 2.0 x10^6 serum-starved cells
Centrifuge the media 2x 300xg to remove cells/ debris
Apply partially clarified media to a 0.2µm filter. MVs are retained by filter
Centrifuge flow-through at 100,000xg to pellet exosomes. Lyse or resuspend the pellet for Western blot or biological analyses
B
Exos
MVs
EVs
WCL
CD-63
IkB-α
Actin
C
50 nm
D
Percent of Exosomes
80%
60%
40%
20%
0%
10-15
15-20
20-25
25-30
30-35
35-40
40-45
45-50
50-55
55-60
diameter (nm)
E
Relative cell death
1.0
0.8
0.6
0.4
0.2
0.0
Serum Starved
2% Serum
Exos

Exosomes derived from Paclitaxel-treated MDAMB-231 cells promote cell survival better than those from control cells.

Since the chemotherapy paclitaxel is commonly used as a frontline treatment for breast cancer patients, we were interested in determining whether the exosomes generated by MDAMB-231 cells would change after being treated with this drug. We first demonstrated the effectiveness of paclitaxel by performing immunofluorescence on MDAMB-231 cells treated without or with 50nM paclitaxel using a tubulin antibody. Figure 3.2A shows that microtubules can be detected throughout the DMSO treated control cell (top panel). However, paclitaxel treatment caused a large increase in the number of microtubules present in the MDAMB-231 cells (bottom panel), consistent with the idea that paclitaxel stabilizes microtubules (18, 37). A proliferation assay was then performed on MDAMB-231 cells treated with either DMSO or a low dose of paclitaxel (50nM). Figure 3.2B shows that paclitaxel treatment completely inhibited the growth of the cancer cells.

Next, we determined how the amount of exosomes generated by MDAMB-231 cells was impacted by paclitaxel treatment. The exosomes generated by an equivalent number of MDAMB-231 cells, treated with either DMSO or paclitaxel, were collected and then subjected to nanoparticle tracking analysis (NTA) to determine exosome amounts. Interestingly, there was consistently an approximately 1.5 fold greater amount of exosomes produced by the paclitaxel treated cells, compared to those treated with the vehicle alone (Figure 3.2C). However, electron microscopy performed on the exosomes generated by the paclitaxel treated MDAMB-231 cells revealed that these vesicles were comparable in size to those generated by control MDAMB-231 cells (compare Figure 3.2D and 3.2E to Figures 3.1C and 3.1D).

Figure 3.2. Exosomes derived from paclitaxel-treated MDAMB-231 cells promote survival beyond exosomes derived from control-treated cells.
(**A**) Immunofluorescence using an anti-tubulin antibody was performed on MDAMB-231 breast cancer cells treated with either DMSO vehicle control, or 50nM paclitaxel. (**B**) To demonstrate the effect of the paclitaxel treatment on cell growth, a proliferation assay was performed on MDAMB-231 cells treated with either DMSO vehicle control, or 50nM paclitaxel. (**C**) The relative amounts of exosomes generated by control (DMSO) MDAMB-231 cells, and cells treated with 50nm paclitaxel (PTX) were determined across several experiments. (**D**) TEM images of exosomes isolated from MDAMB-231 cells treated with 50nM paclitaxel. (**E**) Histogram of the diameter of exosomes collected from MDAMB-231 cells determined by analysis of TEM images. (**F**) Cell death assays performed on NIH-3T3 fibroblasts, comparing the survival-promoting effects of quantified exosomes derived from DMSO or paclitaxel treated MDAMB-231 cells. As a control, cells were also plated in serum-free media, or in the presence of 2% serum. Relative cell death was determined after 48 hours. The experiments were performed a minimum of 3 separate times. The data shown represents the mean ± SD.

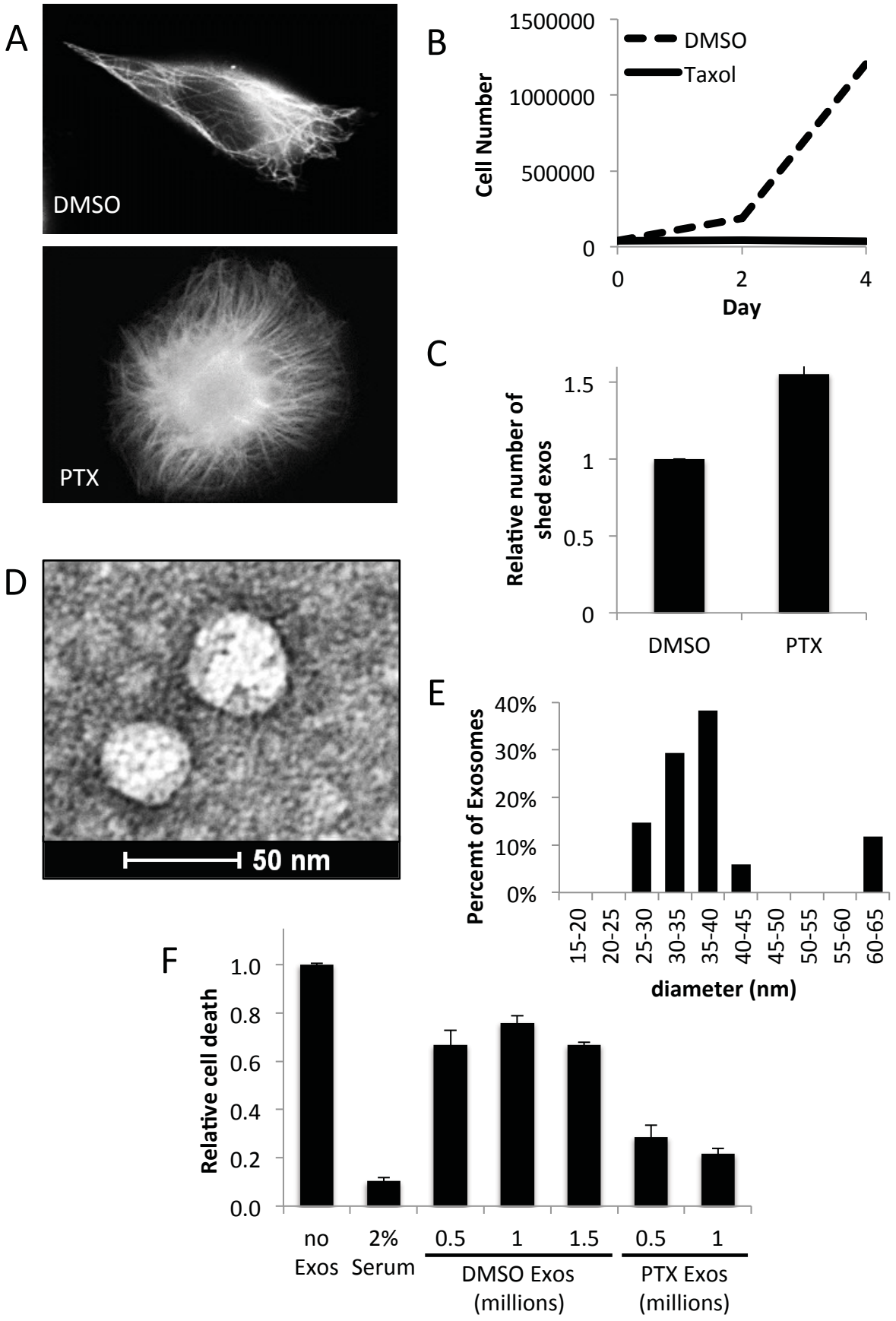
A
DMSO
PTX
B
1500000
1000000
500000
0
Cell Number
DMSO
Taxol
0
2
4
Day
C
Relative number of shed exos
1.5
1
0.5
0
DMSO
PTX
D
50 nm
E
Percemt of Exosomes
40%
30%
20%
10%
0%
15-20
20-25
25-30
30-35
35-40
40-45
45-50
50-55
55-60
60-65
diameter (nm)
F
Relative cell death
1.0
0.8
0.6
0.4
0.2
0.0
no Exos
2% Serum
0.5
1
1.5
DMSO Exos (millions)
0.5
1
PTX Exos (millions)

The ability of the exosomes derived from the paclitaxel-treated MDAMB-231 cells to promote cell survival was then assayed. The exosomes generated by MDAMB-231 cells treated with either DMSO, or 50nM paclitaxel, were collected. Based on our NTA results (see Figure 3.2C), the exosome amounts were normalized and then added to serum-starved cultures of NIH-3T3 cells. A day later, the medium and exosomes on the cells were replenished, and one day after that (48 hours after the start of the assay), the cells were collected and analyzed for apoptosis, as read out by the appearance of nuclear condensation and blebbing. Figure 3.2F shows fibroblasts that had just been serum-starved (bar labeled No Exos) underwent a high level of cell death, compared to cells maintained in medium containing serum (bar labeled 2% Serum), i.e. the positive control. Fibroblasts incubated with exosomes derived from DMSO treated MDAMB-231 cells were again able to reduce the amount of cell death caused by serum starvation, by about 30% (compare bars 1 and 3). Importantly, increasing the amount of exosomes used from these cells did not further reduce the number of cells that died (compare bars 3-5), suggesting that a maximal effect was attained with 0.5 million exosomes/culture. However, when the same experiment was performed with exosomes derived from paclitaxel-treated cells, an even greater survival advantage was observed. Indeed, an ~80% reduction in the amount of serum starvation-induced cell death was attained with these exosomes (Figure 3.2F, compare bars 6 and 7).

These findings suggest that there is most likely something unique about the cargo in the exosomes from paclitaxel-treated MDAMB-231 cancer cells that enables them to strongly protect cells from serum starvation-induced cell death.

Paclitaxel-treated cells generate exosomes that are enriched with survivin.

In order to determine what cargo in exosomes derived from paclitaxel-treated MDAMB-231 cells is responsible for their cell survival promoting capability, lysates of DMSO- or paclitaxel-treated MDAMB-231 cells, as well as from the exosomes and MVs that these cells released, were generated. The lysates were subjected to Western blot analysis using a number of different antibodies against several proteins involved in cell survival. The protein whose expression consistently changed the most in exosomes from the paclitaxel-treated cells was the inhibitor of apoptosis protein, survivin. Figure 3.3A shows that survivin was detected at relatively low levels in exosomes from DMSO treated control cells (top panel, lanes labeled DMSO). However, it was highly enriched in exosomes from the paclitaxel-treated MDAMB-231 cells (top panel, lanes labeled PTX). On average, ~30-fold more survivin was detected in exosomes derived from paclitaxel-treated MDAMB-231 cells compared to exosomes from control-treated cells (Figure 3.3B). Moreover, we found that the enrichment of survivin in exosomes is specific for this class of EVs, as the larger class of EVs, MVs, isolated from the paclitaxel-treated MDAMB-231 cells lacked survivin expression (Figure 3.3A, top panel, lanes labeled PTX). Interestingly, the levels of survivin in the cells did not change significantly in this experiment (Figure 3.3A, lanes labeled WCL), or in an experiment where MDAMB-231 cells were treated with paclitaxel for increasing lengths of time (Figure 3.3C, top panel). This suggests that the increased levels of survivin in exosomes from paclitaxel-treated MDAMB-231 cells cannot be explained by an upregulation of the protein in the cells.

The subcellular localization of survivin in MDAMB-231 cells was then determined by immunofluorescence. The survivin in DMSO-treated cells was predominantly nuclear, as expected (38). However, after exposing the cells to paclitaxel for 12 hours, more survivin could

Figure 3.3. Paclitaxel treatment leads to the enrichment of survivin in exosomes.
(**A**) Western blot analysis using survivin, flotillin, IκBα, and CD-63 antibodies was performed on lysates prepared from exosomes (Exos), microvesicles (MVs), and cell (WCL) fractions after cells were treated with either DMSO or 50nM paclitaxel. Note the increase in survivin signal detected in exosomes derived from paclitaxel treated cells. (**B**) The relative amounts of survivin detected in Exos generated by control (DMSO) MDAMB-231 cells, and cells treated with 50nm paclitaxel (PTX), were determined across several experiments. (**C**) Whole cell lysates prepared from paclitaxel-treated MDAMB-231 cells do not show an increase in survivin expression comparable to the enrichment seen in the exosome fraction. (**D**) Immunofluorescence using an anti-survivin antibody and DAPI (to indicate nuclear localization) was performed on MDAMB-231 cells treated with either DMSO or 50nM paclitaxel. Arrows indicate punctate detection of survivin after paclitaxel treatment. (**E**) Western blot analysis was performed using a survivin antibody on lysates collected from NIH-3T3 fibroblasts, MDAMB-231 cells, U87 glioblastoma cells, SKBR3 cells, and the exosomes generated after cells were treated with DMSO or 50nm paclitaxel. (**F**) Western blot analysis was performed on lysates collected from exosomes derived from MDAMB-231 cells that had been subjected to a panel of chemotherapy agents. Note the increase in survivin localization to the exosomes only after treatment with the microtubule disruptor nocodazole (NDZ) and microtubule stabilizer paclitaxel (PTX). The experiments were performed a minimum of 3 separate times.

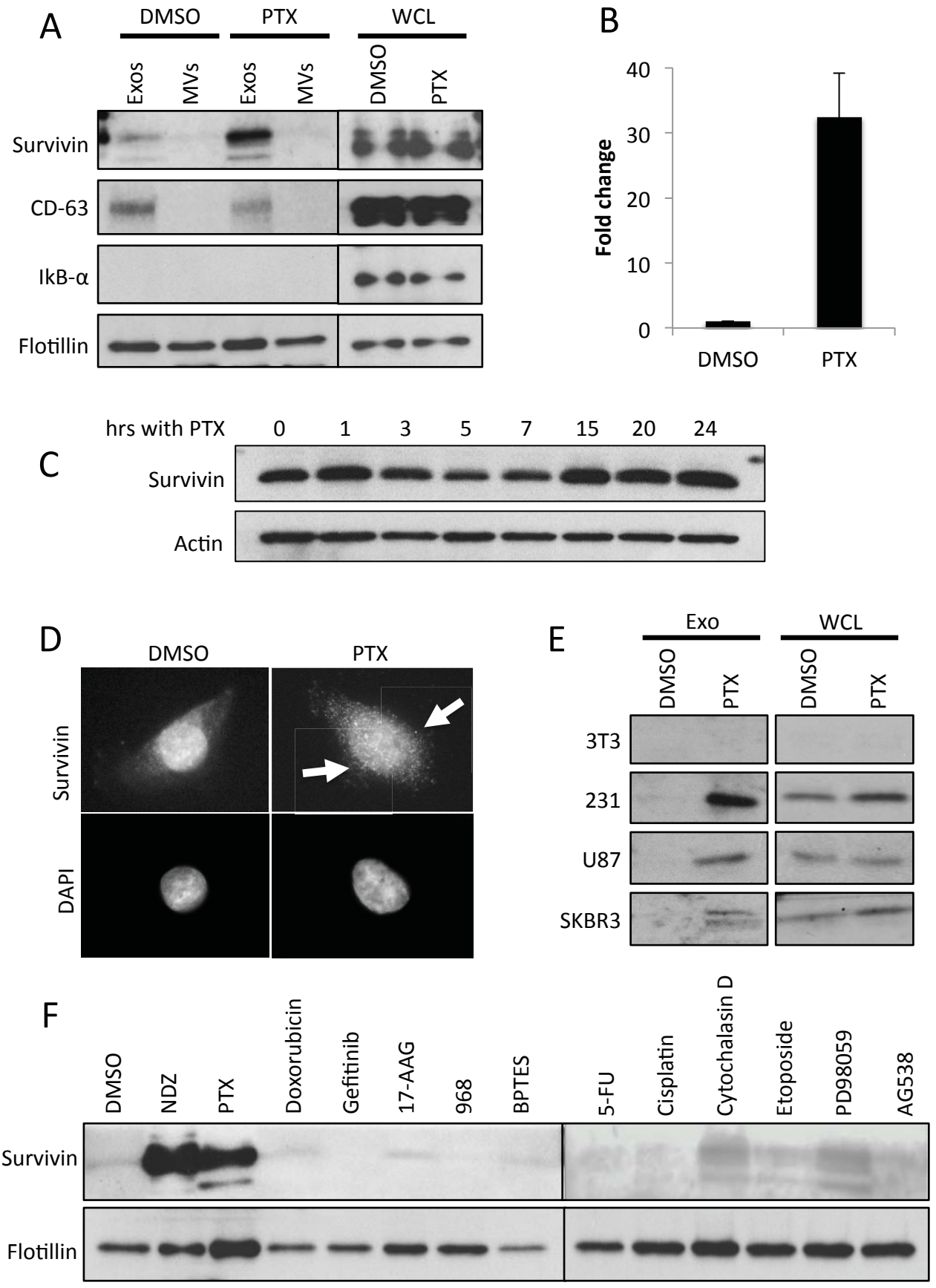
A
DMSO
PTX
WCL
Exos
MVs
Exos
MVs
DMSO
PTX
Survivin
CD-63
IkB-α
Flotillin
B
Fold change
40
30
20
10
0
DMSO
PTX
C
hrs with PTX
0
1
3
5
7
15
20
24
Survivin
Actin
D
DMSO
PTX
Survivin
DAPI
E
Exo
WCL
DMSO
PTX
DMSO
PTX
3T3
231
U87
SKBR3
F
DMSO
NDZ
PTX
Doxorubicin
Gefitinib
17-AAG
968
BPTES
5-FU
Cisplatin
Cytochalasin D
Etoposide
PD98059
AG538
Survivin
Flotillin

be detected in the cytosol, appearing as small puncta (Figure 3.3D, see arrows). We then examined whether treating various cell lines with paclitaxel could alter the levels of survivin present in their exosomes. Exosomes were collected from DMSO or paclitaxel-treated NIH-3T3 cells, which does not express survivin, as well as from aggressive breast cancer cell line MDAMB-231, the glioblastoma cell line U87, and the less aggressive breast cancer cell line SKBR3 (Figure 3.3E). Survivin levels increased in exosomes derived from paclitaxel-treated cancer cells.

Due to other studies demonstrating that survivin activity and cellular localization can change in response to a variety of cell stresses and stimuli, we next investigated whether survivin was similarly enriched in exosomes derived from MDAMB-231 cells treated with various chemotherapeutic agents, or when treated with inhibitors known to block the activation of proteins important for driving the transformed state. The drugs and inhibitors used included microtubule disruptors (nocodazole and paclitaxel), a MEK inhibitor (PD98059), metabolic inhibitors (BPTES and 968), DNA synthesis inhibitors (doxorubicin, 5-FU, etoposide, and cisplatin), inhibitors of growth factor receptors (Gefitinib and AG538), a blocker of actin polymerization (Cytochalasin D), and the HSP90 inhibitor 17-AAG. The exosomes generated by the MDAMB-231 cells treated with each of the drugs/inhibitors were collected and then subjected to Western blot analysis using survivin and flotillin antibodies. Figure 3.3F shows that a roughly equivalent amount of flotillin (an exosome marker) was detected in each of these samples, suggesting that the cells were still capable of generating exosomes in response to each of the treatments (Figure 3.3F, bottom panel). However, when the same exosome lysates were probed for survivin, differences were observed. Only the microtubule disruptor nocodazole caused a similar enrichment of survivin in exosomes as paclitaxel (Figure 3.3F, top panel). This

indicates that the enrichment of survivin in exosomes derived from cells exposed to various stresses is not a common response, but rather appears to occur specifically when microtubule dynamics in cells are disrupted.

Survivin is necessary for exosome-dependent survival.

We set out to determine if survivin in exosomes derived from MDAMB-231 cells treated with paclitaxel was necessary for their strong cell survival promoting capabilities. To this end, we either mock transfected MDAMB-231 cells, or transfected them with a survivin-specific siRNA, and then treated the cells with either DMSO or paclitaxel as outlined in Figure 3.4A. The siRNA reduced survivin expression levels in the cells by at least 90% (Figure 3.4B, blots labeled WCL) and, correspondingly, in the exosomes from the paclitaxel-treated MDAMB-231 cells (Figure 3.4B, blots labeled exosomes). The capability of the exosomes from the paclitaxel-treated cells depleted of survivin to promote cell survival was then assessed. Figure 3.4C shows again that exosomes collected from paclitaxel-treated cells (PTX Exos) are better than those from control cells (DMSO Exos) at promoting the survival of serum-starved NIH-3T3 fibroblasts (compare bars 1 and 2). However, this advantage was completely lost when survivin was knocked down in the exosomes (Figure 3.4C, compare bars 2 and 4). These experiments were also carried out using a less aggressive SKBR3 breast cancer cell line as the recipient cell. Figure 3.4D again shows that exosomes derived from MDAMB-231 cells treated with paclitaxel were able to promote the survival of serum-starved SKBR3 cells, while this effect was again lost when survivin was depleted from the exosomes using siRNA.

Figure 3.4. Knocking down survivin in MDAMB-231 cells decreases their survival-promoting capabilities.
(**A**) Schematic of the cell death assays performed. Serum-starved plates of recipient cells were incubated with exosomes derived from MDAMB-231 cells treated with either DMSO (DMSO Exos), or with 50nM paclitaxel (PTX Exos), and transfected with either mock or survivin-specific siRNA as noted. (**B**) Western blot analysis using survivin and flotillin antibodies was performed on lysates prepared from cells transfected with mock or survivin-specific siRNA, and on the exosomes they shed. (**C**) Results of the cell death assays described in (A) with NIH-3T3 fibroblasts as the recipient cells; relative cell death was determined after 48 hours. (**D**) Results of the cell death assays described in (A) with SKBR3 breast cancer cells as the recipient cells; relative cell death was determined after 5 days. The experiments were performed a minimum of 3 separate times. The data shown represents the mean ± SD.

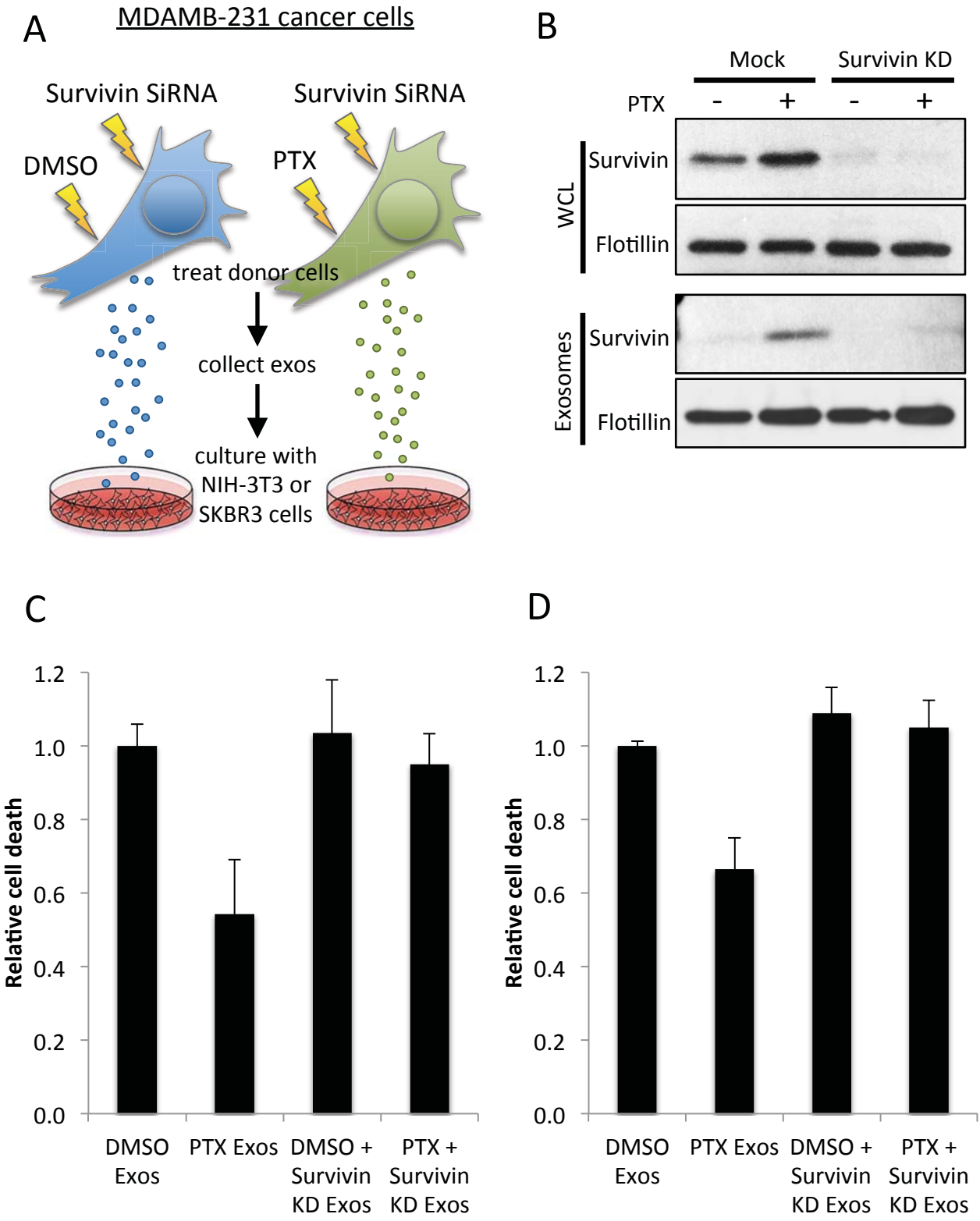
A
MDAMB-231 cancer cells
Survivin SiRNA
Survivin SiRNA
DMSO
PTX
treat donor cells
collect exos
culture with
NIH-3T3 or
SKBR3 cells
B
Mock
Survivin KD
PTX
-
+
-
+
WCL
Survivin
Flotillin
Exosomes
Survivin
Flotillin
C
Relative cell death
1.2
1.0
0.8
0.6
0.4
0.2
0.0
DMSO Exos
PTX Exos
DMSO + Survivin KD Exos
PTX + Survivin KD Exos
D
Relative cell death
1.2
1.0
0.8
0.6
0.4
0.2
0.0
DMSO Exos
PTX Exos
DMSO + Survivin KD Exos
PTX + Survivin KD Exos

Exosomes derived from paclitaxel-treated cells promote chemoresistance.

Next, we wanted to expand our study by determining whether exosomes from paclitaxel-treated MDAMB-231 cells could promote the survival of paclitaxel-treated recipient cells, as would occur in a tumor microenvironment. First, the influence of paclitaxel on SKBR3 cells was determined. Compared to SKBR3 cells treated with only DMSO, SKBR3 cell viability treated with the drug showed over a 40% increase in cell death (Figure 3.5A, compare bars 1 and 2). The paclitaxel-treated SKBR3 cells incubated with exosomes derived from DMSO-treated MDAMB-231 cells did not significantly reduce the cell death rate (bars 2 and 3). In contrast, when the paclitaxel-treated SKBR3 cells were incubated with exosomes derived from paclitaxel-treated MDAMB-231 cells, the relative amount of cell death decreased to levels comparable to that for SKBR3 cells treated with DMSO (compare bars 1 and 4). To demonstrate the role of survivin in mediating this chemoresistance effect, the same experiment was performed, except that exosomes from the paclitaxel-treated MDAMB-231 cells were first depleted of survivin expression by siRNA (Figure 3.5B). The results of this experiment showed that survivin was required for exosomes derived from paclitaxel-treated cells to provide a survival advantage to paclitaxel-treated recipient SKBR3 cells.

Discussion

EVs have garnered a good deal of attention in the past few years for their ability to mediate a wide range of signaling events, most notably in the context of cancer progression. The class of EVs known as exosomes has been strongly tied to the propagation of the transformed phenotype. For example, it has been shown that colon cancer cells expressing an activated mutant form of KRAS shed exosomes containing the mutant KRAS, and that it can be

Figure 3.5. Exosomes derived from paclitaxel treated cells provide a survival advantage to cells treated with paclitaxel that is lost upon survivin knock down.
(**A**) Serum-starved SKBR3 breast cancer cells were treated with either DMSO (PTX treatment -) or with paclitaxel (PTX treatment +) to show the effects of paclitaxel alone on recipient cells (bars 1 and 2). Cell death assays were performed on the SKBR3 cells ± PTX cultured in the presence of exosomes derived from paclitaxel-treated MDAMB-231s. (**B**) Serum-starved SKBR3 cells were treated with 50nM paclitaxel and cultured with exosomes derived from MDAMB-231 cells (Exo donor 231s) treated with either DMSO (PTX treatment -) or with paclitaxel (PTX treatment +) , and transfected with either mock or survivin-specific siRNA, as indicated. Relative cell death was determined after 5 days. The experiments were performed a minimum of 3 separate times. The data shown represents the mean ± SD.

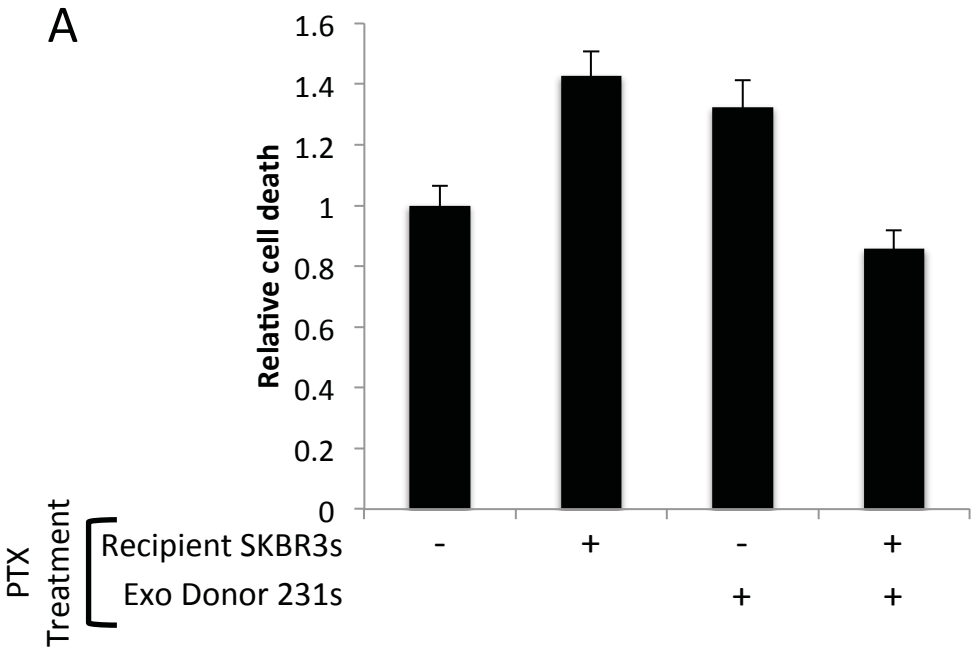
A
1.6
1.4
1.2
1
0.8
0.6
0.4
0.2
0
Relative cell death
PTX Treatment
Recipient SKBR3s - + - +
Exo Donor 231s + +

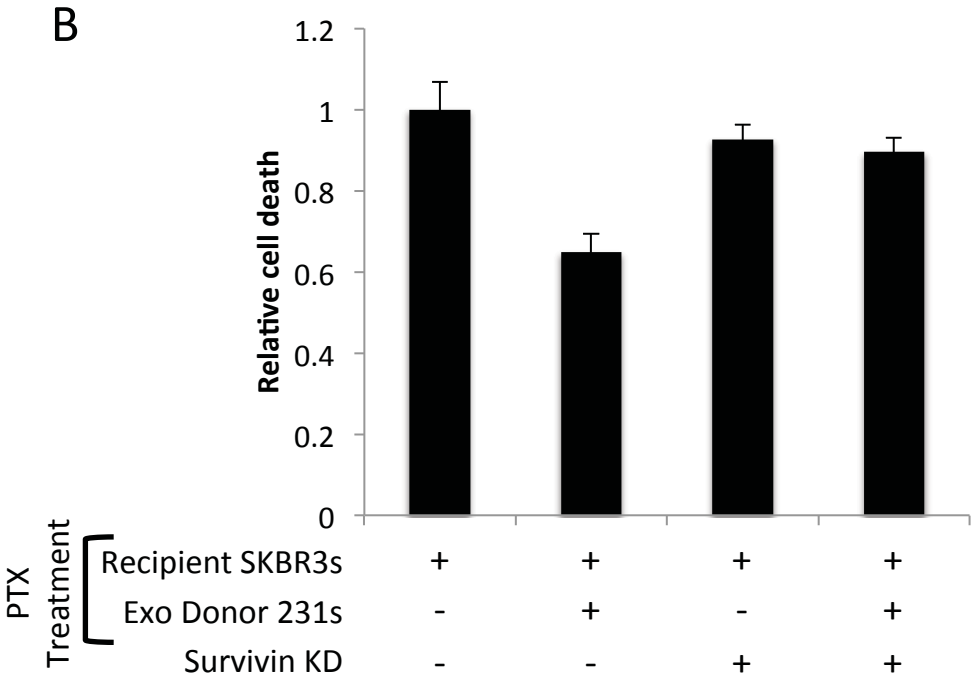
B
1.2
1
0.8
0.6
0.4
0.2
0
Relative cell death
PTX Treatment
Recipient SKBR3s + + + +
Exo Donor 231s - + - +
Survivin KD - - + +

transferred to recipient cells expressing the wild-type form of the gene leading to the enhancement of three-dimensional growth and invasiveness of the recipient cells (39).

In this study, we expand on the role of extracellular vesicles in cancer progression by describing their role in mediating cell survival. Specifically, we set out to determine if the chemotherapy agent paclitaxel had an impact on the properties of exosomes shed by an aggressive breast cancer cell line (MDAMB-231). We discovered that the MDAMB-231 cells treated with paclitaxel not only generated more exosomes, but that these exosomes were enriched with the anti-apoptotic factor survivin. Importantly, this enrichment could not be attributed to an obvious increase in the expression levels of survivin within the cells, or any detection of survivin in the larger microvesicle population before or after paclitaxel treatment.

The presence of survivin in the exosomes derived from paclitaxel-treated cells caused significant changes in the functional capabilities of these exosomes. Namely, these exosomes were able to strongly promote the survival of recipient cells (both fibroblasts and other breast cancer cell lines) exposed to serum starvation or paclitaxel treatment. However, when the paclitaxel-treated cells were first depleted of survivin expression using a survivin-specific siRNA, the exosomes were no longer able to mediate this outcome.

The enrichment of survivin within exosomes is dependent on the disruption of microtubule dynamics. Because survivin interacts with the microtubules during cell cycle progression, it is possible that when microtubule dynamics are interrupted due to the treatment of cells with paclitaxel or nocodazole, survivin is released from interacting with microtubules and is now available to be packaged as exosomal cargo.

As we have shown here, survivin enrichment in exosomes can have a profound impact on their ability to promote survival, even overcoming the challenge of chemotherapy treatment.

This suggests that within a heterogeneous tumor microenvironment, there could be a sharing of survivin-containing exosomes between cancer cells to confer a survival advantage to the tumor as a whole by increasing anti-apoptotic signals. Overall, this study provides a potential mechanism for a shared paclitaxel resistance through the transfer of exosomes.

Materials and Methods

Cell culture and transfections

MBAMB231 and SKBR3 cells were maintained in RPMI with 10% fetal bovine serum, while NIH-3T3 cells were grown in DMEM containing 10% calf serum. Control and Survivin siRNAs (Cell Signaling) were introduced into cells with Lipofectamine 2000 (Invitrogen). Paclitaxel treatment was at 50nm unless otherwise noted.

Immunofluorescence

Cells grown on glass coverslips were either transfected without or with the indicated expression constructs, or with siRNAs, and then cultured as indicated. The cells were fixed with 3.7% (vol/vol) formaldehyde, permeabilized with phosphate buffered saline (PBS) containing 0.1% Triton-X100, and blocked with 10% bovine serum albumin diluted in PBS. The cells were stained with an anti-survivin antibody (Novus Biologicals), followed by incubation with Oregon green 488-conjugated secondary antibodies (Molecular Probes). Digital images of the cells were collected using a Zeiss fluorescence microscope and IPLABS software.

Isolation of vesicles and the preparation of exosome and cell lysates

For the experiments performed involving exosomes, the conditioned media from 4 x10^6 serum-starved cells (which is approximately the equivalent of two 150mm dishes of cells at 70% confluency) was collected and then subjected to two consecutive centrifugations at 300×g to clarify the media of whole cells and cell debris. The partially clarified media was filtered using a Steriflip PVDF filter with a 0.22µm pore size (Millipore) to remove vesicles larger than 0.22µm in diameter and the flow-through was retained. For cell-based assays the exosomes were collected using a centricon with 100,000 kDa size cut-off (Millipore), rinsed three times with PBS, and resuspended in serum-free medium. To generate exosome lysates, the vesicles that passed through the 0.22µm filter were pelleted at 100,000xg for 2 hours and lysed using 200µl of lysis buffer (25 mM Tris, 100 mM NaCl, 1% Triton X-100, 1 mM EDTA, 1 mM DTT, 1 mM $NaVO_4$, 1 mM β-glycerol phosphate, and 1 µg/mL each of aprotinin and leupeptin). Whole cell lysates (WCLs) were prepared by rinsing the 150mm dishes of cells with PBS, adding 1mL of lysis buffer, and scraping the cells off the plate. The resulting exosome and cell lysates were then centrifuged at 13,000 rpm for 10 minutes to remove the Triton X-100 insoluble fraction.

Immunoblot Analysis

The protein concentrations of the WCLs and MV lysates were determined using the Bio-Rad DC protein assay (Bio-Rad). The lysates were normalized by protein concentration, resolved by SDS-PAGE, and then the proteins were transferred to PVDF membranes. The membranes were incubated with various primary antibodies including beta-actin (Abcam), Survivin (Novus Biologicals), and flotillin-2 (Cell Signaling), diluted in in 20 mM Tris, 135 mM NaCl, and 0.02%

Tween 20 (TBST). The primary antibodies were detected with HRP-conjugated secondary antibodies (Cell Signaling) followed by exposure to ECL reagent (Pierce).

Cell Death Assay

Parental NIH-3T3 cells were plated in each well of a six-well dish and then cultured in medium containing 2% calf serum or serum-free medium supplemented with or without 5×10^7 exosomes derived from MDAMB-231 breast cancer cells. Twenty-four hours later the cells were treated with an additional dose of freshly prepared exosomes. A day later (48 hours from the start of the assay) the cells were stained with DAPI for viewing by fluorescent microscopy. Assays evaluating the survival of SKBR3 cells were performed over the course of 5 days. Cells undergoing apoptosis were identified by nuclear condensation or blebbing and the percentage of cell death was calculated by the ratio of apoptotic cells to total cells for each condition at least three times and the results from each experiment were averaged.

Nanoparticle Tracking Analysis (NTA)

For particle concentration determinations, nanoparticle tracking analysis (NTA) was performed with a NanoSight NS300 (Malvern). The samples were diluted in PBS made from ultra-pure water and passed through the beam path and detected by the microscope as points of diffracted light moving rapidly under Brownian motion. A digital video of the particles was analyzed to determine the size of the individual particles based on their movement. Per sample, 5 videos of 60 seconds were captured at 22°C.

Transmission electron microscopy (TEM)

Five µl of an exosome preparation resuspended in PBS made from ultra-pure water were added to a carbon-coated, 300-mesh copper grid and then stained with 1.75% uranyl acetate. Once dry, the samples were imaged using the FEI T12 Spirit 120 kV field emission TEM at Cornell's Center for Materials Research (CCMR), supported by NSF MRSEC award number: NSF DMR-1120296.

REFERENCES

1. N, H., AM, N., M, K., N, N., R, A., W, W., SF, A., CL, K., J, R., Z, T., H, C., A, M., MP, E., DR, L., HS, C., EJ, F., and KA, C. (2012) *SEER Cancer Statistics Review, 1975-2009 (Vintage 2009 Populations)*, National Cancer Institute, Bethesda, MD

2. Jorfi, S., Ansa-Addo, E. A., Kholia, S., Stratton, D., Valley, S., Lange, S., and Inal, J. (2015) Inhibition of microvesiculation sensitizes prostate cancer cells to chemotherapy and reduces docetaxel dose required to limit tumor growth in vivo. *Sci Rep*. **5**, 13006

3. Shedden, K., Xie, X. T., Chandaroy, P., Chang, Y.-T., and Rosania, G. R. (2003) Expulsion of small molecules in vesicles shed by cancer cells: association with gene expression and chemosensitivity profiles. *Cancer Res*. **63**, 4331–4337

4. Tetta, C., Ghigo, E., Silengo, L., Deregibus, M. C., and Camussi, G. (2013) Extracellular vesicles as an emerging mechanism of cell-to-cell communication. *Endocrine*. **44**, 11–19

5. Heneberg, P. (2016) Paracrine tumor signaling induces transdifferentiation of surrounding fibroblasts. *Crit Rev Oncol Hematol*. **97**, 303–311

6. Antonyak, M. A., and Cerione, R. A. (2014) Microvesicles as mediators of intercellular communication in cancer. *Methods Mol Biol*. **1165**, 147–173

7. Al-Nedawi, K., Meehan, B., Micallef, J., Lhotak, V., May, L., Guha, A., and Rak, J. (2008) Intercellular transfer of the oncogenic receptor EGFRvIII by microvesicles derived from tumour cells. *Nat Cell Biol*. **10**, 619–624

8. Muralidharan-Chari, V., Clancy, J. W., Sedgwick, A., and D'Souza-Schorey, C. (2010) Microvesicles: mediators of extracellular communication during cancer progression. *J Cell Sci*. **123**, 1603–1611

9. Patton, J. G., Franklin, J. L., Weaver, A. M., Vickers, K., Zhang, B., Coffey, R. J., Ansel, K. M., Blelloch, R., Goga, A., Huang, B., L'Etoille, N., Raffai, R. L., Lai, C. P., Krichevsky, A. M., Mateescu, B., Greiner, V. J., Hunter, C., Voinnet, O., and McManus, M. T. (2015) Biogenesis, delivery, and function of extracellular RNA. *J Extracell Vesicles*. **4**, 27494

10. Melo, S. A., Sugimoto, H., O'Connell, J. T., Kato, N., Villanueva, A., Vidal, A., Qiu, L., Vitkin, E., Perelman, L. T., Melo, C. A., Lucci, A., Ivan, C., Calin, G. A., and Kalluri, R.

(2014) Cancer exosomes perform cell-independent microRNA biogenesis and promote tumorigenesis. *Cancer Cell*. **26**, 707–721

11. Skog, J., Wurdinger, T., van Rijn, S., Meijer, D. H., Gainche, L., Sena-Esteves, M., Curry, W. T. J., Carter, B. S., Krichevsky, A. M., and Breakefield, X. O. (2008) Glioblastoma microvesicles transport RNA and proteins that promote tumour growth and provide diagnostic biomarkers. *Nat Cell Biol*. **10**, 1470–1476

12. Grange, C., Tapparo, M., Collino, F., Vitillo, L., Damasco, C., Deregibus, M. C., Tetta, C., Bussolati, B., and Camussi, G. (2011) Microvesicles released from human renal cancer stem cells stimulate angiogenesis and formation of lung premetastatic niche. *Cancer Res*. **71**, 5346–5356

13. Antonyak, M. A., Li, B., Boroughs, L. K., Johnson, J. L., Druso, J. E., Bryant, K. L., Holowka, D. A., and Cerione, R. A. (2011) Cancer cell-derived microvesicles induce transformation by transferring tissue transglutaminase and fibronectin to recipient cells. *Proc Natl Acad Sci U S A*. **108**, 4852–4857

14. Liao, J., Liu, R., Shi, Y.-J., Yin, L.-H., and Pu, Y.-P. (2016) Exosome-shuttling microRNA-21 promotes cell migration and invasion-targeting PDCD4 in esophageal cancer. *Int J Oncol*. **48**, 2567–2579

15. Minciacchi, V. R., Freeman, M. R., and Di Vizio, D. (2015) Extracellular vesicles in cancer: exosomes, microvesicles and the emerging role of large oncosomes. *Semin Cell Dev Biol*. **40**, 41–51

16. Yu, S., Cao, H., Shen, B., and Feng, J. (2015) Tumor-derived exosomes in cancer progression and treatment failure. *Oncotarget*. **6**, 37151–37168

17. Henne, W. M., Buchkovich, N. J., and Emr, S. D. (2011) The ESCRT Pathway. *Dev Cell*. **21**, 77–91

18. Weaver, B. A. (2014) How Taxol/paclitaxel kills cancer cells. *Mol Biol Cell*. **25**, 2677–2681

19. Stanton, R. A., Gernert, K. M., Nettles, J. H., and Aneja, R. (2011) Drugs that target dynamic microtubules: a new molecular perspective. *Med Res Rev*. **31**, 443–481

20. Jordan, M. A., Wendell, K., Gardiner, S., Derry, W. B., Copp, H., and Wilson, L. (1996)

Mitotic block induced in HeLa cells by low concentrations of paclitaxel (Taxol) results in abnormal mitotic exit and apoptotic cell death. *Cancer Res*. **56**, 816–825

21. Sah, N. K., Khan, Z., Khan, G. J., and Bisen, P. S. (2006) Structural, functional and therapeutic biology of survivin. *Cancer Lett*. **244**, 164–171

22. Ambrosini, G., Adida, C., and Altieri, D. C. (1997) A novel anti-apoptosis gene, survivin, expressed in cancer and lymphoma. *Nat Med*. **3**, 917–921

23. Hausladen, D. A., Wheeler, M. A., Altieri, D. C., Colberg, J. W., and Weiss, R. M. (2003) Effect of intravesical treatment of transitional cell carcinoma with bacillus Calmette-Guerin and mitomycin C on urinary survivin levels and outcome. *J Urol*. **170**, 230–234

24. Altieri, D. C. (2003) Survivin, versatile modulation of cell division and apoptosis in cancer. *Oncogene*. **22**, 8581–8589

25. Tran, J., Rak, J., Sheehan, C., Saibil, S. D., LaCasse, E., Korneluk, R. G., and Kerbel, R. S. (1999) Marked induction of the IAP family antiapoptotic proteins survivin and XIAP by VEGF in vascular endothelial cells. *Biochem Biophys Res Commun*. **264**, 781–788

26. Xiong, C., Liu, H., Chen, Z., Yu, Y., and Liang, C. (2016) Prognostic role of survivin in renal cell carcinoma: A system review and meta-analysis. *Eur J Intern Med*. 10.1016/j.ejim.2016.06.009

27. Chuwa, A. H., Sone, K., Oda, K., Ikeda, Y., Fukuda, T., Wada-Hiraike, O., Inaba, K., Makii, C., Takeuchi, M., Oki, S., Miyasaka, A., Kashiyama, T., Arimoto, T., Kuramoto, H., Kawana, K., Yano, T., Osuga, Y., and Fujii, T. (2016) Significance of survivin as a prognostic factor and a therapeutic target in endometrial cancer. *Gynecol Oncol*. **141**, 564–569

28. Lens, S. M. A., Vader, G., and Medema, R. H. (2006) The case for Survivin as mitotic regulator. *Curr Opin Cell Biol*. **18**, 616–622

29. Li, F., Ambrosini, G., Chu, E. Y., Plescia, J., Tognin, S., Marchisio, P. C., and Altieri, D. C. (1998) Control of apoptosis and mitotic spindle checkpoint by survivin. *Nature*. **396**, 580–584

30. Giodini, A., Kallio, M. J., Wall, N. R., Gorbsky, G. J., Tognin, S., Marchisio, P. C., Symons, M., and Altieri, D. C. (2002) Regulation of microtubule stability and mitotic

progression by survivin. *Cancer Res*. **62**, 2462–2467

31. Song, Z., Yao, X., and Wu, M. (2003) Direct interaction between survivin and Smac/DIABLO is essential for the anti-apoptotic activity of survivin during taxol-induced apoptosis. *J Biol Chem*. **278**, 23130–23140

32. Altieri, D. C. (2015) Survivin - The inconvenient IAP. *Semin Cell Dev Biol*. **39**, 91–96

33. Tamm, I., Wang, Y., Sausville, E., Scudiero, D. A., Vigna, N., Oltersdorf, T., and Reed, J. C. (1998) IAP-family protein survivin inhibits caspase activity and apoptosis induced by Fas (CD95), Bax, caspases, and anticancer drugs. *Cancer Res*. **58**, 5315–5320

34. Zaffaroni, N., Pennati, M., Colella, G., Perego, P., Supino, R., Gatti, L., Pilotti, S., Zunino, F., and Daidone, M. G. (2002) Expression of the anti-apoptotic gene survivin correlates with taxol resistance in human ovarian cancer. *Cell Mol Life Sci*. **59**, 1406–1412

35. Azmi, A. S., Bao, B., and Sarkar, F. H. (2013) Exosomes in cancer development, metastasis, and drug resistance: a comprehensive review. *Cancer Metastasis Rev*. **32**, 623–642

36. Jorfi, S., and Inal, J. M. (2013) The role of microvesicles in cancer progression and drug resistance. *Biochem Soc Trans*. **41**, 293–298

37. Jordan, M. A., Toso, R. J., Thrower, D., and Wilson, L. (1993) Mechanism of mitotic block and inhibition of cell proliferation by taxol at low concentrations. *Proc Natl Acad Sci U S A*. **90**, 9552–9556

38. Lee, J. Y.-C., Kuo, C.-W., Tsai, S.-L., Cheng, S. M., Chen, S.-H., Chan, H.-H., Lin, C.-H., Lin, K.-Y., Li, C.-F., Kanwar, J. R., Leung, E. Y., Cheung, C. C. H., Huang, W.-J., Wang, Y.-C., and Cheung, C. H. A. (2016) Inhibition of HDAC3- and HDAC6-Promoted Survivin Expression Plays an Important Role in SAHA-Induced Autophagy and Viability Reduction in Breast Cancer Cells. *Front Pharmacol*. **7**, 81

39. Demory Beckler, M., Higginbotham, J. N., Franklin, J. L., Ham, A.-J., Halvey, P. J., Imasuen, I. E., Whitwell, C., Li, M., Liebler, D. C., and Coffey, R. J. (2013) Proteomic analysis of exosomes from mutant KRAS colon cancer cells identifies intercellular transfer of mutant KRAS. *Mol Cell Proteomics*. **12**, 343–355

CHAPTER 4

Conclusions

The field of extracellular vesicles (EVs) is still in its infancy, however there have already been some exciting discoveries demonstrating the significance of these vesicles in many disease states, most notably in cancer progression. However, due to the growing appreciation that normal cell types also make EVs (1-4), there is now a need in the field to better understand how EVs shed by normal and transformed cells differ. Thus, for my first research project, as described in Chapter 2 of this thesis, I set out to determine how EV cargo and function changed upon the induction of cellular transformation.

I discovered that focal adhesion kinase (FAK) is specifically enriched in the larger class of EVs known as MVs, after MEFs were induced to express onco-Dbl, a hyperactive form of a guanine nucleotide exchange factor (GEF) that potently activates the small GTPases Cdc42 and Rho (5-7). The MVs enriched with FAK were able to promote a strong cell survival response, as well as induce a transformed phenotype in NIH-3T3 fibroblasts, as indicated by their ability to form colonies in soft agar. I then went on to show that the ability of the MVs derived from the transformed MEFs to mediate these outcomes was dependent on FAK, as depletion of FAK from the MVs using siRNAs, or inhibition of FAK activity associated with the MVs by treating them with a FAK-specific inhibitor, reversed these effects.

An interesting point raised in this study is that the FAK expression levels in the MEFs did not change significantly after the induction of cellular transformation (i.e. by expression of onco-Dbl). Thus, the large increase in the levels of FAK seen in the MVs derived from the transformed MEFs cannot simply be explained by changes in gene transcription. Rather, these

findings suggest that there is a difference in the way that cells direct specific cargo to MVs depending on whether they are normal (non-transformed) or transformed. To date, there are only a few studies that have focused on understanding the mechanisms underlying the sorting of cargo into EVs. For example, the small GTPase KRAS, and the nuclear ribonucleoprotein A2B1 (hnRNPA2B1), have been implicated in the bulk sorting of miRNA into exosomes, while post-translational modifications, such as sumoylation and GPI anchors, have been shown to influence sorting of EV cargo (8-10). However, whether these mechanisms are deregulated in transformed cells such that more FAK is recruited into MVs is currently unknown. Our inducible MEF system provides us a unique opportunity to investigate this question further. For example, further studies could include expressing truncated forms of FAK to determine if there is a specific domain in FAK required for its enrichment in MVs derived from transformed cells. Additionally, it would be valuable to identify proteins that differentially interact with FAK in control (non-transformed) MEFs versus MEFs expressing onco-Dbl, as these proteins could potentially account for the differential expression of FAK in MVs derived from transformed MEFs, as well as cancer cell lines.

In the pursuit of understanding the roles played by the smaller class of EVs that are generated by the fusion of MVBs with the plasma membrane, I also investigated whether exosome cargo and function could be potentially influenced by subjecting cancer cells to chemotherapies. Thus, I treated MDAMB-231 cells, a highly aggressive, triple negative breast cancer cell line, with the chemotherapy drug paclitaxel, and looked to see whether there were any changes in the exosomes generated by these cells. My initial expectation was that proteins destined to be included as exosome cargo would use microtubules as a trafficking mechanism, and that the disruption of the microtubule network using the microtubule stabilizer paclitaxel,

would prevent the enrichment of at least some cargo in exosomes. However, to my surprise, I found that there was as large increase in the amount of the anti-apoptotic protein survivin present in exosomes shed by paclitaxel-treated MDAMB-231 cells.

The third chapter of this thesis describes the consequences of paclitaxel-treated MDAMB-231 cells shedding exosomes enriched with survivin. Survivin is a member of the inhibitor of apoptosis family of proteins and is normally only expressed during early embryogenesis. However, survivin expression is frequently upregulated in aggressive cancer cells (11-13). Because survivin expression and localization can be altered in response to a variety of cell stresses (14), I wanted to determine if the enrichment of survivin in exosomes was specific to paclitaxel. Interestingly, I found that there was no significant increase in the amounts of survivin detected in the exosomes generated by MDAMB-231 cells exposed to a variety of growth factor receptor inhibitors, cytoskeleton disruptors, kinase inhibitors, or inhibitors of DNA synthesis. The only inhibitor capable of enriching survivin in exosomes like paclitaxel was another modifier of microtubules, nocodazole. This is particularly intriguing because nocodazole functions by enhancing the catastrophic disassembly of microtubules, whereas paclitaxel stabilizes assembled microtubule subunits to prevent the proper progression through the cell cycle (15-18). This suggests that survivin enrichment in exosomes is not a general cell stress response, and is specific to the disruption of normal microtubule dynamics.

The exact molecular mechanism by which the disassembly or stabilization of microtubules in cancer cells leads to the enrichment of survivin in exosomes is currently under investigation in the laboratory. Preliminary data generated by Arash Latifkar, a fellow graduate student in the group, suggests that the NAD-dependent deacetylase Sirtuin 1 (Sirt1) may be involved in this process. It has been previously reported that Sirt1 expression is down regulated

by paclitaxel, and combined with the finding that Sirt1 regulates survivin (19, 20), raises the interesting possibility that Sirt1 may mediate the ability of paclitaxel to increase the levels of survivin in exosomes. Consistent with this idea, Arash has also recently found that transfecting MDABM-231 cells with siRNAs targeting Sirt1 leads to exosomes that contain more survivin, similar to paclitaxel treatment.

Through my studies, I have examined the biological significance of exosomes enriched with survivin. Specifically, I found that the exosomes derived from control MDAMB-231 cells were able to promote the survival of serum-starved NIH-3T3 fibroblasts by approximately 30%. However, those collected from MDAMB-231 cells treated with paclitaxel, promoted cell survival by almost 80%. I went on to show the ability of the exosomes from the cancer cells treated with the chemotherapy to promote survival was due to the increase in survivin levels, as depletion of survivin from these exosomes by siRNA completely eliminated this survival advantage.

In the clinical setting, acquired resistance to paclitaxel is common (18, 21), so I also investigated whether exosomes from paclitaxel-treated MDAMB-231 cells could promote the survival of recipient cancer cells exposed to the same chemotherapy, as would occur in a tumor microenvironment. When paclitaxel-treated SKBR3 breast cancer cells were incubated with exosomes derived from paclitaxel-treated MDAMB-231 cells, chemoresistance occurred. Once again, the exosome-mediated survival advantage could be eliminated when survivin was depleted from the exosomes. This provides an example where chemotherapy treatment can alter exosomal cargo in order to transfer a survival signal within the tumor microenvironment, leading to drug resistance.

EVs are potent mediators of cellular function within a tumor microenvironment. Cancer cells are able to transmit signals of growth and survival to neighboring cancer cells and stromal cells to propagate the transformed phenotype (22-25). The enrichment of FAK and survivin in EVs derived from cancer cells appear to be two proteins in EVs that play important roles in promoting the effects of EVs. These findings are highlighted in Figure 4.1, which shows a cancer cell shedding both MVs and exosomes into the surrounding microenvironment. The EVs can then be taken up by neighboring cancer cells, as well as normal cells, to promote their growth and survival. These cancer-specific EVs also have the potential to get into the bloodstream where they can have an effect at a distant site, or be isolated from the serum of cancer patients for use as a source of diagnostic markers.

The search for cancer-specific biomarkers has expanded greatly with the finding that EVs derived from tumors can be detected in the bloodstream of patients known as a "liquid biopsy" (26-28). This has the potential to provide valuable data for patient care, especially for heterogeneous tumors where a normal biopsy would likely only capture a small fraction of the tumor, and for tumors that may require invasive surgeries in order to acquire a biopsy, for example in the case of brain tumors (29). Any of the macromolecules contained within EVs can have the potential for being used as diagnostic markers of cancer, as well as for determining the genetic makeup of the tumor for proper selection of therapeutic agents, or gauging therapy response (30).

The findings from the studies presented in Chapters 2 and 3 of this thesis are especially exciting when coupled with the observation that FAK and survivin are only found in EVs derived from oncogenically transformed cells. FAK is present in the MVs derived from highly aggressive breast cancer cell lines, but cannot be detected in the MVs derived from the non-

Figure 4.1
Diagram depicting EVs within the tumor microenvironment.
Cancer cells shed microvesicles containing FAK that increase the growth and survival of neighboring cells. After treating the cancer cells with paclitaxel, exosomes enriched with survivin are released and can promote the growth of recipient cancer cells.

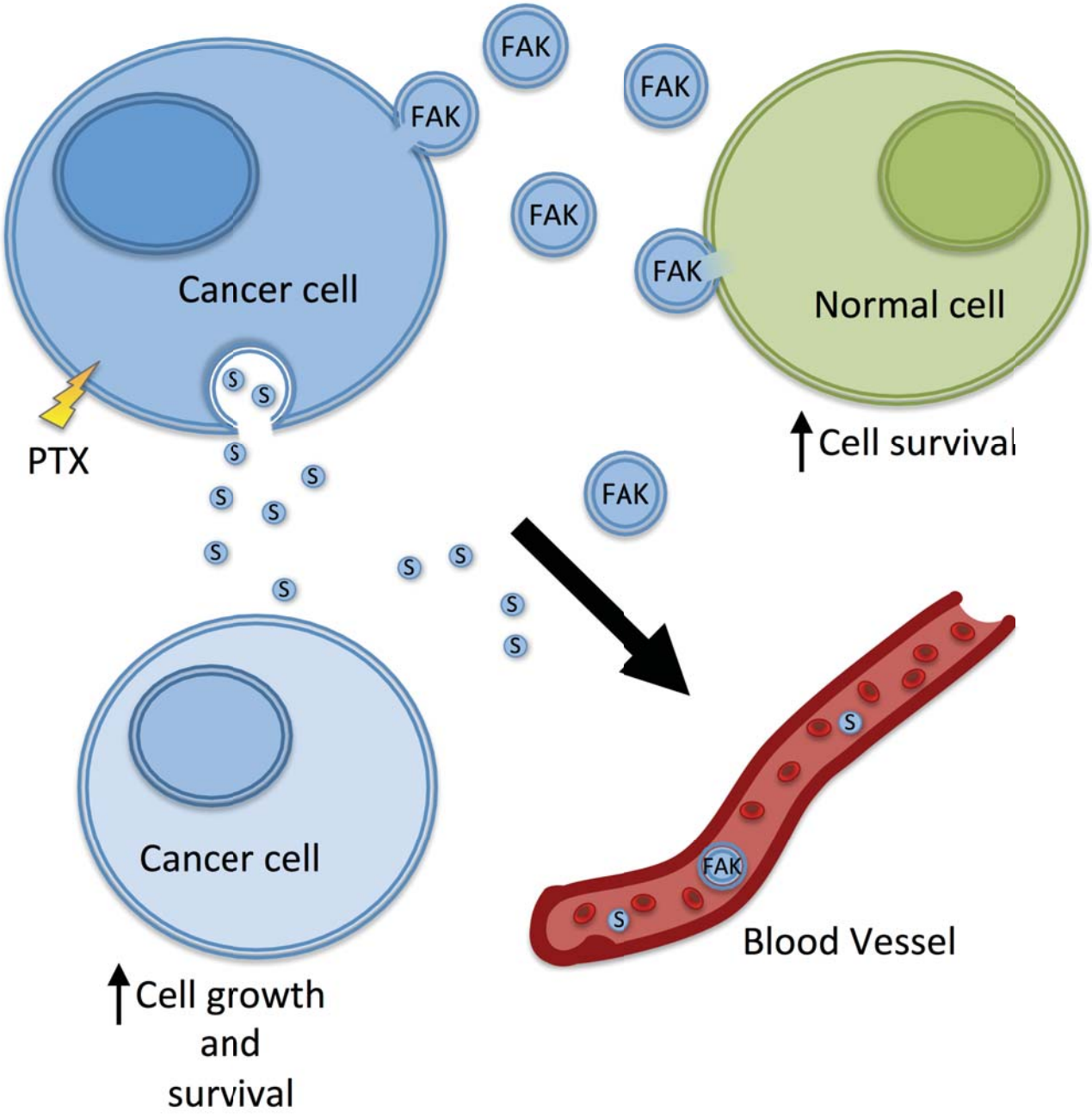
FAK
FAK
FAK
FAK
FAK
Cancer cell
Normal cell
PTX
S
Cell survival
FAK
Cancer cell
Blood Vessel
Cell growth
and
survival

transformed mammary epithelial cell line MCF-10A. This opens the door to the possibility that the detection of FAK in MVs isolated from patients could be used as an indicator of cancer. Additionally, survivin is specifically enriched in exosomes derived from cancer cells treated with paclitaxel, suggesting that the detection of survivin in exosomes from patients treated with this chemotherapy could be used as a marker of drug resistance.

Ultimately, it will be important to expand my findings to *in vivo* models. For example, MDAMB-231 cells could be injected into mice to allow tumor formation. Once a tumor has formed, the plasma from the mice could be collected and the MVs isolated. The MVs could then be evaluated for the expression of FAK. Additionally, the tumor-bearing mice could be treated with DMSO or paclitaxel to determine if survivin can be detected in exosomes derived from the plasma of mice treated with the chemotherapy.

EVs have the potential to dramatically alter how we diagnose and treat diseases, especially cancer. However, there is still a significant amount of basic research needed in the field before we will truly understand the mechanisms behind EV formation, cargo sorting, and interactions with recipient cells. It has recently emerged that there may be sub-classes of EVs beyond the distinction between MVs and exosomes (31, 32), highlighting the need for stringent biochemical characterization of the different vesicle populations. With this thesis, I have contributed to our knowledge of the cargo and biological impact of different classes of extracellular vesicles shed by oncogenically transformed cells and how they play a role in promoting cell survival, growth, and chemotherapy resistance.

REFERENCES

1. Desrochers, L. M., Bordeleau, F., Reinhart-King, C. A., Cerione, R. A., and Antonyak, M. A. (2016) Microvesicles provide a mechanism for intercellular communication by embryonic stem cells during embryo implantation. *Nat Commun*. **7**, 11958

2. Santi, A., Caselli, A., Ranaldi, F., Paoli, P., Mugnaioni, C., Michelucci, E., and Cirri, P. (2015) Cancer associated fibroblasts transfer lipids and proteins to cancer cells through cargo vesicles supporting tumor growth. *Biochim Biophys Acta*. **1853**, 3211–3223

3. Nolte-'t Hoen, E. N. M., Buermans, H. P. J., Waasdorp, M., Stoorvogel, W., Wauben, M. H. M., and 't Hoen, P. A. C. (2012) Deep sequencing of RNA from immune cell-derived vesicles uncovers the selective incorporation of small non-coding RNA biotypes with potential regulatory functions. *Nucleic Acids Res*. **40**, 9272–9285

4. Waldenstrom, A., Genneback, N., Hellman, U., and Ronquist, G. (2012) Cardiomyocyte microvesicles contain DNA/RNA and convey biological messages to target cells. *PLoS One*. **7**, e34653

5. Olivo, C., Vanni, C., Mancini, P., Silengo, L., Torrisi, M. R., Tarone, G., Defilippi, P., and Eva, A. (2000) Distinct involvement of cdc42 and RhoA GTPases in actin organization and cell shape in untransformed and Dbl oncogene transformed NIH3T3 cells. *Oncogene*. **19**, 1428–1436

6. Stalnecker, C. A., Ulrich, S. M., Li, Y., Ramachandran, S., McBrayer, M. K., DeBerardinis, R. J., Cerione, R. A., and Erickson, J. W. (2015) Mechanism by which a recently discovered allosteric inhibitor blocks glutamine metabolism in transformed cells. *Proc Natl Acad Sci U S A*. **112**, 394–399

7. Lin, R., Cerione, R. A., and Manor, D. (1999) Specific contributions of the small GTPases Rho, Rac, and Cdc42 to Dbl transformation. *J Biol Chem*. **274**, 23633–23641

8. Cha, D. J., Franklin, J. L., Dou, Y., Liu, Q., Higginbotham, J. N., Demory Beckler, M., Weaver, A. M., Vickers, K., Prasad, N., Levy, S., Zhang, B., Coffey, R. J., and Patton, J. G. (2015) KRAS-dependent sorting of miRNA to exosomes. *Elife*. **4**, e07197

9. Villarroya-Beltri, C., Baixauli, F., Gutierrez-Vazquez, C., Sanchez-Madrid, F., and Mittelbrunn, M. (2014) Sorting it out: regulation of exosome loading. *Semin Cancer Biol*. **28**, 3–13

10. Kunadt, M., Eckermann, K., Stuendl, A., Gong, J., Russo, B., Strauss, K., Rai, S., Kugler, S., Falomir Lockhart, L., Schwalbe, M., Krumova, P., Oliveira, L. M. A., Bahr, M., Mobius, W., Levin, J., Giese, A., Kruse, N., Mollenhauer, B., Geiss-Friedlander, R., Ludolph, A. C., Freischmidt, A., Feiler, M. S., Danzer, K. M., Zweckstetter, M., Jovin, T. M., Simons, M., Weishaupt, J. H., and Schneider, A. (2015) Extracellular vesicle sorting of alpha-Synuclein is regulated by sumoylation. *Acta Neuropathol*. **129**, 695–713

11. Sah, N. K., Khan, Z., Khan, G. J., and Bisen, P. S. (2006) Structural, functional and therapeutic biology of survivin. *Cancer Lett*. **244**, 164–171

12. Li, F., Ambrosini, G., Chu, E. Y., Plescia, J., Tognin, S., Marchisio, P. C., and Altieri, D. C. (1998) Control of apoptosis and mitotic spindle checkpoint by survivin. *Nature*. **396**, 580–584

13. Altieri, D. C. (2003) Survivin, versatile modulation of cell division and apoptosis in cancer. *Oncogene*. **22**, 8581–8589

14. Grdina, D. J., Murley, J. S., Miller, R. C., Mauceri, H. J., Sutton, H. G., Li, J. J., Woloschak, G. E., and Weichselbaum, R. R. (2013) A survivin-associated adaptive response in radiation therapy. *Cancer Res*. **73**, 4418–4428

15. Dubel, S., and Little, M. (1988) Microtubule-dependent cell cycle regulation is implicated in the G2 phase of Hydra cells. *J Cell Sci*. **91 (Pt 3)**, 347–359

16. Allan, V. J., and Vale, R. D. (1991) Cell cycle control of microtubule-based membrane transport and tubule formation in vitro. *J Cell Biol*. **113**, 347–359

17. Jordan, M. A., Toso, R. J., Thrower, D., and Wilson, L. (1993) Mechanism of mitotic block and inhibition of cell proliferation by taxol at low concentrations. *Proc Natl Acad Sci U S A*. **90**, 9552–9556

18. Dumontet, C., and Sikic, B. I. (1999) Mechanisms of action of and resistance to antitubulin agents: microtubule dynamics, drug transport, and cell death. *J Clin Oncol*. **17**, 1061–1070

19. Wang, R.-H., Zheng, Y., Kim, H.-S., Xu, X., Cao, L., Luhasen, T., Lee, M.-H., Xiao, C., Vassilopoulos, A., Chen, W., Gardner, K., Man, Y.-G., Hung, M.-C., Finkel, T., and Deng, C.-X. (2008) Interplay among BRCA1, SIRT1, and Survivin during BRCA1-associated tumorigenesis. *Mol Cell*. **32**, 11–20

20. Peck, B., Chen, C.-Y., Ho, K.-K., Di Fruscia, P., Myatt, S. S., Coombes, R. C., Fuchter, M. J., Hsiao, C.-D., and Lam, E. W.-F. (2010) SIRT inhibitors induce cell death and p53 acetylation through targeting both SIRT1 and SIRT2. *Mol Cancer Ther*. **9**, 844–855

21. Stanton, R. A., Gernert, K. M., Nettles, J. H., and Aneja, R. (2011) Drugs that target dynamic microtubules: a new molecular perspective. *Med Res Rev*. **31**, 443–481

22. Kahlert, C., and Kalluri, R. (2013) Exosomes in tumor microenvironment influence cancer progression and metastasis. *Journal of Molecular Medicine*. **91**, 431–437

23. Billottet, C., and Jouanneau, J. (2008) [Tumor-stroma interactions]. *Bull Cancer*. **95**, 51–56

24. Tetta, C., Ghigo, E., Silengo, L., Deregibus, M. C., and Camussi, G. (2013) Extracellular vesicles as an emerging mechanism of cell-to-cell communication. *Endocrine*. **44**, 11–19

25. Antonyak, M. A., and Cerione, R. A. (2014) Microvesicles as mediators of intercellular communication in cancer. *Methods Mol Biol*. **1165**, 147–173

26. Taylor, D. D., and Gercel-Taylor, C. (2009) The origin, function, and diagnostic potential of RNA within extracellular vesicles present in human biological fluids. *J Cell Physiol*. **218**, 460–466

27. van der Pol, E., Boing, A. N., Harrison, P., Sturk, A., and Nieuwland, R. (2012) Classification, functions, and clinical relevance of extracellular vesicles. *Pharmacol Rev*. **64**, 676–705

28. Shao, H., Chung, J., Balaj, L., Charest, A., Bigner, D. D., Carter, B. S., Hochberg, F. H., Breakefield, X. O., Weissleder, R., and Lee, H. (2012) Protein typing of circulating microvesicles allows real-time monitoring of glioblastoma therapy. *Nat Med*. **18**, 1835–1840

29. Mahmoudi, K., Ezrin, A., and Hadjipanayis, C. (2015) Small extracellular vesicles as tumor biomarkers for glioblastoma. *Mol Aspects Med*. **45**, 97–102

30. Chen, C., Skog, J., Hsu, C.-H., Lessard, R. T., Balaj, L., Wurdinger, T., Carter, B. S., Breakefield, X. O., Toner, M., and Irimia, D. (2010) Microfluidic isolation and transcriptome analysis of serum microvesicles. *Lab Chip*. **10**, 505–511

31. Willms, E., Johansson, H. J., Mager, I., Lee, Y., Blomberg, K. E. M., Sadik, M., Alaarg, A., Smith, C. I. E., Lehtio, J., Andaloussi, El, S., Wood, M. J. A., and Vader, P. (2016) Cells release subpopulations of exosomes with distinct molecular and biological properties. *Sci Rep*. **6**, 22519

32. Smith, Z. J., Lee, C., Rojalin, T., Carney, R. P., Hazari, S., Knudson, A., Lam, K., Saari, H., Ibanez, E. L., Viitala, T., Laaksonen, T., Yliperttula, M., and Wachsmann-Hogiu, S. (2015) Single exosome study reveals subpopulations distributed among cell lines with variability related to membrane content. *J Extracell Vesicles*. **4**, 28533